749

TRANSPORTATION
RESEARCH RECORD 749

Embankment Stabilization and Soil Mechanics

TRB
TRANSPORTATION RESEARCH BOARD
NATIONAL ACADEMY OF SCIENCES

The Transportation Research Record series consists of collections of papers in a given subject. Most of the papers in a Transportation Research Record were originally prepared for presentation at a TRB Annual Meeting. All papers (both Annual Meeting papers and those submitted solely for publication) have been reviewed and accepted for publication by TRB's peer review process according to procedures approved by a Report Review Committee consisting of members of the National Academy of Sciences, the National Academy of Engineering, and the Institute of Medicine.

The views expressed in these papers are those of the authors and do not necessarily reflect those of the sponsoring committee, the Transportation Research Board, the National Academy of Sciences, or the sponsors of TRB activities.

Transportation Research Records are issued irregularly; approximately 40 are released each year. Each is classified according to the modes and subject areas dealt with in the individual papers it contains. TRB publications are available on direct order from TRB, or they may be obtained on a regular basis through organizational or individual affiliation with TRB. Affiliates or library subscribers are eligible for substantial discounts. For further information, write to the Transportation Research Board, National Academy of Sciences, 2101 Constitution Avenue, NW, Washington, DC 20418.

TRANSPORTATION RESEARCH RECORD 749

Embankment Stabilization and Soil Mechanics

TRANSPORTATION RESEARCH BOARD

COMMISSION ON SOCIOTECHNICAL SYSTEMS
NATIONAL RESEARCH COUNCIL

NATIONAL ACADEMY OF SCIENCES
WASHINGTON, D.C. 1980

Transportation Research Record 749
Price $6.00
Edited for TRB by Frances R. Zwanzig

modes
1 highway transportation
3 rail transportation

subject areas
25 structures design and performance
62 soil foundations
63 soil and rock mechanics

Library of Congress Cataloging in Publication Data
National Research Council. Transportation Research Board.
Embankment stabilization and soil mechanics.

(Transportation research record; 749)
1. Embankments–Addresses, essays, lectures. 2. Slopes (Soil mechanics)–Addresses, essays, lectures. 3. Soil stabilization–Addresses, essays, lectures. I. Title. II. Series.
TE7.H5 no. 749 [TE210.8] 380.5s [624.1'62] 80-21107
ISBN 0-309-030590-5 ISSN 0361-1981

Sponsorship of the Papers in This Transportation Research Record

DIVISION A–REGULAR TECHNICAL ACTIVITIES
C. V. Wootan, Texas A&M University, chairman

Committee on Low-Volume Roads
Melvin B. Larsen, Illinois Department of Transportation, chairman
Richard G. Ahlvin, John A. Alexander, J. R. Bell, Mathew J. Betz, A. S. Brown, Everett C. Carter, Paul E. Conrad, Robert C. Deen, Martin C. Everitt, Asif Faiz, Gordon M. Fay, Raymond J. Franklin, Marian T. Hankerd, Clell G. Harral, William G. Harrington, Raymond H. Hogrefe, J. M. Hoover, Lynne H. Irwin, Delano S. Jespersen, Clarkson H. Oglesby, Adrian Pelzner, George B. Pilkington II, George W. Ring III, Eldo W. Schornhorst, Eugene L. Skok, Jr., Nelson H. Taber, Ronald L. Terrell, Eldon J. Yoder, John P. Zedalis

GROUP 2–DESIGN AND CONSTRUCTION OF TRANSPORTATION FACILITIES
R. V. LeClerc, Washington State Department of Transportation, chairman

Structures Section
Ivan M. Viest, Bethlehem Steel Corporation, chairman

Committee on Tunnels and Underground Structures
Don A. Linger, Federal Highway Administration, chairman
Ellis L. Armstrong, Robert B. Begin, O. H. Bentzen, Gilbert L. Butler, G. Wayne Clough, Edward J. Cording, Charles H. Downey, Lawrence R. Eckert, Philip Egilsrud, Eugene L. Foster, Edward D. Graf, Delon Hampton, Jerome S. B. Iffland, Chih-Cheng Ku, Robert S. Mayo, Terence G. McCusker, Phillip R. McOllough, Ikuo Nagai, Pierrepont E. Sperry, Forrest H. Stairs, Jr., Rooney J. Stebbins, James D. Washington, Lyman D. Wilbur

Soil Mechanics Section
Lyndon H. Moore, New York State Department of Transportation, chairman

Committee on Embankments and Earth Slopes
Raymond A. Forsyth, California Department of Transportation, chairman
Thomas A. Bellatty, Bruce N. Bosserman, Roger D. Goughnour, Wilbur M. Haas, Larry G. Hendrickson, William P. Hofmann, Robert D. Holtz, Charles C. Ladd, Richard E. Landau, Robert M. Leary, Richard P. Long, Glen L. Martin, Kenneth M. Miller, Lyndon H. Moore, Lyle K. Moulton, Gerald P. Raymond, Walter C. Waidelich, William G. Weber, Jr., Gary C. Whited

Committee on Foundations of Bridges and Other Structures
Clyde N. Laughter, Wisconsin Department of Transportation, chairman
Arnold Aronowitz, Michael Bozozuk, Bernard E. Butler, W. Dale Carney, Harry M. Coyle, Gerald F. Dalquist, M. T. Davisson, Albert F. Dimillio, Bengt H. Fellenius, Frank M. Fuller, G. G. Goble, Richard J. Goettle III, Stanley Gordon, Stanley Haas, Hal W. Hunt, Philip Keene, G. A. Leonards, Alex Rutka, Richard J. Suedkamp, Aleksandar S. Vesic, John L. Walkinshaw, James Doyle Webb, William J. Williams

Geology and Properties of Earth Materials Section
David L. Royster, Tennessee Department of Transportation, chairman

Committee on Exploration and Classification of Earth Materials
Robert B. Johnson, Colorado State University, chairman
Carl D. Ealy, Martin C. Everitt, Edward A. Fernau, William Byran Greene, Robert K. H. Ho, Frank L. Jogodits, Gene O. Johnson, Robert D. Krebs, Donald E. McCormack, Olin W. Mintzer, Frank R. Perchalski, Alex Rutka, Robert L. Schuster, J. Chris Schwarzhoff, Robert B. Sennett, Andrew Sluz, Sam I. Thornton, J. Allan Tice, Gilbert Wilson

Committee on Soil and Rock Properties
William F. Brumund, Golder Associates, chairman
C. O. Brawner, Samuel P. Clemence, Carl D. Ealy, James P. Gould, Ernest Jonas, T. Cameron Kenney, Charles C. Ladd, G. A. Leonards, C. William Lovell, Gerald P. Raymond, Robert L. Schiffman, Hassan A. Sultan, William D. Trolinger, David J. Varnes, Harvey E. Wahls, John L. Walkinshaw

John W. Guinnee, Transportation Research Board staff

Sponsorship is indicated by a footnote at the end of each report. The organizational units and officers and members are as of December 31, 1979.

Contents

Authors of the Papers in This Record

Baladi, Gilbert Y., Department of Civil Engineering, Michigan State University, East Lansing, MI 48824
Bang, S., Department of Civil Engineering, University of Notre Dame, Notre Dame, IN 46556
Bartoskewitz, Richard E., Texas Transportation Institute, Texas A&M University, College Station, TX 77843
Bauer, G. E., Department of Civil Engineering, Carleton University, Ottawa, Ont., Canada
Betz, Mathew J., Department of Engineering, Arizona State University, Tempe, AZ 85281
Brawner, C. O., Consultant, 780 West Greenwood Road, West Vancouver, B.C. V7S IX7, Canada
Brumund, William, Golder Associates, 5125 Peachtree Road, Atlanta, GA 30341
Coyle, Harry M., Department of Civil Engineering and Texas Transportation Institute, Texas A&M University, College Station, TX 77843
Cutter, W. A., Atec Associates, Inc., 5150 E. 65th Street, Indianapolis, IN 46220
Dash, Umakant, Pennsylvania Department of Transportation, P.O. Box 2926, Harrisburg, PA 17120
Deschenes, J. H., Terratech, Ltd., 275 Benjamin Hudon, Montreal, P.Q., Canada
Despain, Ronald, Johannessen and Girand Consulting Engineers, Inc., 6611 North Black Canyon Highway, Phoenix, AZ 85015
Fowler, Jack, U.S. Army Engineer Waterways Experiment Station, Box 631, Vicksburg, MS 39180
Goble, G. G., Department of Civil, Environmental, and Architectural Engineering, University of Colorado, Boulder, CO 80309
Haliburton, T. Allan, Department of Civil Engineering, Oklahoma State University, Stillwater, OK 74074
Holtz, R. D., Department of Civil Engineering, Purdue University, West Lafayette, IN 47906
Huang, Yang H., Department of Civil Engineering, University of Kentucky, Lexington, KY 40506
Jovino, Pierre Luigi, Fondedile Corp., 739 Boyleston Street, Boston, MA 02116
Lamb, Stephen E., New York State Department of Transportation, 1220 Washington Avenue, State Campus, Albany, NY 12232
Langan, J. Patrick, U.S. Army Engineer District, Mobile, P.O. Box 2288, Mobile, AL 36601
Lentz, Rodney W., Department of Civil Engineering, University of Missouri, Rolla, MO 65401
Leonards, G. A., Department of Civil Engineering, Purdue University, West Lafayette, IN 47906
McCammon, Norman C., Golder Associates, 224 W. 8th Avenue, Vancouver, B.C. V5Y 1N5, Canada
Moses, Fred, Department of Civil Engineering, Case Western Reserve University, Cleveland, OH 44106
Murray, Richard P., New York State Department of Transportation, 1220 Washington Avenue, State Campus, Albany, NY 12232
Romstad, K. M., Department of Civil Engineering, University of California, Davis, CA 95616
Scott, J. D., R. M. Hardy and Associates, 4810 93rd Street, Edmonton, Alta., Canada
Shen, C. K., Department of Civil Engineering, University of California, Davis, CA 95616
Shields, D. H., R. M. Hardy and Associates, Ltd., 4052 Gravely Street, Burnaby, B.C. V5C 3TC, Canada
Snyder, Richard, Goble and Associates, 12434 Cedar Road, Cleveland, OH 44106
Wyllie, Duncan C., Golder Associates, 224 W. 8th Avenue, Vancouver, B.C. V5Y 1N5, Canada

In-Place Roadway Foundation Stabilization

Richard P. Murray

A new stabilization technique that uses a two-dimensional pile system and relieving platform is described. This technique has been used to preserve a short section of NY-23A about 16 km (10 miles) west of Catskill, New York. The two-lane roadway, built on the side of a steep mountain valley, suffered major damage in a 1935 hurricane. Reconstruction at that time used a series of stone-filled timber cribs and stone walls to support the roadway embankment. Subsequent weathering has caused deterioration of the exposed timber crib faces and resultant loss of stone filling from within the cribs. This loss of support has caused movement of the pavement. One location in particular, where the roadway was supported by a series of four timber cribs, was considered critical because a failure would be rapid and would involve the entire roadway. In early 1977, the stone wall in this area had moved so much that it threatened to topple. This wall was replaced by precast concrete wall units, which solved the immediate problem but not the deep-seated stability problem. Permanent stabilization alternatives included relocation into the hillside, a structure at grade, support of the downhill slope, and in-place treatment. Design constraints included maintaining one-way traffic during construction and minimizing environmental damage. In-place stabilization incorporating the root-pile concept was selected. Plans and specifications were prepared on this basis. This paper describes the project site, design features, analysis of the contractor's proposal, construction details, and postconstruction observations. Recommendations for the use of this in-place stabilization method on future contracts are made.

Each year, many highways in the United States are damaged by landslides. It is estimated that more than $100 million is spent annually to repair landslide damage. Studies have shown that up to 95 percent of all landslides are caused by water (1). The project described in this paper, however, did not involve a water-related slide: In this case, deterioration of timber cribs had removed support from upper retaining structures and the roadway. The movement of slides due to such causes is slow, and frequent patching of the pavement can keep the surface safe for travel. However, as movement progresses, these slides reach a point where complete failure is imminent and major stabilization techniques must be used. The choice of stabilization methods is often limited by design constraints such as lack of additional right-of-way, the need to minimize environmental damage, and the need to maintain traffic flow during construction. These constraints often require new and innovative stabilization methods. This paper describes the case history of the design and construction of an embankment-stabilization project having all of these constraints.

SITE DESCRIPTION

The project was located on NY-23A, about 160 km (100 miles) north of New York City and 16 km (10 miles) west of Catskill (see Figure 1). This road connects the Hudson Valley, a major north-south travel route, with the northern Catskill Mountains through a steep, narrow valley. The road is 6.4 m (21 ft) wide and rises approximately 365 m (1200 ft) in 5.6 km (3.5 miles). The Catskill Mountains are a year-round tourist and resort area that provides recreation activities for the urban New York area. Summer recreation, fall foliage, and winter skiing make the roadway heavily traveled with cars, buses, and commercial trucks throughout the year.

A cross section of the landslide area shows the need for stabilization (see Figure 2). The embankment slope combining the stone wall and the series of timber cribs has an overall inclination of about 75°. Borings taken adjacent to the dry stone wall showed a layered cobble and boulder fill over very compact glacial till that extends to bedrock. Borings taken on the uphill side of the road did not encounter the cobble and boulder fill.

The timber cribs were installed in 1935 after hurricane rains had destroyed many areas of the road (see Figures 3 and 4). Over the past 40 years, the timber facing deteriorated and either disappeared (Figure 5) or was seriously weakened. This resulted in a loss of support for the upper retaining structures and the roadway. In the main failure area (see Figure 6), the retaining structure settled and tipped, which created a depression of the pavement that required periodic maintenance. In the area just west of the main failure area (see Figure 7), deterioration and movement of the lower timber cribs removed support for the oversteepened soil slope, which led to subsidence of the shoulder and guide rail.

Slope indicator data showed movements at 3 m (10 ft) and 5.8 m (19 ft) below the roadway surface. The movements at 3 m were related to displacement of the dry stone wall. In 1977, a portion of this wall appeared ready to collapse and was replaced. The continuing movements at 5.8 m were approximately at the interface between the cobble fill and the glacial till (thus reinforcing the failure-mechanism theory that the deterioration of the timber crib facing was the cause of the loss of support for the facilities above). Failure at this level would remove at least half of the roadway and thus close the road.

CORRECTIVE DESIGN

Because the project is located within the Catskill State Park, strict controls to minimize environmental and esthetic damages had to be observed. Traffic conditions dictated that at least one-way traffic had to be maintained at all times. Possible design alternatives of relocation into the hillside, an at-grade structure supported by drilled-in caissons, and stabilization of the downhill slope with a rock fill were studied and rejected for not meeting the New York State Department of Transportation (NYSDOT) criteria. Reconstruction of the existing walls in the same location was impossible due to the restricted access to the cribs [15 m (49 ft) or more below the roadway] and the necessity to remove the roadway that this process would entail. Treating the face with shotcrete was determined to be impractical and not permanent. Thus, a solution was required that would provide a permanent stable platform for the roadway without the support of the timber crib walls; i.e., in-place stabilization was needed.

Several in-place stabilization methods were investigated. A structure at grade was considered in detail and rejected because of lack of accessibility of the site for large equipment, costs, and the necessity to close the road. A line of drilled-in caissons forming a wall was rejected because of the limited working area for large equipment, questionable cost estimates, and uncertainty as to whether or not sufficient bridging to support the roadway would develop between the caissons.

The last method considered was one involving drilling a three-dimensional array of small-diameter root piles to create an in-place gravity-stabilized retaining wall by knitting together the in situ soil, boulder, and rock masses. This patented process was selected because it fulfilled all of the design criteria.

Because the root-pile method was a patented process, legal complications arose regarding awarding a sole-source procurement contract of this magnitude. New York State law requires that all large contracts be awarded on a competitive-bid process and, therefore, it was necessary to develop some form of alternative-bid contract. Designs from other foundation specialty companies were solicited and found to be unsatisfactory. Alternative bids of root piles versus complete relocation into the hillside were considered and rejected. The NYSDOT legal department stated that the specifications must allow other contractors an opportunity to submit equivalent designs. NYSDOT was reluctant to be put in the position of having to evaluate alternative designs, but the roadway failure was accelerating and the project was essential, and so an "or equal" provision was included.

The plans and specifications were developed around the concept that the contractor would design and construct an earth-pile retaining wall based on a system of

Figure 1. Project location.

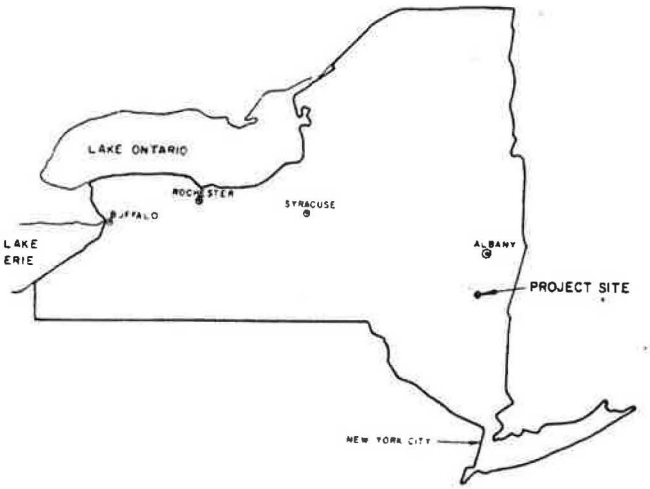

Figure 2. Cross section of critical section showing need for stabilization.

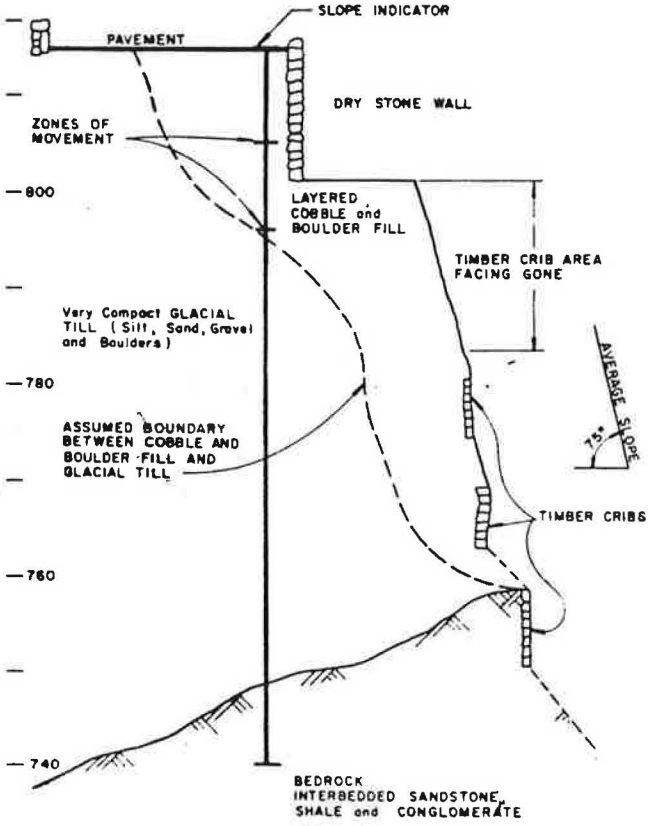

Figure 3. Conditions after 1935 hurricane.

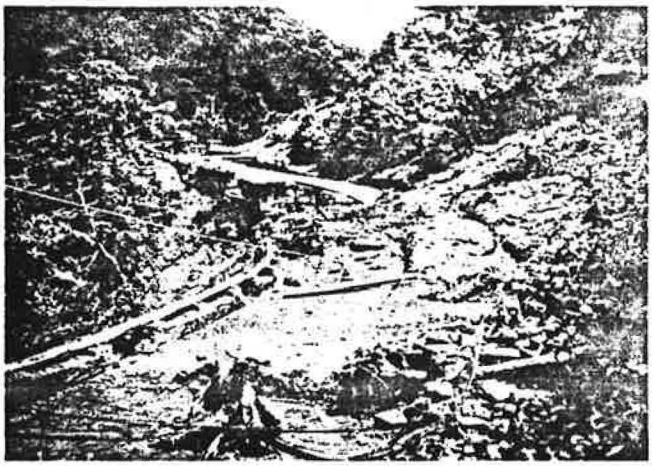

Figure 4. Construction of stone-filled timber cribs used to repair 1935 hurricane damage.

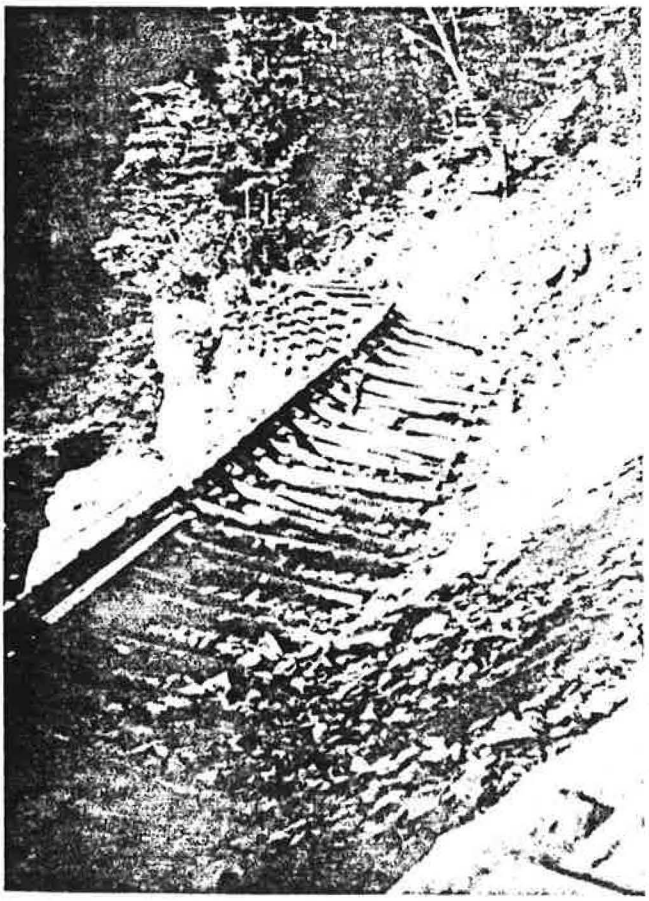

Figure 5. Current condition of timber cribs.

Figure 6. Main failure area.

cast-in-place reinforced concrete piles similar to those used in the root-pile method and topped with a reinforced concrete cap beam or an approved equal. The specifications required that the piles have a minimum diameter of 10 cm (4 in) and that the retaining wall contain an average of at least two 10-cm piles per linear foot (0.3 m) of wall measured at the ground surface. The payment items included excavation, piles, additional fluid mortar, concrete, and steel. Due to the unique location, topography, access problems, and storage space at the project site, the contract documents included as much information as possible to assist the contractor in the design, as well as a requirement that the site be visited before bid submission. Every effort was made to provide the contractor with enough information to design and construct the retaining structure.

The design that was approved for use involved installation of a two-dimensional system of four or five rows of reinforced concrete piles battered 15° in both directions from the vertical and supporting a reinforced concrete cap beam. Figure 8 shows a typical pile layout and section at the critical section. The length of the

Figure 7. Area west of main failure area.

Figure 8. Typical pile layout at critical section.

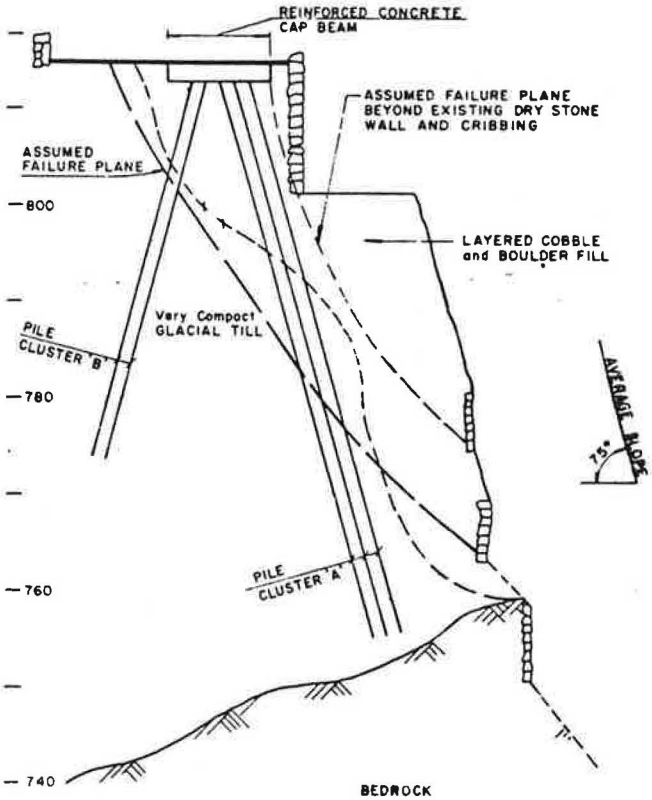

piles was varied based on the cross sections, and more piles were installed in the more critical areas. The pile and cap beam structure was analyzed as a rigid frame with sidesway. The legs (pile clusters A and B) were assumed to be fixed at the failure plane (because of their embedment below this point) and to act as beams and thus provide the capability to resist moments. These are valid assumptions because the loose, open rock allows the fluid mortar to fill the voids and the reinforcing steel knits the whole system together. All lateral resistance above the failure plane in front of pile cluster A was disregarded. Any material remaining in this position adds to the stability of the system. The soil above the failure plane, consisting mainly of layered cobbles and boulders, was assumed to have a unit weight of 1842

kg/m³ (115 lb/ft³), an angle of internal friction of 30°, and cohesion equal to 0.

The steps in the design analysis are shown in Figures 9-13. [The example analyzed in these figures does not represent the most critical section (that shown in Figure 8) but, rather, is based on preliminary data. The conditions at the critical section were discovered only during construction and were analyzed by the NYSDOT Soil Mechanics Bureau by using an approximate, somewhat conservative method.]

The forces exerted on the piles by the earth above the failure plane were resolved (see Figures 9 and 10) into axial and transverse loads on the two pile clusters. The transverse loads acting on the piles were distributed increasing linearly with depth. A rigid-frame analysis

Figure 9. Design analysis: resolution of forces from wedge 1.

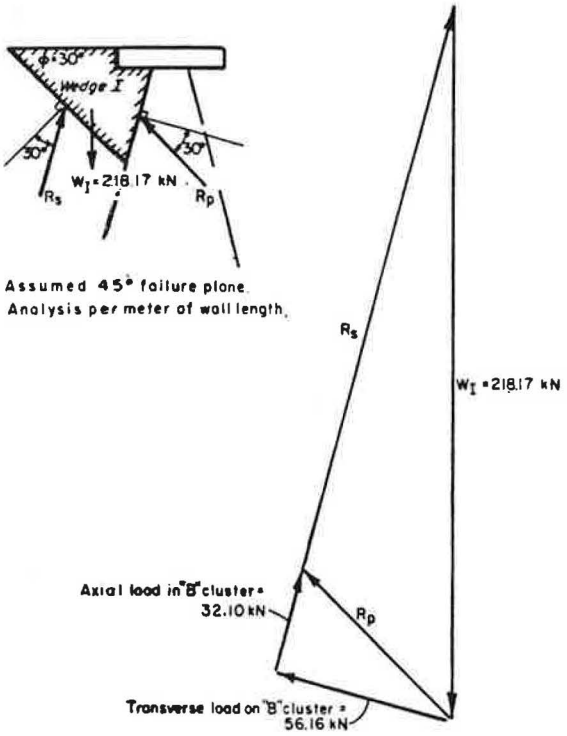

Figure 10. Design analysis: resolution of forces from wedge 2.

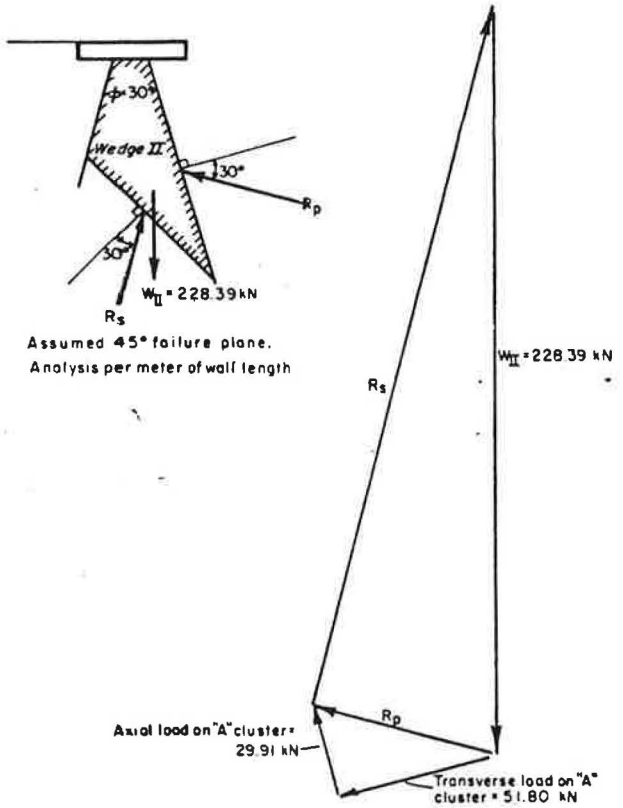

Figure 11. Design analysis: forces acting on rigid frame.

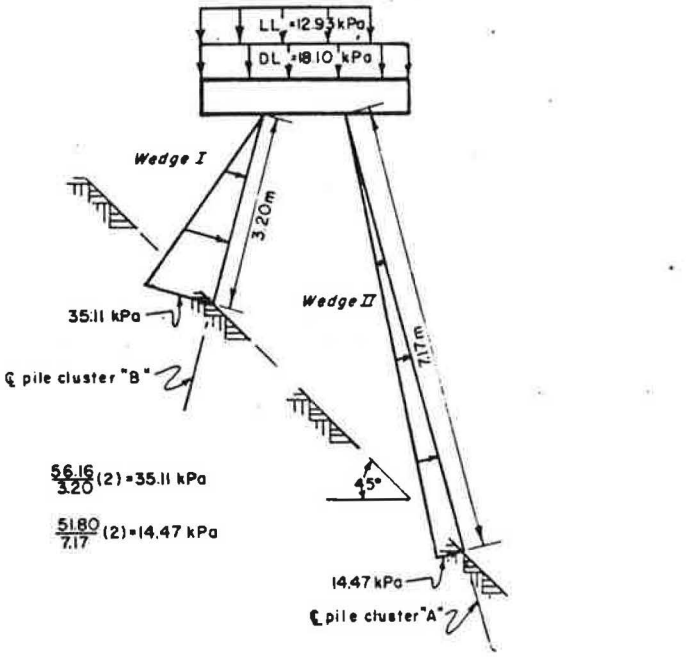

Figure 12. Design analysis: moments and shears determined by rigid-frame analysis with sidesway.

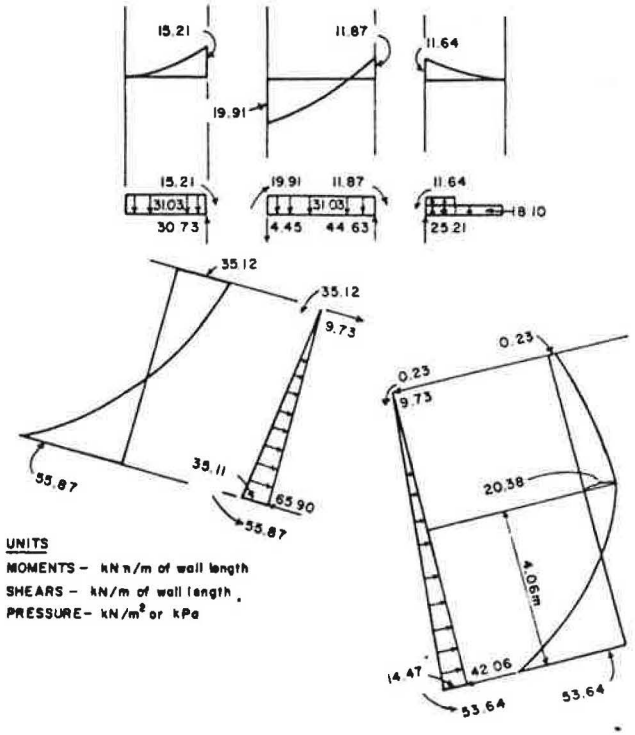

Figure 13. Design analysis: calculation of axial load on (a) pile cluster A and (b) pile cluster B.

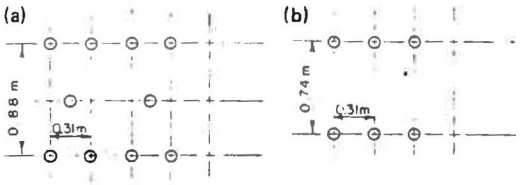

Figure 14. Construction: series of drills at work site.

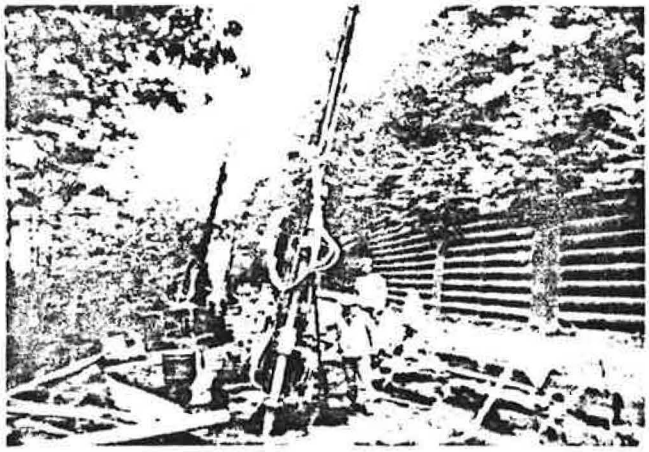

with sidesway was performed for the geometry and loading shown in Figure 11. The resulting moments and shears are shown in Figure 12. The axial loads from the bending moments were added to those obtained in the steps shown in Figures 9 and 10. The allowable pile loads were calculated as shown below (1 kN/m = 0.222 lbf/ft and 1 kN = 224 lbf):

For pile cluster A, which has the geometry shown in Figure 13a,

Axial force per meter = (25.21 + 44.63)cos 15° + 29.91 = 97.37 kN/m,
Force from bending moment = 53.64/0.88 = 60.95 kN/m, and
Maximum axial load per pile = 158.32/8.74 = 18.11 kN (which is less than the design capacity of 111.25 kN).

For pile cluster B, which has the geometry shown in Figure 13b,

Axial force per meter = (30.73 - 4.45)cos 15° + 32.10 = 57.48 kN,
Force from bending moment = 55.87/0.74 = 75.50 kN/m,
Total axial load = 57.48 ± 75.50 = 132.98 kN or -18.02 kN, and
Maximum axial load per pile = 132.98/6.56 = 20.27 kN (which is less than the design capacity of 111.25 kN).

The contractor's computations were checked by the Soil Mechanics Bureau by using an approximate and conservative method. The ability of the pile clusters to sustain the computed bending moments was also investigated. It was found that, to enable each pile cluster to act as a composite beam, the shear strength of the rock fill between the piles had to be increased by permitting penetration of fluid mortar from the piles. After the design computations had been reviewed, the design was approved.

CONSTRUCTION

Construction began in August 1977. The contractor elected to excavate below the cap beam and pour an unreinforced concrete mud mat or working platform. This mat enabled him to lay out the piles on a smooth surface and to work in all kinds of weather. The pile layout was checked against the contractor's approved drawing and drilling began as shown in Figure 14. In a small number of holes, steel casings were used but, in most, there were no casings. The fluid mortar was hand poured into the holes, and 3.2-cm-diameter (no. 10) Dywidag threaded rods (reinforcing bars) were inserted. The rods had been cut into 3-m lengths, due to the necessity of installing them by hand. The pile lengths were determined by the length of the reinforcing steel placed and did not exceed the design length. The contractor was ordered to continue work until the piles and cap beam were completed to ensure the overall stability of the area.

Before the piles were installed, slope indicators were installed at various locations to monitor the stability during and after construction. Analysis of the movement data indicated that, as the piles were installed, the movements shifted to a lower depth in the compact glacial till due to the load transfer in the piles. Records indicate that up to 13 cm (5 in) of movement of the top of the existing dry stone wall occurred during construction operations. The movements slowed considerably as the front rows of piles were completed but remained in a constant state of flux from shallow to deep and vice versa due to readjustments of the shearing stresses from the soil to the piles. The piles transferred the loads deeper. Since completion of the cap beam on December 15, 1977, only minor movements have been recorded.

PERFORMANCE

The project was opened to traffic in 1978. It has been through two winters and springs, i.e., the most critical times of the year, with no significant adverse effects. The minor settlements of the pavement adjacent to the cap beam are believed to be due to discontinuity in the pavement cross section—the cap beam and the unexcavated pavement provide a rigid base, whereas the area between was filled with subbase material. The subbase material consolidated under traffic loading, which resulted in formation of a depression. There are also two areas on the downhill side of the work where the soil and rock have moved away from the cap beam. These movements were expected and were taken into account in the design shown in Figure 8. As this material moves away from the earth-pile retaining wall, the design concept of not relying on it for stability will be tested.

This method of in-place stabilization has proved to be effective and meets all of the design criteria. The contractor was able to work within one lane and maintain traffic on the other lane. Some dust was generated by the drilling operations; however, the effects on the environment were negligible. The cost of the earth-pile retaining wall and related items (no paving items) was about $10 000/linear m ($3000/linear ft) of stabilization. Much of this cost was due to the design constraints, the project location, and the area terrain.

RECOMMENDATIONS

New York State anticipates only limited future application of this stabilization method, principally due to its high cost. There may be other failure areas where con-

straints will dictate the use of this method. In these cases, the state will design the treatment rather than making use of the design-construct concept. Bidding competition by the many contractors who are not staffed to develop a design-construct contract should result in lower bid prices.

REFERENCE

1. R. G. Chassie and R. D. Goughnour. States Intensifying Efforts to Reduce Highway Landslides. Civil Engineering, Vol. 46, No. 4, 1976.

Publication of this paper sponsored by Committee on Embankments and Earth Slopes.

Embankment Stabilization by Use of Horizontal Drains

Stephen E. Lamb

An embankment 24 m (about 80 ft) high that traverses a narrow valley on I-81 about 56 km (35 miles) south of Syracuse, New York, began to fail several years after construction. In the spring of 1973, the pavement dropped several centimeters to bring the cumulative patch to 46 cm (about 18 in). Complete failure of the embankment was anticipated for the spring of 1974 because past movements had been largest during the spring and recent monitoring had indicated an increase in the rate of movement. A design for a stabilization project to counteract the effects of the hydrostatic pressure that was believed to be causing the failure was prepared that consisted of a berm and shear key at the toe of the embankment. Implementation of this design, however, could not be completed before spring. Therefore, it was decided to stabilize the embankment by decreasing the excess hydrostatic pressure by installing a system of horizontal drains, a project that could be completed before spring and at a cost saving of $1 000 000. The project was completed in early spring of 1974, and the embankment has been stable since then. This paper describes the design, construction, and postconstruction evaluation of the project. In addition, observations and comments are made that should be of assistance in evaluating this method of stabilization for future projects.

The problem discussed in this paper occurred in an embankment 24 m (approximately 80 ft) high that crosses a steep-sided valley 122 m (approximately 400 ft) wide. The embankment is part of I-81 in central New York State; in April 1973, about eight years after its construction, a severe crack was observed in the southbound roadway (see Figure 1). The pavement had dropped several centimeters and, by mid-July, approximately 46 cm (18 in) of asphalt paving had been placed to maintain the highway profile. A field review to determine the extent of the distress showed that stabilization would be beyond the scope of maintenance personnel.

DESIGN INVESTIGATION AND ANALYSIS

The investigation of the area consisted of a survey, a drilling program, and establishment of horizontal-movement-control stakes. The drilling program consisted of 21 borings. In 17 of the borings, observation wells were established to monitor groundwater fluctuations and to locate the depth of movement in the foundation soils (1). A plan of the site is shown in Figure 2.

Inspection of a 91-cm (36-in) diameter, corrugated metal pipe culvert in the center of the unstable area showed separations at several joints and a few separations between the joints. Also, the underdrains placed at the original ground surface during original construction were flowing.

The cross section shown in Figure 3 indicates the soil profile and observed static water table. The observation wells indicated a variable artesian pressure below the silt and clay layer, and measurements in these wells indicated significant lateral movement in the lower part of the silt and clay strata.

An analysis of the data obtained by the end of July 1973 suggested that a progressive wedge-type shear failure was occurring through the silt and clay. The most significant factor contributing to the failure was that, since construction, the static water table had risen 21 m (approximately 70 ft) in the embankment.

Analyses indicated that a counterweight berm would not be adequate to provide stability. One apparent solution was to form a key against sliding by a close-order sequence of excavation and backfilling and then construct a berm above the key. Analysis of this indicated that the slope would be stable but that the method would require an excavation for the key that extended approximately 9 m (30 ft) below the existing ground surface and cost about $1 million, because of limited access for equipment. Next, an at-grade structure spanning the failure area was considered, but the cost estimate for this was also about $1 million. Therefore, the decision was made to prepare plans to stabilize the area by using a shear key-berm solution, because a structure would require long-term maintenance. The design for this could have been completed by April 1974; however, the construction would not have been completed until several months later.

Because a major failure during the critical spring period was a significant possibility, a review was made of another method for solving this problem. In the western United States, groundwater is sometimes removed from slopes by installing horizontal drains. Such drains cannot be considered a permanent solution because of the complexity of underground water movements, but their cost is only approximately 4 percent (i.e., $40 000) of the cost of the more-permanent treatments. Consequently, a recommendation was made to attempt to achieve stabilization by installing horizontal drains.

A contract was negotiated, and work began in March 1974. Basically, the contract included a general description of the work to be performed and a 30-day completion date with a liquidated damage clause.

Because the schedule of the project did not provide sufficient time to complete the borings until just before beginning the contractual work, the description of the work to be performed was written before all the subsurface information could be obtained. However, the description was sufficiently general to allow making modifications after reviewing all the information.

The location and spacing of the drains was determined

from an educated guess rather than a theoretical analysis. Basically, the drains were to be installed in a fan-shaped pattern from the toe of the embankment at two different inclinations. The upper level was to be installed above and parallel to the silt and clay strata to achieve the maximum possible drawdown in the embankment material and to prevent recharge during peak runoff. The lower level was placed so as to provide drainage for the lower permeable strata (see Figures 3 and 4).

CONSTRUCTION

There are several practical problems of installation that are important in the design and inspection of horizontal drain projects.

The equipment requires a level working surface approximately 6 m (20 ft) wide. The working surface at the site was established by constructing a small cut-fill section at the toe of the embankment.

Before drilling was begun, the equipment was leveled on a timber mat. The horizontal alignment was established by sighting along stakes located at the top and toe of the slope, and the vertical alignment was established by loosening the swivels and adjusting the leveling jacks by using a 15-cm (6-in) machinist's level on the initial length of drilling rod (see Figure 5; note scissor swivel and adjustable jack on ends of carriage). The 0.1-0.15 m^3/min (30-40 gal/min) water required for drilling was obtained by damming the culvert outlet.

The heavy-walled, flush-coupled steel drill casing had an expendable bit adaptor with a J-slot on the first section. One or two O-ring seals were placed in the grooves in the adaptor to prevent drill cuttings from lodging between the disposable bit and the adaptor and possibly freezing the bit to the adaptor.

The 3-m (10-ft) sections of drill casing were advanced with water and rotation until the planned length was reached. The disposable bit was then advanced without rotation or water until the bit jammed against firm material. To uncouple the bit, the rotation of the casing was reversed for approximately one-quarter to one-half turn and then the casing was hydraulically withdrawn to dislodge the bit.

Two problems were encountered during the drilling operation: (a) flowing silt and sand plugging the drill

Figure 1. Problem site: highlighted pavement crack.

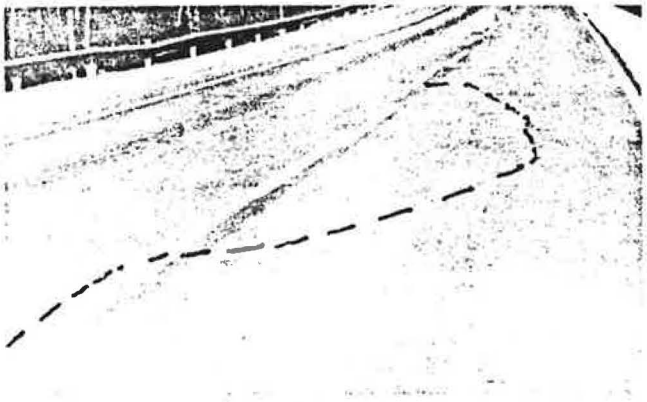

Figure 2. Plan view.

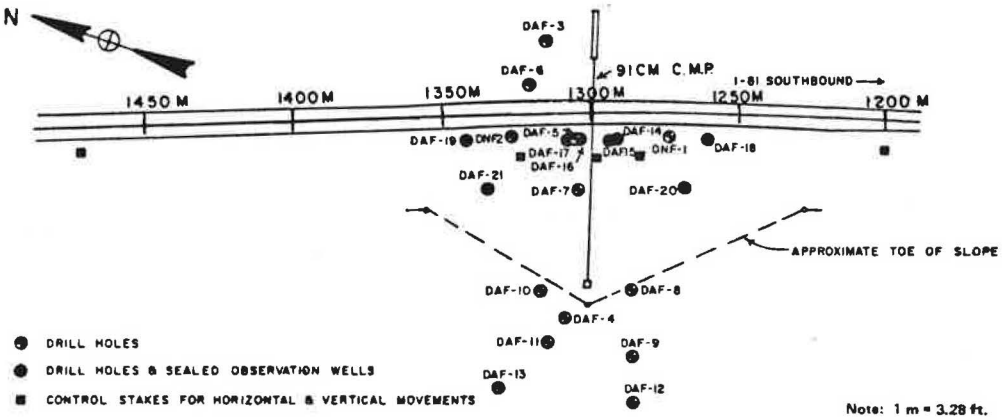

Figure 3. Cross section: typical soil profile.

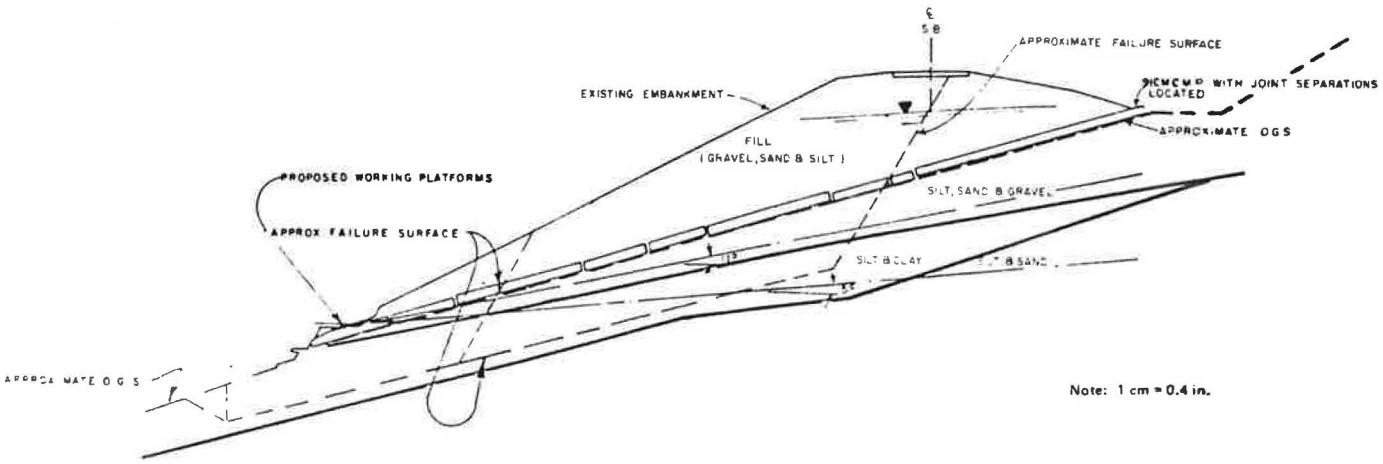

Figure 4. Drain layout: plan view.

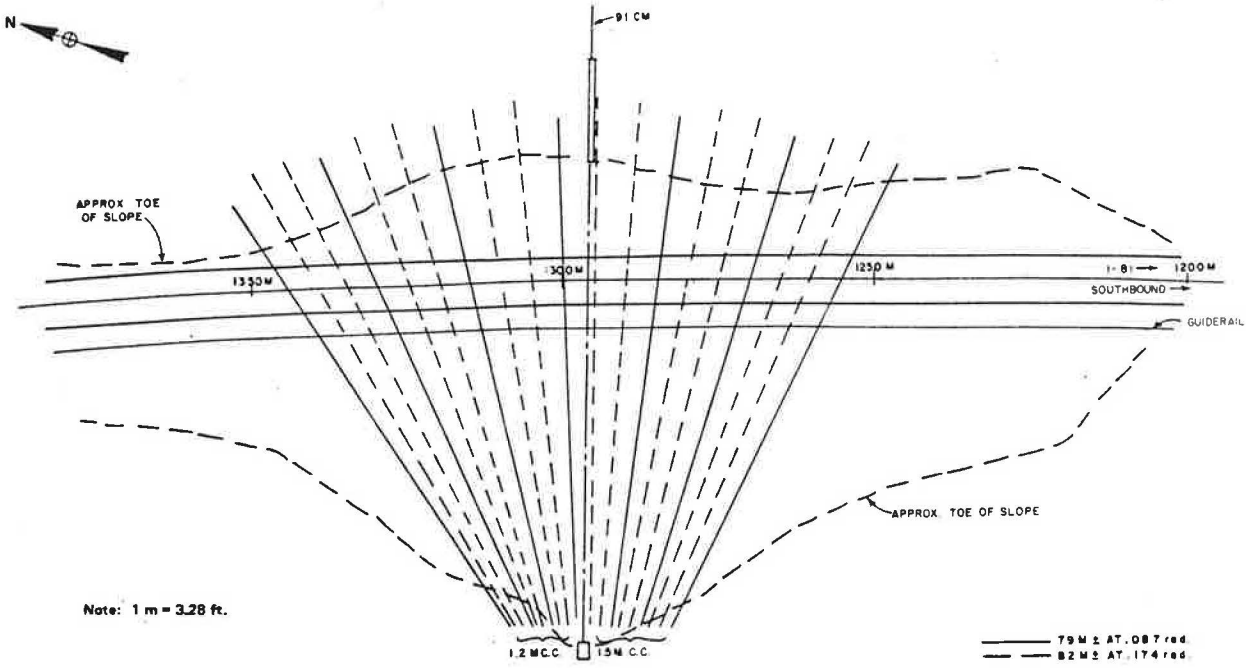

Figure 5. Vertical alignment of drilling equipment.

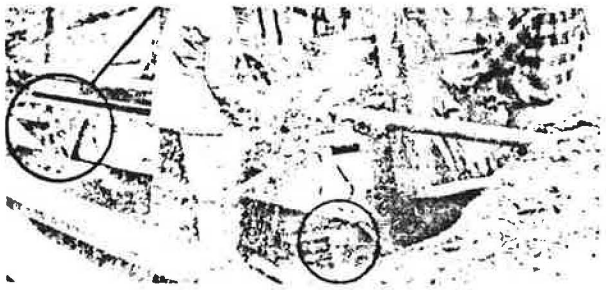

casing and (b) inability to dislodge the disposable bit. These problems can be avoided by using a one-way valve and spacer in the bit assembly when drilling in loose sand or silt and by attaching the bit and O-ring seals carefully.

The drain pipe was 5-cm (2-in nominal) diameter polyvinyl chloride (PVC) that had 0.25-mm (0.010-in) wide slots in a trislot configuration around the perimeter at 6-mm (0.25-in) intervals. Each drain consisted of joined 3-m sections of slotted pipe, except that the last two sections were unslotted to prevent piping at the drain outlet. The drain pipe was plugged at the upper end and inserted into the drill casing. As additional lengths of pipe were inserted into the casing, each joint was glued. The casing was extracted in 3-m sections from around the PVC pipe, which was held in place in the slope by a floating-lock piston device. This locking device is a one-way water-tight piston that, as the casing is withdrawn, is retained within the drill casing by water pressure. Occasionally, the piston bound in the drill casing, but this problem could usually be solved by rapping the casing with a sledge hammer as the casing was being withdrawn.

A few drains did not function after completion. A review of the installation sequence suggested that this problem was probably caused by the separation of a PVC pipe connection when the piston locking device bound in the casing. This situation was satisfactorily corrected by pop riveting some of the connections.

Grease was applied to the threads of the drill casing each time a section of casing was added, an operation that resulted in the formation of a grease ring on the inside of the casing as the connections were tightened. This excess grease then smeared over the drainage slots in the PVC pipe when the pipe was installed through the casing. Because the grease is not water soluble, this smearing significantly reduces the effective area available for water to enter the pipe. [For example, on a 76-m (250-ft) section of pipe that was removed from the casing because the drill bit could not be dislodged, approximately 30 percent of the effective drainage area was smeared with grease.] The grease cannot be eliminated because the lubricant is required for the drilling. Therefore, the amount of grease applied should be minimal, and its application to the casing connections should be carefully done.

The work involved the installation of 1585 m (5200 ft) of drains and was completed in 3 weeks.

POSTCONSTRUCTION DATA COLLECTION AND EVALUATION

After completion of the drain installation, data were first obtained weekly on the movement of the control stakes, the water elevation in the observation wells, and the flow rate from each drain. In October 1974, the recording interval was modified to annually for the movement of the control stakes and biweekly for both the water elevation in the observation wells and the flow rate from each drain. In July 1975, the reading intervals for the water elevations and flow rates were again modified, this time to four times per year—April, July, October, and January. No additional cracking has been noted during periodic visual inspections of the pavement in the area. Also, the survey data from the control stakes indicate that there have been no significant horizontal or vertical movements since the drain installation was completed.

The total flow rate and the flow rates from each level of drains are shown in Figure 6. Records from a nearby weather station indicate that the upper level of drains

Figure 6. Flow data.

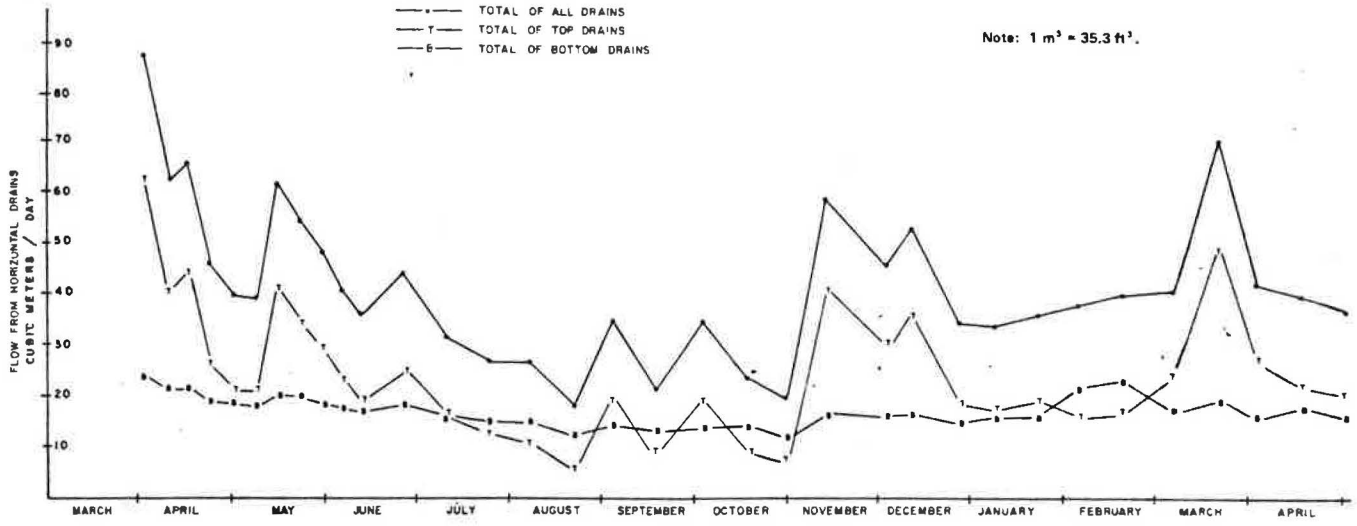

Figure 7. Typical drawdown curve: observation well DAF-14.

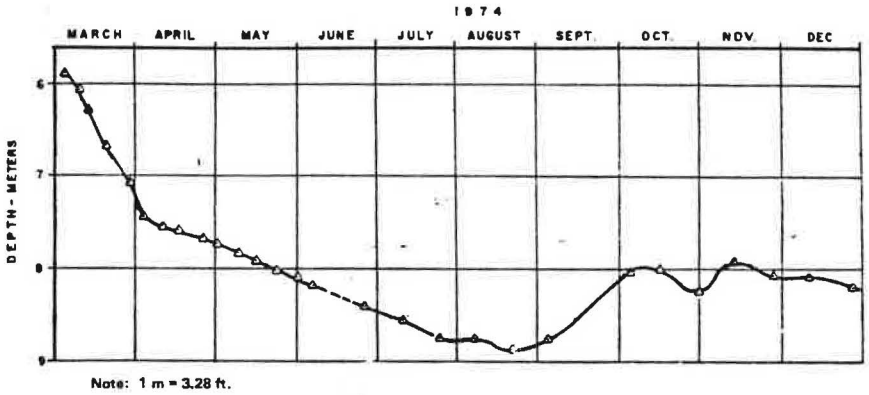

may be sensitive to rainfall. The flow data obtained after April 1975 indicate that the total flow is generally increasing. However, these readings were obtained during traditionally wet seasons. The data shown suggest that more information is desirable for a long-term performance evaluation of the drains.

The typical drawdown curve shown in Figure 7 indicates that the static water table above the silt and clay strata was generally lowered 3 m during 1974. This drop, coupled with a 1.5-m (5-ft) reduction of the water table in both the silt and clay and the underlying silt and sand was sufficient to provide stability. The data to date indicate that the drop in the water table will be long term.

The flow rates of the individual drains varied from dripping to approximately 0.03 m^3/min (8 gal/min).

Several of the completed drains were checked in September 1975 to determine their slopes. This check was initiated because, in a subsequent horizontal-drain project, all the drains rose above the desired inclination. The drilling equipment used in the two projects was similar but not identical. The elevations of the drains were checked at 15 and 30 m (50 and 100 ft) by using a small-diameter polyethylene tube filled with water as a level.

Any difference in the inclinations between the as-installed values and those found in the September 1975 check were attributed to the method used to set the initial inclination rather than to wandering of the steel casing. Basically, the information obtained indicated that the drains did not significantly rise on this project.

Water flowing from the drains did not freeze during the winter if the flow rates were more than 0.004 m^3/min (0.1 gal/min).

CONCLUSIONS

The drains have lowered the groundwater table and eliminated the factors that caused the pavement failure and the movements have stopped.

A 1979 survey indicated that there has been no movement in the past five years and that the flow from the drains is basically unchanged. Thus, the horizontal drains have apparently permanently solved the problem and also saved $1 000 000.

RECOMMENDATIONS

1. The site evaluation should include the installation of a complete monitoring system. This system should include provisions for monitoring (a) the water table in the area and (b) horizontal and vertical movements of the ground surface and should be permanent and protected from damage during construction and due to vandalism.
2. A prebid inspection should be held for interested prospective bidders during which questions could be answered. This would enable the attending bidders to more accurately estimate the cost of the work and result in lower bid prices.
3. For greater precision, the vertical inclination of each drain should be set by using a level having a minimum length of 0.6 m (2 ft).

4. The contractor's installation procedure should be reviewed to ensure that the PVC pipe is continuous after installation. Perhaps techniques such as a minimum set time, pop riveting the joints, or maintaining positive pressure on the PVC pipe while extracting the casing will be necessary to ensure this.
5. The contract should require the contractor to apply grease to the casing during drilling carefully so as to minimize the grease smear on the PVC drain pipe.

REFERENCE

1. V. C. McGuffey. Plastic Pipe Observation Wells for Recording Groundwater Levels and Depth of Active Slide Movements. Highway Focus, Aug. 1971.

Publication of this paper sponsored by Committee on Embankments and Earth Slopes.

Abridgment

Dynamic Compaction of Granular Soils

G. A. Leonards, W. A. Cutter, and R. D. Holtz

The densification of a loose granular fill by dynamic compaction is described. The effective depth of compaction was found to be described by the relationship $D \simeq \frac{1}{2}(Wh)^{\frac{1}{2}}$ when D and h are expressed in meters and W is expressed in metric tons. The degree of compaction achieved was found to correlate with the product of the energy per drop and the total energy applied per unit surface area.

This paper describes the use of dynamic compaction to densify a loose granular fill in preparation for the construction of a warehouse at the National Starch and Chemical Corporation's Indianapolis plant [further details of this work are described elsewhere (1)]. During the 1930s, embankments of granular material—a sand spoil from an adjacent gravel pit operation—had been placed along the northern property line and through the central portion of the development area. The two embankments merged on the east side of the property to enclose a triangular-shaped tract of land.

The original plans called for constructing the warehouse on a controlled granular fill entirely located between the two spoil embankments. However, subsequent to the filling and grading operations of this area, it was decided to enlarge the warehouse and to shift its location eastward. These changes meant that both the northeast and the southeast corners of the warehouse structure would be situated over the old spoil embankments, which had been constructed simply by end dumping. Because the project was being constructed as quickly as possible, the old spoil embankments had to be improved as expeditiously as possible.

Basically, the spoil materials were a loose, fine-to-medium sand (having thin gravelly seams) covered by a well-compacted sand whose thickness increased with increasing distance from the crest of the old spoil piles (see Figure 1). The percentage of fines (those passing a 75-μm sieve) ranged from 2 to 10 and was typically 5-6. The depth to the underlying original ground surface was about 5-6 m, and the groundwater table was 9-10.5 m below the current ground surface. After examining a variety of ways for dealing with the problem, it was decided that densification would be both the cheapest and the most expedient method. Estimates were made of relative costs and times to completion for excavation and replacement by controlled, compacted backfill versus deep compaction in situ, and deep compaction by a heavy falling weight was selected for trial.

PRELIMINARY TRIALS

Preliminary trials were carried out by using the weights, drop heights, and drop patterns shown in Figure 2. Based on measurements of crater depth after successive drops, it was decided to limit the number of drops at each point to seven. Standard penetration (N) and Dutch cone penetration (q_c) tests were obtained before and after completion of the pattern shown in Figure 2a, and the results were sufficiently promising to justify the second trial, in which the 5.9 [metric] ton weight was dropped 12 m in the pattern shown in Figure 2b. Except for the first 0.6-1 m, a large improvement in penetration resistance was achieved down to the underlying clay layer. The clay layer apparently absorbed energy remarkably well and prevented deeper densification. Because the clay layer was at an even greater depth in the area to be improved, it was concluded that dynamic compaction by using the weight, drop height, and pattern shown in Figure 2b at each footing location should be satisfactory.

RESULTS OF DYNAMIC COMPACTION

A grid was outlined at each footing location and compaction was carried out. Figure 3 is typical of the results achieved. In all cases, sufficient compaction ($N \geq 15$) was obtained to the desired depth (5 m) and the footings were proportioned by using a contact pressure of 168 kPa. The warehouse has now been in service for more than two years, and measurements show that the maximum total settlement has been less than 5 mm. Area compaction of lesser intensity was applied between the footings to support the slab on ground used for the warehouse floor. Although measurements have not been made on the floor slab, it has not settled noticeably.

VIBRATION EFFECTS

Because of the possibility of further extensions to the plant, the relationship between the distance of a drop point from an existing structure and the induced vibrations was evaluated. A seismograph was placed on an exterior footing (before the columns were cast), and the 5.9-ton weight was dropped 12 m at locations 3-24 m from the footing. The frequency of vibration was approximately 7 Hz, and the measured velocities were essentially ground motions. The peak particle velocity appeared to vary inversely with the logarithm of the distance from the drop point; on a drained granular soil, particle velocities of ≤50 mm/s at a distance of 3 m from the drop point were found.

Figure 1. Typical soil boring results.

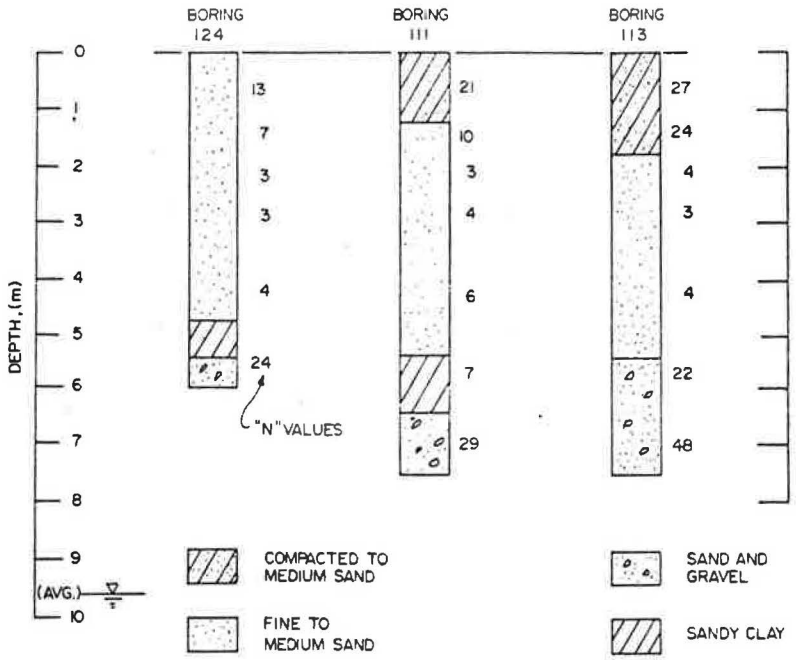

Figure 2. Number of drops and drop patterns.

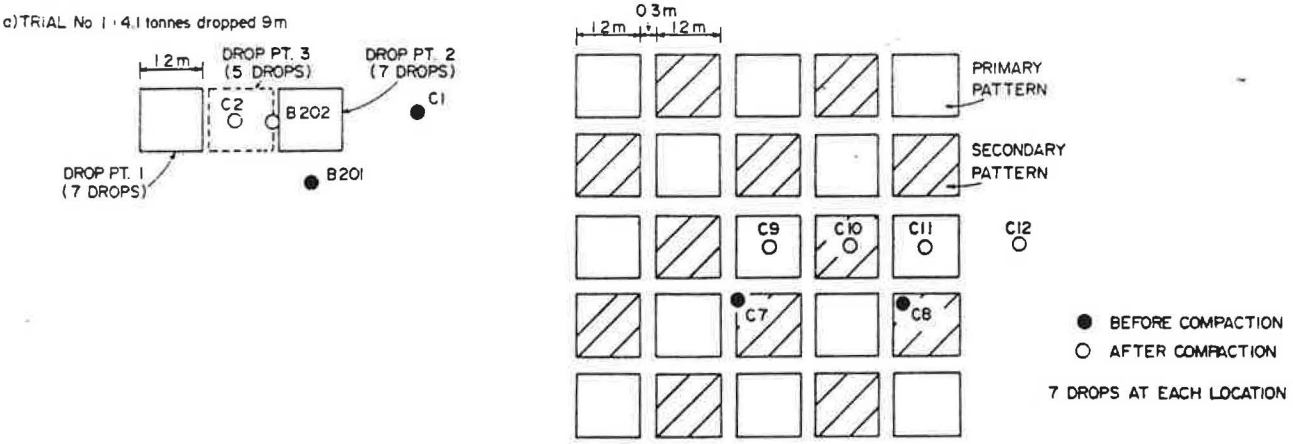

Figure 3. Relationship between cone penetration resistance and depth before and after dynamic compaction: footing H-1.

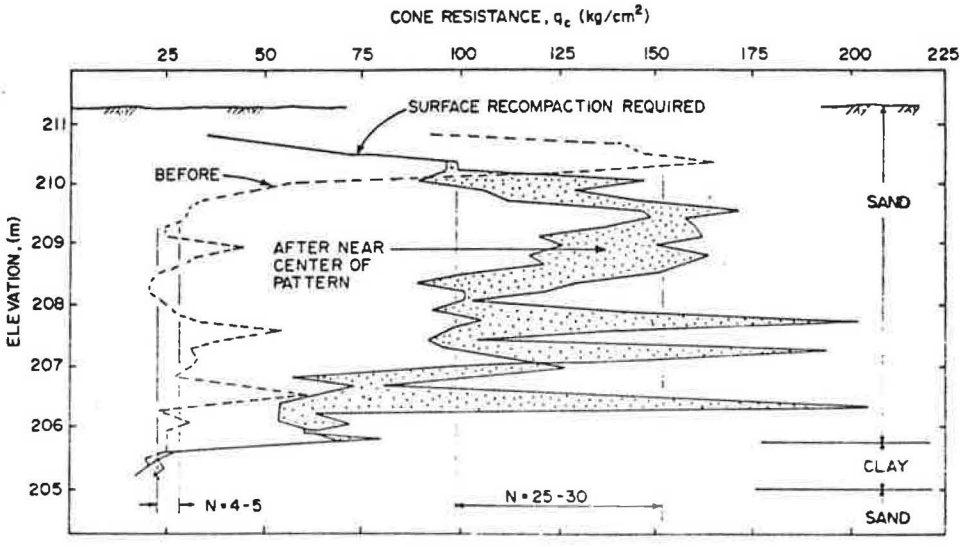

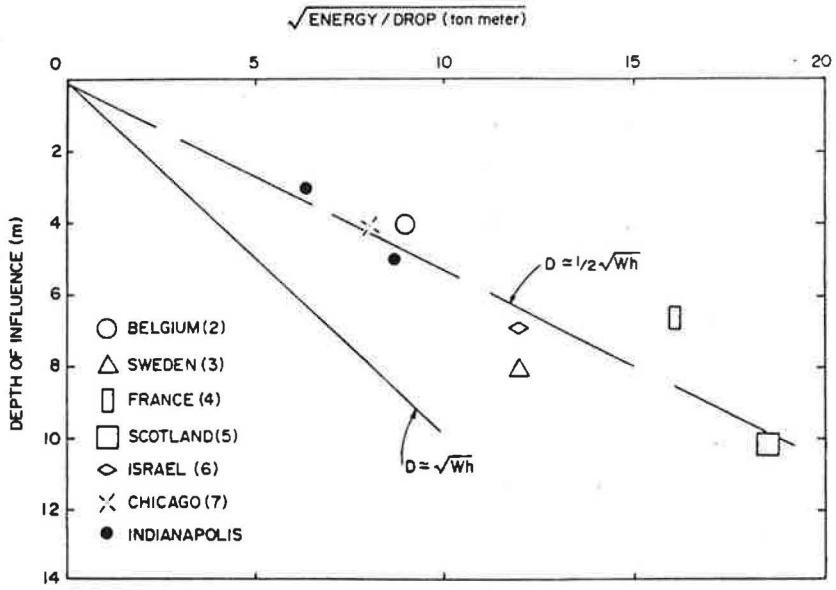

Figure 4. Relationship between depth of influence of compaction and square root of energy per drop.

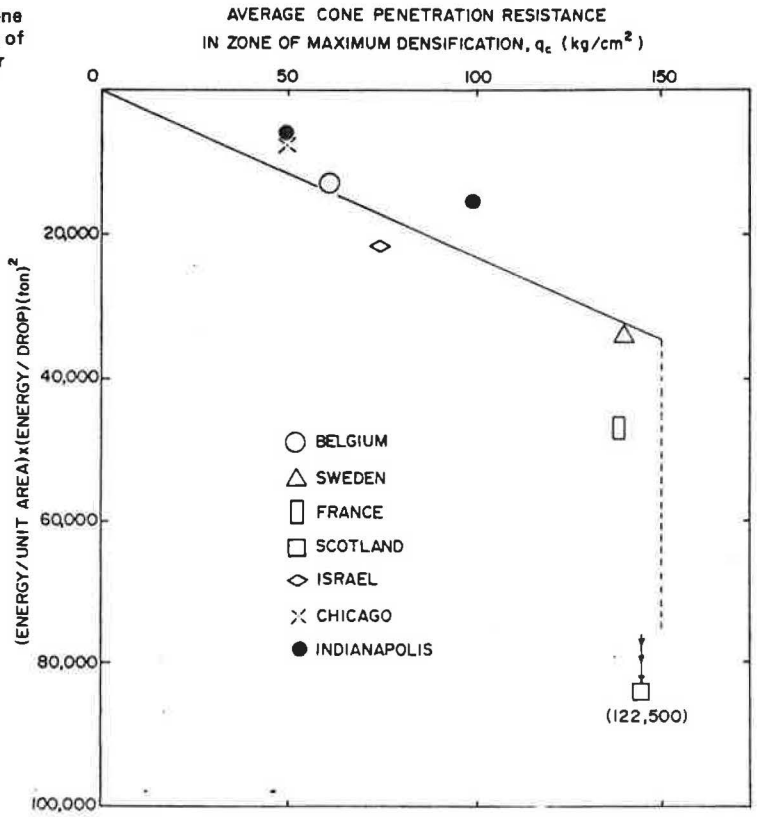

Figure 5. Relationship between cone penetration resistance and product of energy per unit area and energy per drop.

COMPARISON WITH PUBLISHED DATA

As a guide for future work, the results obtained in Indianapolis were compared with those available in the literature. Figure 4 shows the relationship between the energy per drop and the depth to which significant densification took place. A suitable criterion for the depth of influence would depend on the soil type and its initial state of compaction; for the work reported in this paper, the criterion was an increase in N-value of 3-5. A common rule of thumb (2) is expressed by the relationship

$$D \simeq (Wh)^{1/2} \quad (1)$$

where

D = depth of influence in meters,
W = falling weight in tons, and
h = height of drop in meters.

It appears, however, that the use of this rule tends to overestimate the effective depth of compaction substantially and that

$$D \simeq \tfrac{1}{2}(Wh)^{1/2} \quad (1a)$$

more nearly reflects available experience.

The degree of compaction attained depends not only

on the energy per drop but also on the sequence of drop points and the number of drops at each point. Available data from Belgium (3), Sweden (4), France (5), Scotland (6), Israel (7), and Chicago (8), as well as these, suggest that, for dry granular soils, the degree of compaction (as measured by q_c) correlates best with the product of the energy per drop and the total energy applied per unit of surface area (Figure 5). It appears that there may be an upper bound to the densification that can be achieved, corresponding approximately to $q_c = 150$ kg/cm^2, but more data are needed to verify this result.

CONCLUSIONS

1. In granular soils, the depth to which densification is significant is controlled mainly by the energy per drop: Relationship 1a given above is recommended as a guide for preliminary trials. The presence of clay layers or seams will greatly attenuate the effective depth of compaction.
2. The upper meter of soil is usually left in a relatively loose state, and surface recompaction is required.
3. For dry granular soils, the degree of compaction achieved seems to correlate best with the product of the energy per drop and the total energy applied per unit surface area. It appears that there may be an upper bound to the compaction that can be attained and that this corresponds to $q_c \simeq 150$ kg/cm^2 (N = 30-40).

REFERENCES

1. G. A. Leonards, W. A. Cutter, and R. D. Holtz. Dynamic Compaction of Granular Soils. Journal of the Geotechnical Engineering Division, Proc., ASCE, Vol. 106, No. GT1, Jan. 1980, pp. 35-44.
2. L. Menard and Y. Broise. Theoretical and Practical Aspects of Dynamic Consolidation. Géotechnique, Vol. 25, No. 1, 1975, pp. 3-18.
3. E. DeBeer and A. Van Wambeke. Consolidation Dynamique par Pilonnage Intensif, Aire d'Essai d'Embourg. Annales des Travaux Publics de Belgique, No. 5, Oct. 1973, pp. 295-318.
4. S. Hansbo, B. Pramborg, and P. O. Nordin. The Vänern Terminal: An Illustrative Example of Dynamic Consolidation of Hydraulically Placed Fill. Les Edition Sols-Soils, No. 25, 1973, pp. 5-11.
5. J. P. Gigan. Compactage par Pilonnage Intensif de Remblais de Comblement d'un Bras de Seine. Laboratoires des Ponts et Chaussées, Paris, Bull. de Liaison, Vol. 90, July-Aug. 1977, pp. 81-102.
6. J. M. West and B. E. Slocombe. Dynamic Consolidation as an Alternative Foundation. Ground Engineering, Vol. 6, No. 6, 1973, pp. 52-54.
7. D. David. Deep Compaction. D. David Engineers, Ltd., Ramat Aviv, Israel, Bull., no date.
8. R. G. Lukas. Densification of Loose Deposits by Pounding. Journal of the Geotechnical Engineering Division, Proc., ASCE, Vol. 106, No. GT4, April 1980, pp. 435-461.

Publication of this paper sponsored by Committee on Embankments and Earth Slopes.

Construction of a Root-Pile Wall at Monessen, Pennsylvania

Umakant Dash and Pier Luigi Jovino

A case history of the design, analysis, construction, and performance evaluation of a root-pile wall is presented in this paper. The root-pile wall was contracted for construction by the Pennsylvania Department of Transportation to correct a landslide near Monessen. The structure consisted of four hundred and fifty-eight 12.5-cm (5-in) diameter cast-in-place concrete piles placed at different inclinations to both the vertical and the horizontal axes. The piles were connected at the top by a 76.2-cm (30-in) thick by 1.82-m (6-ft) wide cap beam constructed in two 30.48-m (100-ft) sections. The cap beam was constructed first, and the root piles were then installed by extending drill holes through the cap beam to bedrock at predetermined locations and inclinations, inserting a single no. 9 deformed reinforcing steel bar (grade 60) into each drill hole, and grouting the holes. Nine survey targets were marked at the top of the cap beam to measure both horizontal and vertical movements and seven slope inclinometers were installed at various points both upslope and downslope from the structure to measure horizontal movements of the structure and the surrounding soil. This paper describes the soil and groundwater conditions, soil test results, slope stability analyses, design of the root-pile wall, and the findings of the horizontal and vertical measurements of wall movement. The following summary, observations, and conclusions are made: (a) a root-pile structure provides a fast and economical alternative to many conventional structures; (b) before the installation of the root piles, the movements of the cap beam varied from less than 2.5 cm (1 in) at the north end to more than 45.7 cm (18 in) at the sound end—these movements were due to movements of unstable soil in the slide area; (c) after the installation of the root piles, there were significant movements [up to 5 cm (2 in)] in the cap beam as well as in the soil below it, which indicated that some movement of the root-pile structure was needed before resistance to earth pressure could be mobilized; (d) no significant soil movement through the root piles could be detected—the small-diameter piles and the soil between them appeared to work as a single composite structure; and (e) conventional design procedures for retaining walls appear to provide adequate overall design for root-pile walls (the geometry of the root-pile structure described in this paper is patented and may not be the optimum design for all situations).

During the construction of a four-lane highway along the Monongahela River, just north of I-70, a series of landslides occurred. One of these landslides, at the northern end of the project, involved the new highway construction, as well as two water lines and a city street above the slope about 76 m (250 ft) from the northbound lanes.

A root-pile wall was designed and constructed to correct the landslide along PA-306 in Monessen, Pennsylvania. Several alternatives (such as tieback, reinforced-earth, and concrete-gravity walls) were considered, but the root-pile method of correction was

Figure 1. Cross section at center of landslide area.

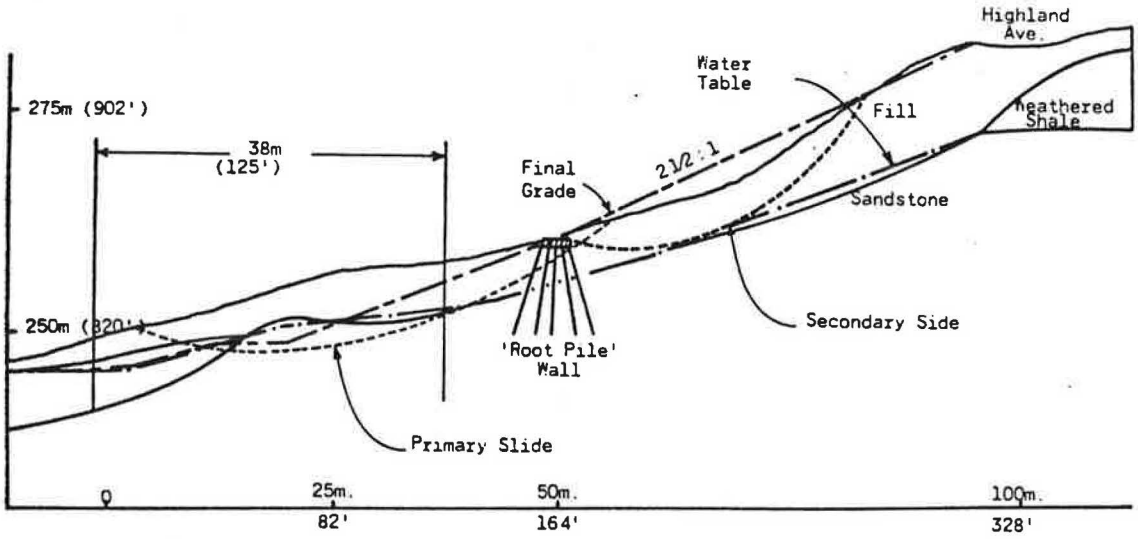

Figure 2. Aerial photograph of site.

selected because it would require the least amount of disturbance and the minimum time and have a cost comparable with that of the other systems. Another consideration in the selection decision was that this would allow evaluation of the procedure to determine its feasibility for future corrective works.

Root piles are small-diameter reinforced-concrete piles developed by the Fondedile Corporation specifically for strengthening soil or rock that is otherwise incapable of supporting its own load and/or an external load (1, 2). The method is efficient and economical and suitable for a variety of underpinning, restoration, and stabilization work.

SITE CONDITIONS

Stratigraphically, the slide area was confined to the upper portion of the Conemaugh formation of the Pennsylvania period. These strata vary from hard massive sandstone to red shales and have minor limestone interbeds. The overburden contains surface debris from mining operations, as well as foundations and other construction materials from demolished houses in the area.

A cross section at the center of the landslide area, including soil types and groundwater elevations, is shown in Figure 1. The section also shows the locations of the highway at the bottom, the root-pile wall near the middle, and the city street (Highland Avenue) near the top of the failed slope.

Figure 2 is an oblique aerial photograph taken soon after the failure and shows the general site conditions, the scarps, the acid mine-drainage channel, the location of a water pipe, and the location of the root-pile wall. The overburden soils (fill and colluvium) consisted of silty clays and clayey silts (AASHO A-6 and A-7) intermixed with rock fragments, cinders, and building materials.

The groundwater elevation varied from near the surface to about 3 m (10 ft) below the surface. Extremely wet conditions prevailed for most of the year, particularly around the acid mine-drainage channel.

SLOPE STABILITY

Slope stability analyses were performed by using a generalized soil profile and groundwater near the surface. The top and bottom scarps and the rock line were used as part of the assumed failure surface (Figure 1). Several slope-stability-analysis trials were made by using the Morgenstern-Price method and varying the effective angle of internal friction with each trial until a factor of safety nearly equal to 1.0 was obtained. The most-probable values of soil strength parameters obtained by using this method were $c = 4.79$ kPa (100 lbf/ft^2) and $\phi = 17°$. The maximum mass density (γ) [2146 kg/m^3 (134 lb/ft^3)] was obtained by using the Proctor compaction test.

DESIGN

The design of a root-pile structure involves (a) selection of the location; (b) selection of the size; (c) selection of the pile arrangement—including spacing, inclination, length, and size of the individual piles; (d) checking the loads and stresses on the individual piles; and (e) checking probable movements of the structure. The method used for the pile arrangement at present (1979) is mostly derived from experience and is patented by the Fondedile Corporation (3, 4). The effective soil parameters used in the design of the root-pile wall were those cited above.

The resultant earth pressure (P) can be calculated by using Equation 1 and Figure 3.

$$P = (\tfrac{1}{2})\gamma h^2 Ka \qquad (1)$$

Figure 3. Design of root-pile wall.

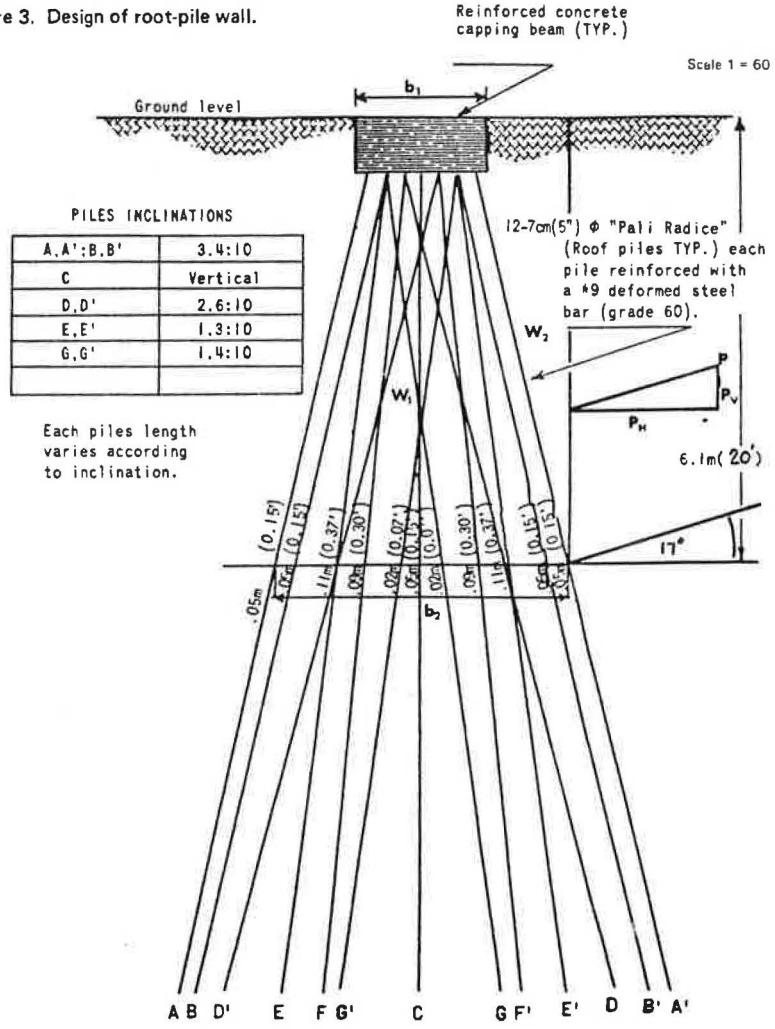

where h = height and Ka = coefficient of active earth force.

By assuming no effect of cohesion, $P = (1/2) \times 2146 \times 6.09^2 \times 0.757 = 295$ kN [66 400 lbf (66.4 kips)].

If the resultant direction is assumed to be at an angle of 17° to the horizontal, then $P_v = P \sin 17° = 86.4$ kN [19 400 lbf (19.4 kips)] and $P_H = P \cos 17° = 282.6$ kN [63 500 lbf (63.5 kips)].

The weight within the root-pile structure (W_1) is calculated by using Equation 2.

$$W_1 = \gamma h[(b_1 + b_2)/2] \quad (2)$$

where b_1 = width of cap beam and b_2 = width of root-pile structure at bedrock.

Thus, $W_1 = 2146 \times 6.09 \times [(1.82 + 3.96)/2] = 37\,778$ kg (83 112 lb) = 370.5 kN [83 300 lbf (83.3 kips)].

The weight of the soil wedge (W_2) is calculated by using Equation 3.

$$W_2 = \gamma h[(b_2 - b_1)/2] \quad (3)$$

Thus, $W_2 = 2146 \times 6.09 \times [(3.96 - 1.82)/2] = 13\,987$ kg (30 771 lb) = 137.2 kN [30 820 lbf (30.82 kips)].

The total vertical force (V) is given by Equation 4.

$$V = P_v + W_1 + W_2 \quad (4)$$

Thus, V = 86.4 + 370.5 + 137.2 = 594 kN [133 500 lbf (133.5 kips)].

The distance of the resultant (d) from "0" (Figure 3) is then $[(370.5 \times 1.98) + (137.2 \times 3.25) + (86.4 \times 3.96) - (282.6 \times 2.02)] \div (370.5 + 137.2 + 86.4) = 1.60$ m (5.24 ft)
and the eccentricity (e) is (3.96/2) - 1.60 = 0.38 m (1.25 ft).

At the base, where bedrock elevation is 6.09 m below the surface, the horizontal distances of the centers of the various root piles from the central (vertical) pile (i.e., pile C) are 0.27, 0.76, 1.16, 1.72, and 1.98 m (0.90, 2.50, 3.80, 5.65, and 6.50 ft). The corresponding numbers of piles per unit length of wall are obtained by considering a typical unit of root-pile wall (which repeats along the length of the entire structure) and dividing the total number of piles at the given distance from the center of the typical unit by the length of the typical unit (see Figure 4a) and are 0.23, 0.98, 1.21, 0.49, and 0.49/m (0.07, 0.30, 0.37, 0.15, and 0.15/ft), respectively.

The area moment of inertia (I) is $2[(0.23 \times 0.27^2) + (0.98 \times 0.76^2) + (1.21 \times 1.16^2) + (0.49 \times 1.72^2) + (0.49 \times 1.98^2)] = 11.16$ m^4 (26.8×10^6 in^4).
The total area of the root piles (A) is 2(0.23 + 0.98 + 1.21 + 0.49 + 0.49) = 6.80 m^2 (73.2 ft^2).

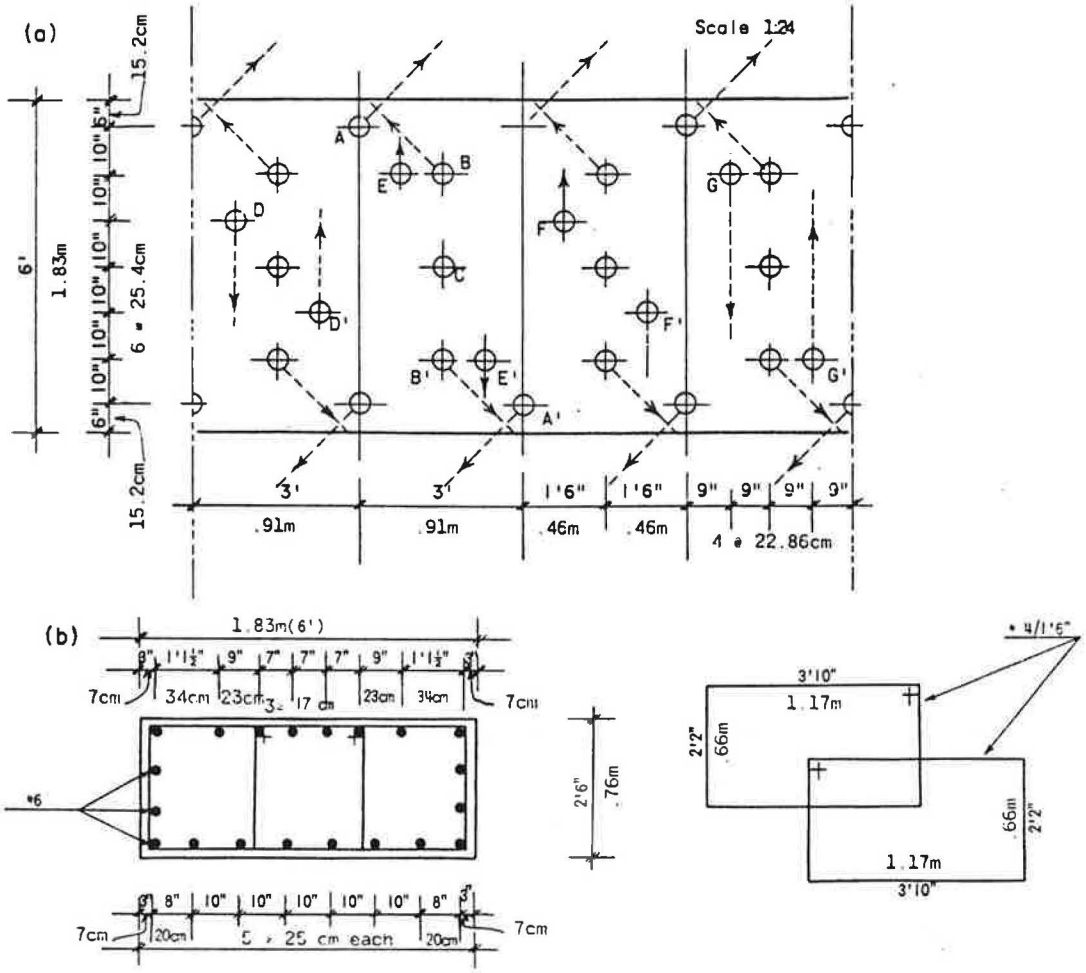

Figure 4. Cap beam: (a) pile locations and (b) reinforcement details.

Figure 5. Form work for cap beam.

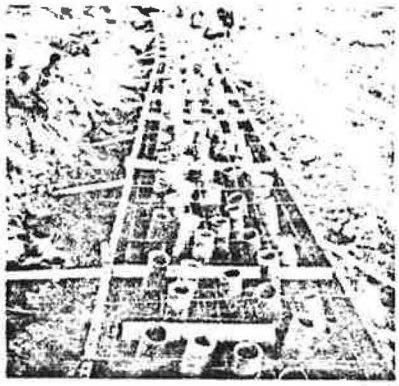

Figure 6. Drilling of holes through cap beam and preparation for grouting.

The pile loads are P_{max} = (594.0/6.80) + (594.0 × 0.38)/11.16 = 107.6 kN [24 180 lbf (24.18 kips)] and P_{min} = (594.0/6.80) - (594.0 × 0.38)/11.16 = 67.12 kN [15 090 lbf (15.09 kips)] and thus are within the allowable limits for the piles used.

For a 12.7-cm (5-in) diameter pile reinforced with a no. 9 bar, the allowable shear in concrete is 690 kPa × 126.64 cm^2 = 8.74 kN [1960 lbf (1.96 kips)],
the allowable shear in steel is 110 316 kPa × 5.09 cm^2 = 56.22 kN [12 630 lbf (12.63 kips)], and
the total allowable shear is 8.74 + 56.22 = 64.96 kN [14 600 lbf (14.60 kips)].
As the average number of piles over the length is 6.82/m (2.08/ft), the average shear resistance is 443 kN/m [13 500 lbf/ft (13.5 kips/m)].
Therefore, the factor of safety against shear is shear resistance from structure ÷ total horizontal force on structure = 443/282.6 = 1.56.

CONSTRUCTION

The construction of the root-pile wall was begun in December 1978. The cap beam was constructed in two 30.5-m (100-ft) sections (see Figure 4b). Figure 5 shows the form work for the cap beam. After the com-

pletion of the cap beam, construction was suspended during January and February 1979. There were movements of up to 46 cm (18 in) in the cap beam during this period. The holes for the vertical piles along the centerline of the cap beam were drilled first, and then the inclined holes were drilled. Most of the vertical holes were grouted before inclined holes were drilled. Figures 6 and 7 show the drilling operation, and Figures 8 and 9 show the mixing and grouting operations. The construction of the root pile was completed in April 1979.

Immediately after the holes were drilled through the cap beam, they were cleaned by using air pressure and a no. 9 reinforcing steel rod was placed in the drill hole. The grout was then poured into the hole until it was completely filled. No external pressure was applied to the grout during the grouting operation.

The grout mix consisted of 1 bag of cement, 22.7 L (6 gal) of water, and 0.071 m^3 (2.5 ft^3) of sand.

During the excavation for the northbound lanes downslope from the wall, the slope between the wall and the northbound lanes failed. This failure occurred during the second week of April 1979. Figures 10-13 show the

Figure 7. Drilling operation.

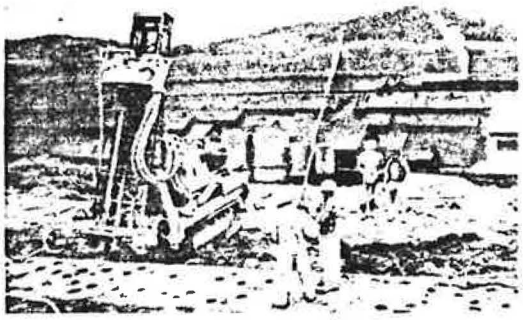

Figure 8. Mixing of grout.

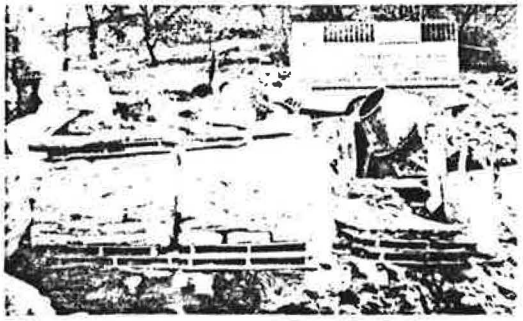

Figure 9. Grouting under gravitational pressure.

Figure 10. Soil movement during excavation downslope from root-pile wall.

Figure 11. Additional movement that broke slope inclinometer pipes below wall.

Figure 12. Broken root piles.

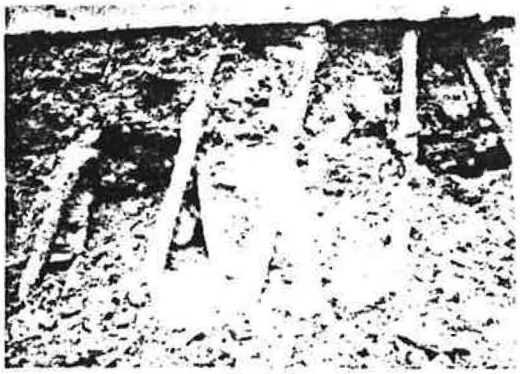

Figure 13. Testing of piles for soundness.

Figure 14. Slide conditions near large water pipe and removal of failed soil.

Figure 15. Root-pile wall after removal of downslope failed soil.

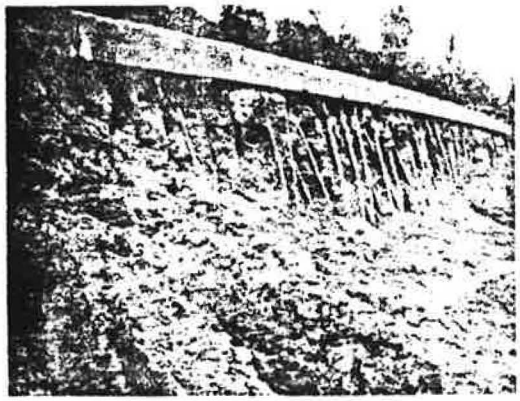

Figure 16. Completion of downslope soil removal.

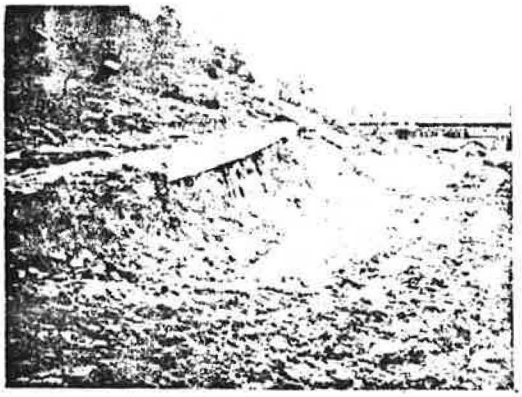

failed slope, as well as the condition of the root piles after the slope failure.

It was then decided to remove the entire failed slope in front of the root-pile wall and reconstruct the slope at a gradient of 2.5 horizontal to 1 vertical, using a well-compacted fill and a 1-m (3-ft) thick layer of granular material against the root-pile wall.

The drainage ditches were dug at right angles to the wall to drain a significant amount of the water that had ponded at the bottom of the exposed part of the wall and to serve as a permanent drainage system. Figures 14-17 show the general conditions after removal of the soil within the failed slope. Figure 18 shows the drainage ditch filled with stone.

Figure 17. General view before reconstruction.

Figure 18. Installation of drainage ditch.

Figure 19. Beginning of reconstruction.

The reconstruction work, particularly the compaction near the root-pile wall, had to be done with special care so as not to damage the piles. Figures 19-22 show the conditions during reconstruction in front of the wall.

The reconstruction work was completed in July 1979.

PERFORMANCE

The horizontal and vertical movements of the cap beam were monitored by taking survey readings at nine different points. These readings indicated that, before the installation of the root piles, the movements at the south end were about 46 cm (18 in) and those at the north end were less than 2.5 cm (1 in). The cap-beam movements ceased, however, after the installation of the root piles.

A total of eight slope inclinometers were installed—four on the downslope side and four on the upslope side

Figure 20. Placement of granular material against root-pile wall.

Figure 21. Placement of fill next to root piles.

of the cap beam. The slope inclinometers on the downslope side (nos. 2, 4, 6, and 8) were sheared off during the slope failure of April 1979. The horizontal movements recorded from slope inclinometers nos. 1, 3, 5, and 7 are shown in Figure 23.

SUMMARY

The root-pile wall at Monessen provided a positive solution to the landslide problem. The method was rapid, requiring about eight weeks of actual construction time, although the total elapsed time was about four months, due to bad weather and other circumstances. The construction required practically no removal of existing soils or structures. The drilling and grouting could be done even in wet site conditions.

The original design of 7.6 m (25 ft) for the average length of root pile had to be changed to 8.8 m (29 ft) because the depth to sound bedrock was greater than had been anticipated. This delayed the completion of the

Figure 22. Reconstructed fill in front of root-pile wall.

Figure 23. Relationship between depth and deflection: (a) slope indicator 1, (b) slope indicator 3, (c) slope indicator 5, and (d) slope indicator 7.

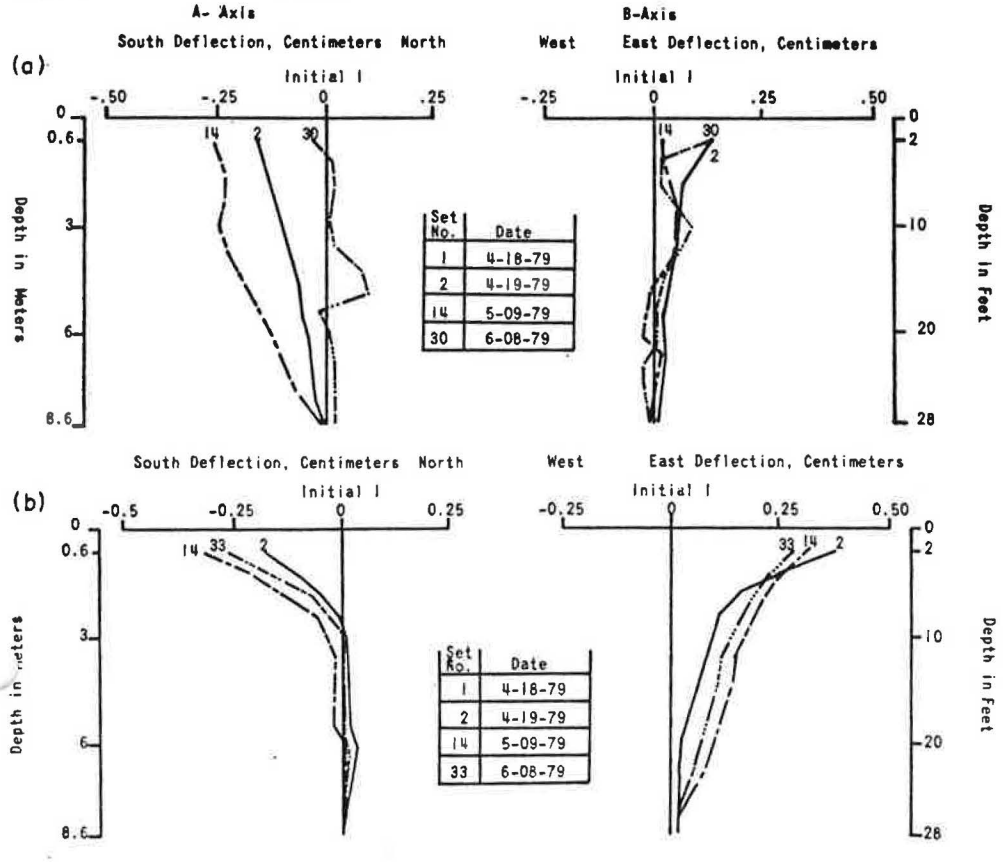

Figure 23. Continued.

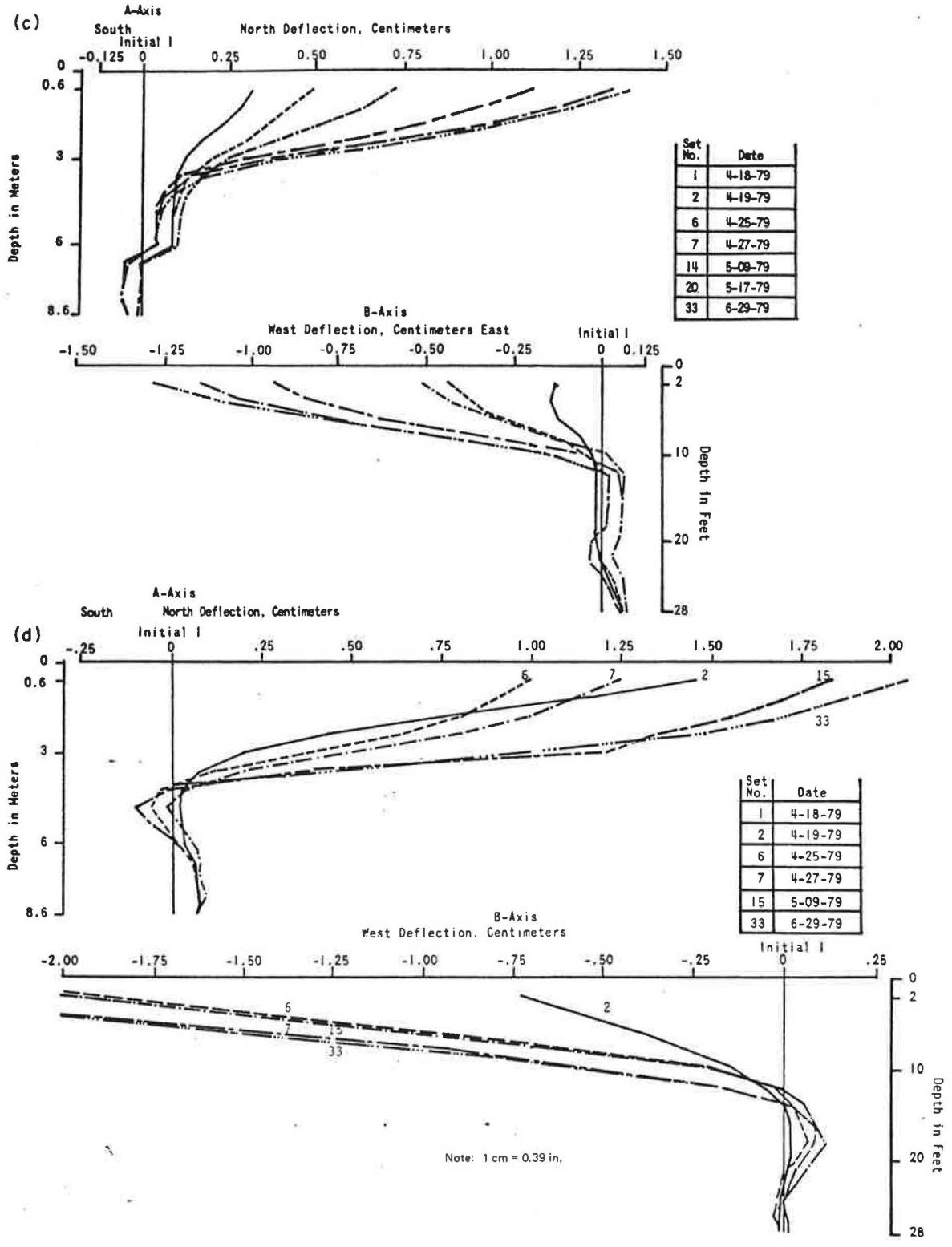

construction and increased the total cost but had little or no effect on the design. There was a time delay of about 12 weeks between the casting of the cap beam and the installation of the first series of root piles. The movements of the cap beam could have been avoided by installing the root piles soon after the cap beam was constructed. The internal design of the root-pile structures is not well understood and is primarily based on experience. The arrangement of root piles (e.g., the number, size, spacing, and inclination) is based on empirical methods. The root-pile arrangement is patented and no rational method is generally available. Therefore, the actual design factor of safety cannot easily be determined.

The external stability of the root-pile wall is analyzed by using classical methods for gravity-wall analysis. This is simplistic because it does not consider soil-

structure interaction aspects but appears, however, to be conservative.

The performance of the structure at Monessen provided a valuable test case for the adequacy of the current design practice because the structure supported the slope above it despite the unexpected slope failure below.

CONCLUSIONS AND RECOMMENDATIONS

Based on the experience with and the available structure-movement data from this project, the following conclusions are made:

1. The root-pile structure provides a fast and economical alternative to many conventional structures.
2. Before the installation of the root piles, the movements of the cap beam varied from less than 2.5 cm at the north end to more than 46 cm at the south end. These movements were due to movements of unstable soil in the slide area.
3. After the installation of the root piles, there were significant movements [up to 5 cm (2 in)] in the cap beam as well as in the soil below it. This indicates that some movement of the root-pile structure was needed before resistance to earth pressure could be mobilized.
4. No significant soil movement through the root piles could be detected; i.e., the small-diameter piles and the soil between them appeared to work as a single composite structure.
5. The construction of the root-pile wall was rapid and caused little or no disturbance to the existing terrain.
6. Conventional design procedures for retaining walls appear to provide overall design for root-pile walls. The geometry of the root-pile structure described in this paper is patented and may not be the optimum design for all situations. Therefore, the design procedure for the geometry and size of the individual piles within the root-pile structure should be investigated further. A rational method, one that considers soil-structure interaction, should be developed for the design of root-pile structures and verified by using actual field measurements of prototype construction.
7. There should be more test cases of root-pile construction; the instrumentation should be adequate to measure loads and movements so that the design methods can be evaluated.

ACKNOWLEDGMENT

The construction of this root pile was carried out under the supervision of Engineering District 12 of the Pennsylvania Department of Transportation. William R. Galanko and William T. Mesaros of the district provided assistance throughout the duration of the project. The help of Donald L. Keller, Phillip E. Butler, Kenneth J. Rush, and others in the Bureau of Materials, Testing, and Research is appreciated. We also thank the Ram Construction Company, the general contractor for the project, and the Fondedile Corporation of Boston, Massachusetts, who did most of the root-pile wall construction work.

REFERENCES

1. F. Lizzi. Special Patented Systems of Underpinning and Root Piles with Special Reference to Problems Arising from the Construction of Subways in Built-up Areas. Fondedile Corp., Boston, MA, 1972.
2. Fondedile System. Fondedile Corp., Boston, MA, no date.
3. F.A. Bares. Use of Pali Radice (Root Piles) for the Solution of Difficult Foundation Problems. Presented at ASCE Transportation Engineering Meeting, Montreal, July 1974, Preprint MTL-41.
4. Fondedile Corp. Root-Pattern Piles Underpinning. Proc., Symposium on Bearing Capacity of Piles, Central Building Research Institute, Roorkee, India, Feb. 1964.

Publication of this paper sponsored by Committee on Embankments and Earth Slopes.

Analysis of an Earth-Reinforcing System for Deep Excavation

S. Bang, C. K. Shen, and K. M. Romstad

A limit-analysis procedure for a reinforced lateral earth support system is described. The system is composed of a wire-mesh-reinforced shotcrete panel facing, an array of reinforced anchors grouted into the soil mass, and rows of reinforcing bars that form horizontal wales at each anchor level. Excavation starts from the ground level and, after each layer, reinforcement is applied immediately on the exposed surface and into the native soil. This system thus forms a temporary earth support that has the advantages of requiring no pile driving, not loosening or sloughing the soil, and providing an obstruction-free site for foundation work. It has been successfully used for large areas of excavation to depths of up to 18 m in various ground conditions. However, in the past, no rational and proven analytical design procedure was available, a problem that resulted in considerable reservation toward the use of the system among engineers and contractors. The two-dimensional plane-strain limit-analysis formulation includes consideration of design parameters such as soils type, depth of excavation, length of the reinforcing members, inclination, and spacing. The analysis procedure can be used to evaluate the overall stability of the system and to determine the proper size, spacings, and length of the reinforcement for a given site condition.

In recent years, underground construction has been widely used as a logical part of the solution to many urban and city problems. Sewer and water conduits and other utility lines are usually installed underground in large cities, and vehicular tunnels and underground stations can decrease both intracity and intercity traffic congestion and thus improve both air quality and traffic safety. Even more important is that increased underground building construction is a desirable alternative that saves energy. To meet the challenge of increasing

demand, it is imperative that effective, economical, and safe underground excavation technology be developed.

This paper describes a limit-analysis procedure for a relatively new, reinforced lateral earth support system for deep excavation. This system has been used in Vancouver, British Columbia, in Edmonton, Alberta, and more recently in Portland, Oregon (1), to depths up to 18 m. Varying ground conditions have been encountered, including sandy and clayey fills, glacial tills, sandy and silty alluvial deposits, and very soft weathered rocks. The advantages of this system over those of conventional, temporary lateral earth support systems have been reported elsewhere (2, 3). Although the cost of construction is comparable to that of conventional systems, the time required to complete an excavation job can be decreased by 30-50 percent if the new system is used.

Briefly, the system is composed of a 0.1-m-thick, wire-mesh-reinforced shotcrete panel facing; an array of reinforcing members spaced 0.9-1.8 m apart and grouted into the soil mass; and rows of four no. 4 reinforcing bars forming horizontal wales at each anchor level (see Figure 1). Excavation starts at the ground level and, after each layer, reinforcement is applied immediately on the exposed surface and into the native soil. The system offers an unusual way to form a temporary earth support and has the advantages of requiring no pile driving, not loosening or sloughing the soil, and providing an obstruction-free site for foundation work.

BACKGROUND

Designs for and analyses of this system have usually assumed the classical Rankine's active failure wedge, and the spacing and length of the reinforcing members have been determined by using a procedure similar to the conventional tied-back anchor system design. However, there are some fundamental behavioral differences between the nature of this system and that of other lateral earth support systems. Conventional systems are designed to retain the soil adjacent to a vertical cut,

Figure 1. Typical cross section.

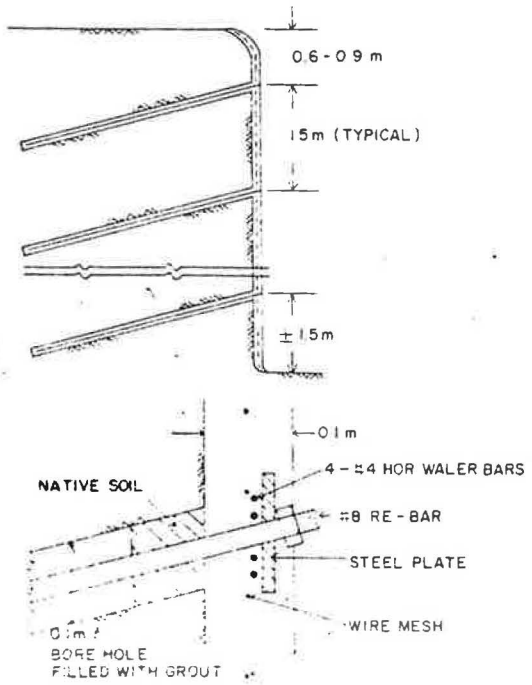

whereas this system is based on strengthening the adjacent native soil so that the system itself can withstand a vertical cut to a depth that normally requires the installation of lateral support. Furthermore, the strengthened soil mass develops its strength through a network of closely spaced reinforcing members that are grouted into the soil. This system can be viewed as a reinforced-earth retaining wall having adequate strength and stability to contain the movement of soil masses both within and behind it.

A simple design method for reinforced-earth walls has been suggested by Lee and others (4) based on the assumption that the classical Rankine's plane failure surface passes through the toe of the wall facing at an angle of $[45 + (\phi/2)]°$ to the horizontal. A similar assumption is made in the method proposed by Holm and Bergdahl (5), which takes into consideration a failure plane having different inclinations and points of intersection with the wall facing.

Although the classical plane failure-surface assumption simplifies the analysis procedure, it is highly unlikely that the failure surface of an adequately designed reinforced-earth wall would give a triangular failure wedge. Laboratory-model tests of reinforced-earth walls (6, 7) have indicated that their failure surfaces are curved and cannot be effectively represented by the conventional plane failure-surface assumption.

Romstad and others (8) approached the design of a reinforced-earth wall by hypothesizing that the failure surface will consist of two planes having a transition at the back edge of the reinforcing strips when it extends beyond the reinforced-earth zone or will be a plane through the toe of the wall when it lies entirely within the reinforced zone.

A similar approach has been used by Smith and Wroth (7). Their hypothesized failure surface is the same as that suggested by Romstad and others. They assume that the resultant of the earth pressure developed between the reinforced and the unreinforced soil blocks forms an angle ϕ to the horizontal. The overall stability of the wall is then evaluated by comparing the strip force calculated from the force equilibrium of the reinforced block with the total frictional force calculated from the overburden and the effective strip legnth beyond the assumed failure surface. The disadvantage of this approach is that the factor of safety calculated for a stable reinforced-earth wall is highly unconservative because full friction is assumed to be developed at all times. Therefore, the results are valid only when the wall is on the verge of failure.

LIMIT ANALYSIS AT EQUILIBRIUM

To date, there have been no prototype failure studies of this new lateral earth support system. Other indirect methods, therefore, must be used to approximate the failure mechanism. As shown in Figure 2, contours of factors of safety can be obtained by a finite-element analysis of the system (9) and, thus, a potential failure surface can be approximated; this potential failure surface passes more or less through the toe of the wall to form a curved surface. As discussed above, most of the proposed design methods for reinforced earth walls (7, 8) approximate this curved failure surface by two planes that have an abrupt change of direction at the back of the reinforced zone. In this analysis, however, it is assumed that the failure surface is more appropriately represented by a parabolic curve passing through the toe of the wall. The parabola can intersect the ground surface at any point by changing the value of "a", as shown in Figure 3. The potential failure surface is then the parabola that has the lowest overall factor of

Figure 2. Factor-of-safety contours determined by finite-element analysis.

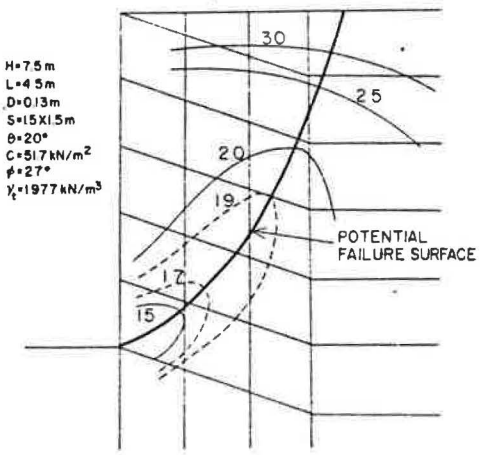

Figure 3. Postulated failure surface: general case.

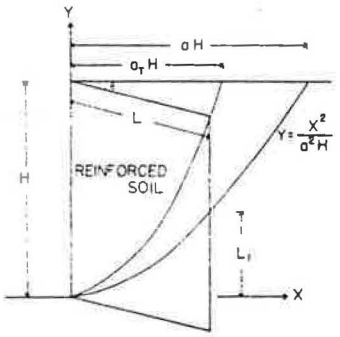

Figure 4. Postulated failure surface: (a) case 1 ($a > a_T$) and (b) case 2 ($a < a_T$).

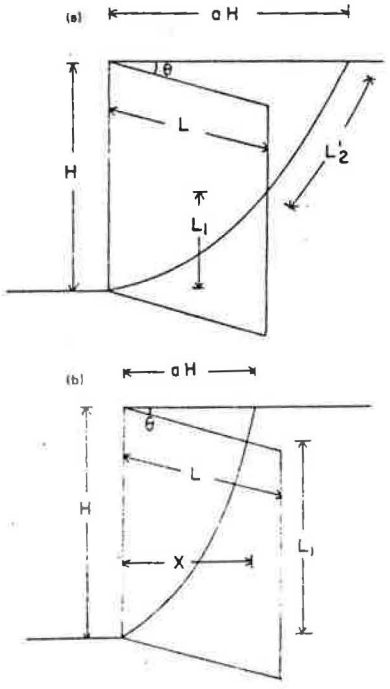

safety. Two cases must be considered separately: case 1 in which the failure surface extends beyond the reinforced zone and case 2 in which the failure surface lies entirely within the reinforced soil mass (see Figure 4).

Figure 5. Free-body diagram.

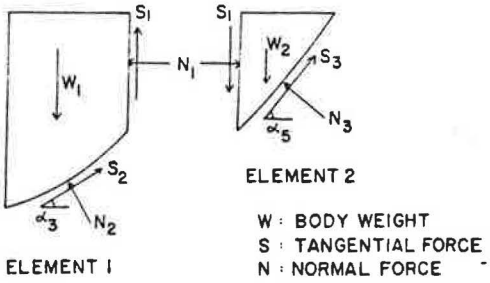

Case 1: $a \geq a_T$

Figure 5 shows the free-body diagrams of the reinforced soil block (element 1) and the unreinforced soil block (element 2). The directions of the tangential forces acting along the bottom of each element, S_2 and S_3, are assumed to be parallel to the corresponding chords, i.e.,

$$\alpha_3 = \tan^{-1}(L_1/L\cos\theta) \quad (1a)$$

$$\alpha_5 = \tan^{-1}(H - L_1)/(aH - L\cos\theta) \quad (1b)$$

where

$$L_1 = y|_{x = L\cos\theta} = L^2\cos^2\theta/a^2H \quad (2)$$

The equilibrium equations of element 1 are thus

$$N_2 = (W_1 - S_1)\cos\alpha_3 - N_1\sin\alpha_3 \quad (3)$$

$$S_2 = (W_1 - S_1)\sin\alpha_3 + N_1\sin\alpha_3 \quad (4)$$

where

$$W_1 = HL\gamma\cos\theta - \int_0^{L\cos\theta} (x^2/a^2H)\gamma\,dx$$

$$= \gamma\,[HL\cos\theta - (L^3\cos^3\theta/3a^2H)] \quad (5)$$

$S_1 = \beta N_1$ (i.e., β = ratio of S_1 to N_1),
$N_1 = \frac{1}{2}K\gamma(H - L_1)^2$,
α = unit weight of soil, and
K = stress (σ) ratio = σ_h/σ_v.

The equilibrium of element 2 is expressed by

$$N_3 = (W_2 + S_1)\cos\alpha_5 + N_1\sin\alpha_5 \quad (6)$$

$$S_3 = (W_2 + S_1)\sin\alpha_5 - N_1\cos\alpha_5 \quad (7)$$

where

$$W_2 = \gamma\,[H(aH - L\cos\theta) - \int_{L\cos\theta}^{aH} (x^2/a^2H)\,dx] \quad (8)$$

Therefore, the total driving force (S_D) along the assumed failure surface is

$$S_D = S_2 + S_3 = (W_1 - S_1)\sin\alpha_3 + (W_2 + S_1)\sin\alpha_5 + N_1(\cos\alpha_3 - \cos\alpha_5) \quad (9)$$

The total resisting force (S_r) along the failure surface can be expressed as

$$S_r = C'L_2 + N_3\tan\phi_2' + N_2'\tan\phi_1' + T_T \quad (10)$$

where

C' = developed cohesion,
ϕ'_1 = developed friction angle for element 1,
ϕ'_2 = developed friction angle for element 2,
$N'_2 = N_2 + T_N$,
T_N = normal component of the resultant of the axial force in the reinforcing members $= \Sigma T_i \cos(90 - \alpha_3 - \theta)$,
T_T = tangential component of the resultant of the axial force in the reinforcing members $= \Sigma T_i \sin(90 - \alpha_3 - \theta)$,
ΣT_i = resultant of the axial force in the reinforcing members behind the assumed failure surface (this calculation is described below), and
L_2 = length of the entire failure arc, i.e.,

$$L_2 = \int_0^{aH} [1 + (dy/dx)^2]^{1/2} dx$$
$$= (H/2)(a^2 + 4)^{1/2} (a^2H/4) \ln |[2 + (a^2 + 4)]/a^{1/2}| \quad (11)$$

The coefficient β, the ratio between the normal force and the tangential force at the interface of element 1 and element 2, can then be obtained from the equilibrium of element 2. The driving force in element 2 is S_3, and the resisting force can be obtained by using Coulomb's equation.

$$S_3 = C'L'_2 + N_3 \tan \phi'_2 = (W_2 + S_1)\sin\alpha_5 - N_1 \cos\alpha_5 \quad (12)$$

where L'_2 = length along the failure arc of element 2, i.e.,

$$L'_2 = \int_{L\cos\theta}^{aH} [1 + (dy/dx)^2]^{1/2} dx$$
$$= (H/2)(a^2 + 4)^{1/2} - (L\cos\theta/2a^2H)(a^4H^2 + 4L^2\cos^2\theta)^{1/2} - -$$
$$+ (a^2 H/4) \ln |[2aH + aH(a^2 + 4)^{1/2}]/[2L\cos\theta + (a^4H^2 + 4L^2\cos^2\theta)^{1/2}]| \quad (13)$$

Therefore

$$\beta = 2[C'L'_2 + W_2(\cos\alpha_5 \tan\phi' - \sin\alpha_5) + N_1(\cos\alpha_5 + \sin\alpha_5 \tan\phi')]$$
$$\div K\gamma(H - L_1)^2 (\sin\alpha_5 - \cos\alpha_5 \tan\phi') \quad (14)$$

Because S_1 cannot be greater than $N_1 \tan\phi'$, β must be less than $\tan\phi'$, (i.e., if $\beta < \tan\phi'$, $\beta = \beta$ and if $\beta \geq \tan\phi'$, $\beta = \tan\phi'$).

Case 2: $a < a_T$

A similar expression can be derived for the case in which the failure surface lies entirely within the reinforced soil mass, i.e., when $a < a_T$. For this case,

$$\alpha_3 = \tan^{-1}(L_1/x) \quad (15a)$$

$$\alpha_5 = \tan^{-1}[x \tan\phi/(aH - x)] \quad (15b)$$

The total driving force and the total resisting force developed along the assumed failure surface are expressed in the same manner as for the case in which $a \geq a_T$. The equilibrium equation of element 2 is again used to obtain the ratio (β) between the normal and tangential forces at the interface of element 1 and element 2.

$$\beta = 2[C'L'_2 + W_2(\cos\alpha_5 \tan\phi' - \sin\alpha_5) + N_1(\cos\alpha_5 + \sin\alpha_5 \tan\phi')]$$
$$\div K\gamma(x \tan\theta)^2 (\sin\alpha_5 - \cos\alpha_5 \tan\phi') \quad (16)$$

where

$$L'_2 = \int_x^{aH} [1 + (dy/dx)^2]^{1/2} dx$$
$$= (H/2)(a^2 + 4)^{1/2} + (x/2a^2H)/(a^4H^2 + 4x^2)^{1/2}$$
$$+ (a^2H/4) \ln |[2aH + aH(a^2 + 4)^{1/2}]/[2x + (a^4H^2 + 4x^2)^{1/2}]| \quad (17)$$

$$W_2 = H(aH - x)\gamma - \int_x^{aH} (x^2/a^2H)\gamma dx$$
$$= \gamma[(2aH^2/3) + (x^3/2a^2H) - Hx] \quad (18)$$

$$N_1 = (K\gamma/2)(x \tan\theta)^2 \quad (19)$$

Calculation of Resultant Force in Reinforcing Members

The resultant force of the reinforcing members, ΣT_i, is the sum of the forces of the individual members. Each force is obtained by calculating the frictional resistance of the portion of the member (its effective length) behind the assumed failure surface. The frictional resistance is the shear stress developed between the reinforcing member and the surrounding soil, i.e.,

$$T_i = \pi D l_i (\tau_{ns} + C')/S_H \quad (20)$$

where

l_i = effective length of the reinforcing member,
τ_{ns} = shear stress $= \sigma_n \tan\phi'$,
$\tan\phi'$ = developed frictional coefficient,
σ_n = normal stress,
S_H = horizontal spacing of reinforcement,
C' = developed cohesion = C/FS, and
FS = overall factor of safety.

This frictional resistance of each reinforcing member must be smaller than the yield strength of the member; i.e.,

$$T_i < A_s f_y / S_H \quad (21)$$

where A_s = cross-sectional area of reinforcement and f_y = yield stress of reinforcement. From the theory of elasticity,

$$\sigma_n = \sigma_x \sin^2\theta + \sigma_y \cos^2\theta + \tau_{xy} \sin 2\theta \quad (22a)$$

and

$$\tau_{ns} = -\tau_{xy}\cos 2\theta + (1/2)(\sigma_y - \sigma_x)\sin 2\theta = \sigma_n \tan\phi' \quad (22b)$$

Therefore,

$$\tau_{xy} = (1/\cos 2\theta)[(1/2)(\sigma_y - \sigma_x)\sin 2\theta - \sigma_n \tan\phi'] \quad (23)$$

and

$$\sigma_n = \sigma_x \sin^2\theta + \sigma_y \cos^2\theta + \tan 2\theta\,[(1/2)(\sigma_y - \sigma_x)\sin 2\theta$$
$$- \sigma_n \tan\phi'] = (\sigma_y \cos^2\theta - \sigma_x \sin^2\theta)/(\cos 2\theta$$
$$+ \sin 2\theta \tan\phi') \quad (24)$$

where

$\sigma_y = \gamma \bar{Z}_1$,
$\sigma_x = K\sigma_y$, and
$\bar{Z}_1 = Z_1 + (L\cos\theta - x_1)(\tan\theta/2)$
= distance from the ground surface to the center of the effective length (see Figure 6).

Figure 6. Calculation of effective length of reinforcing members.

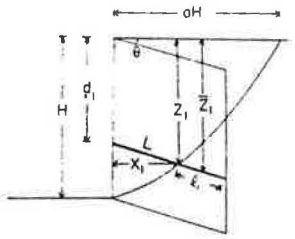

$d_i = S_v \cdot i - S_v/2 \quad (i = 1, \ldots, N)$
S_v = Vertical Spacing
N = Number of Reinforcing Members
$\ell_i = L - X_i / \cos\theta$

$$X_i = \frac{-\tan\theta + \sqrt{\tan^2\theta + 4(H - d_i)/(\alpha^2 H)}}{2/(\alpha^2 H)}$$

$Z_i = H - X_i^2/(\alpha^2 H)$
$\bar{Z}_i = Z_i + (L\cos\theta - X_i)\tan\theta/2$

Figure 7. Typical results of limit analysis.

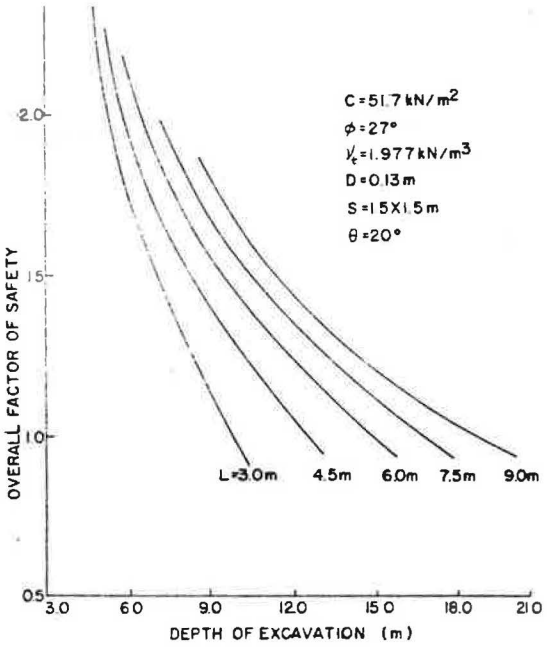

Because the reinforcing members are installed after the excavation, the lower-most member is not considered when the depth of excavation (H) is an exact multiple of the vertical spacing (S_v) of the reinforcement. If the depth of excavation is not an exact multiple of the vertical spacing, the number of reinforcing members is assumed to be the integer portion of the H/S_v ratio.

EVALUATION OF OVERALL STABILITY

The overall stability of the excavation system can be evaluated in terms of Equations 9 and 10. At any stage, the driving force and the resisting force developed along the assumed failure surface must be in equilibrium, i.e.,

$$S_D = S_F \tag{25}$$

The overall factor of safety (FS) is the factor of safety when

$$FS_C = FS_\phi = FS \tag{26}$$

where

FS_c = factor of safety with respect to cohesion and
FS_ϕ = factor of safety with respect to friction.

The factor of safety with respect to cohesion (or with respect to friction) is the ratio between the available cohesion (friction) and the developed cohesion (friction), i.e., $C' = C/FS$ and $\tan\phi' = \tan(\phi/FS)$ (if $\phi_1' = \phi_2'$). Because these equations are tedious and because both the driving-force and the resisting-force expressions contain a variable FS term, direct solution is not possible. Therefore, an iterative method was used to calculate the overall factor of safety. The iteration begins by assuming that $FS_c = FS_\phi = L/H$ and then calculates S_D and S_F.

A computer program was developed to calculate this overall factor of safety. For a given set of geometric and strength parameters, this program calculates the minimum factor of safety by searching a series of potential failure surfaces passing through the toe of the wall. A typical result of this limit equilibrium analysis for a soil having C = 51.7 kPa and $\phi = 27°$ is shown in Figure 7. The spacings and diameter of the reinforcing members are 1.5x1.5 m and 0.13 m, respectively. The angle of inclination is 20° to the horizontal. The effect of the length of the reinforcing members on the overall stability is shown by the steepness of the curves; the shorter the members, the steeper the curve. For a given depth of excavation, the increase in the factor of safety with increasing reinforcing length is greater when the members are relatively short. For instance, at an excavation depth of 9.0 m, the overall factor of safety increases by 0.35 when the length of the reinforcement increases from 3 to 4.5 m but by only 0.1 when the length of reinforcement increases from 4.5 to 6.0 m. This figure can be used as a stability design chart for calculation of the necessary length of the reinforcing members for a given depth of excavation. It can also be used as a stability analysis chart for estimation of the overall factor of safety of an existing system. Similar charts for different geometries of reinforcement and/or different types of soil can be developed.

DISCUSSION AND CONCLUSION

The currently available limit-analysis methods (7, 8) for reinforced-earth walls are based on a failure surface consisting of two planes having abrupt changes at the back of the reinforced zone. Because a real failure surface is more likely to be a continuous surface, this analysis uses a parabolic curve to represent the failure surface. The potential failure surfaces predicted by the finite-element analysis and by the limit analysis are compared in Figure 8. The agreement between these two predicted curves is excellent.

Recently, the failure of this system (10) was studied by means of centrifuge model tests. Soil displacements were measured in the model, and maximum shear strain contours were plotted as shown in Figure 9, in which the shaded area indicates the potential failure zone. A limit analysis was also performed for this model, and the shape of the parabolic curve having a factor of safety of 1.0 was computed and plotted on the same figure. That this curve in large portion lies within the potential failure zone strongly supports the validity of the limit-analysis formulation.

The results of the limit analysis were also compared, for a particular example, with the works of Lee and others (4) and Romstad and others (8) (which hypothesize single- and double-plane failure surfaces, respectively). The properties of the example used and the critical

Figure 8. Comparison of predicted potential failure surfaces.

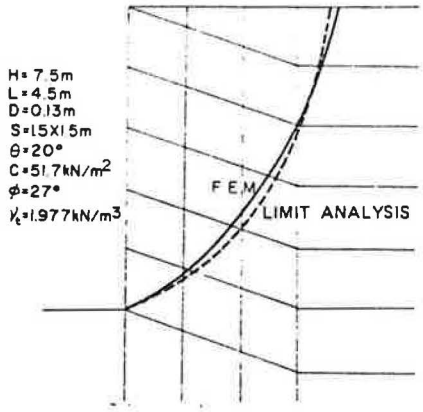

Figure 9. Maximum shear strain contour of centrifuge model at failure.

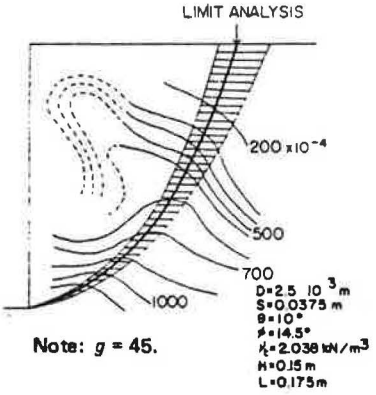

heights of the wall calculated by each method are summarized below:

Property	Value
Cohesion (kPa)	0
Friction (°)	36
Unit weight of soil (kN/m³)	1.96
Diameter of reinforcing bars (cm)	2.5
Surface area of reinforcing bars (m²/m)	0.13
Spacing of reinforcing bars (cm x cm)	60 x 60

	Critical Height (m)	
Failure Surface	L = 9 m	L = 10.5 m
Single plane	12.3	15.3
Double plane	18.6	19.8
Parabolic	15.0	16.5

The method proposed by Lee and others predicts the lowest values because it does not consider the development of frictional resistance along the hypothesized failure surface. The double-plane failure-surface assumption predicts the highest critical heights because of the formation of the acute angle near the toe of the wall. The parabolic failure-surface assumption predicts intermediate values (see Figure 10). The differences between the critical heights predicted by either the single- or the double-plane failure-surface assumptions and those predicted by the parabolic failure-surface assumption are approximately 10-25 percent. The less the amount of reinforcement, the larger the difference.

Thus, the proposed limit-analysis method provides a rigorous treatment for the design of a reinforced lateral earth support system for deep excavation.

Figure 10. Comparison of predicted failure heights and surfaces.

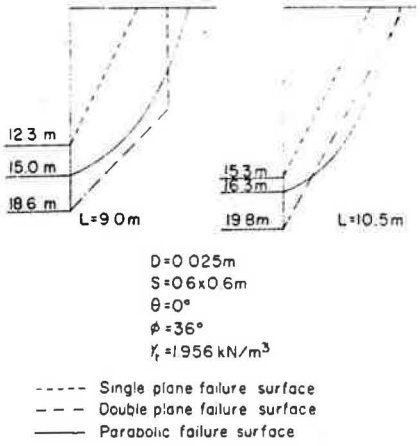

ACKNOWLEDGMENT

The research reported in this paper was supported by a National Science Foundation grant. We are grateful for this support.

REFERENCES

1. Sprayed Concrete Wall Cuts Overall Costs by 30 Percent on Underpinning and Shoring. Engineering News Record, Aug. 1976.
2. S. Bang. Analysis and Design of Lateral Earth Support System. Department of Civil Engineering, Univ. of California, Davis, Ph.D. thesis, Sept. 1979.
3. C. K. Shen, S. Bang, L. R. Herrmann, and K. M. Romstad. A Reinforced Lateral Earth Support System. Paper presented at ASCE Spring Convention and Exhibit, Pittsburgh, PA, April 1978.
4. K. L. Lee, B. D. Adams, and J. J. Vagneron. Reinforced Earth Retaining Walls. Journal of the Soil Mechanics Division, Proc., ASCE, Vol. 99, No. SM 10, Oct. 1973.
5. G. Holm and U. Bergdahl. Fabric Reinforced Earth Retaining Walls: Results of Model Tests. Proc., International Conference on Soil Reinforcement, Tokyo, Japan, Vol. 1, March 1979.
6. P. M. Petrick. Laboratory Study of Tensions in Slabs and Deformations of Reinforced Earth Works. Proc., International Conference on Soil Reinforcement, Tokyo, Japan, Vol. 1, March 1979.
7. A. Smith and C. P. Wroth. The Failure of Model Reinforced Earth Walls. Paper presented at ASCE Spring Convention and Exhibit, Pittsburgh, PA, April 1978.
8. K. M. Romstad, Z. Al-Yassin, L. R. Herrmann, and C. K. Shen. Stability Analysis of Reinforced Earth Retaining Structures. Paper presented at ASCE Spring Convention and Exhibit, Pittsburgh, PA, April 1978.
9. L. R. Herrmann. User's Manual for Reinforced Earth Analysis. Department of Civil Engineering, Univ. of California, Davis, Jan. 1978.
10. C. K. Shen, Y. S. Kim, S. Bang, and J. F. Mitchell. Centrifuge Modeling of a Lateral Earth Support. Paper presented at ASCE Fall Convention and Exhibit, Atlanta, GA, Oct. 1979.

Publication of this paper sponsored by Committee on Embankments and Earth Slopes.

Design and Construction of Fabric-Reinforced Embankment Test Section at Pinto Pass, Mobile, Alabama

T. Allan Haliburton, Jack Fowler, and J. Patrick Langan

A 244-m (800-ft) long sand embankment test section was successfully constructed on a very soft foundation at Mobile, Alabama, to verify the concept that a geotechnical fabric can be used as tensile reinforcement and to gain the experience needed to construct an additional 1280 m (4200 ft) of embankment. Based on expected behavior, criteria for fabric selection and special construction sequences were developed. Instrumentation was installed in the test section to evaluate embankment, fabric, and foundation behavior. Construction was accomplished by low-ground-pressure dozers. Conventional dump trucks were used to haul the embankment fill. Several different fabric-placement schemes were evaluated. The embankment was constructed to design elevation without failure and, despite foundation pore-pressure levels that exceeded the height of the embankment, the bearing displacements and consolidation settlements were relatively small. The concept was found to be a technically feasible, operationally practical, and cost-effective method for rapid construction of embankments at locations where an unreinforced embankment would fail.

In a study concerning the use of Pinto Island, Mobile Harbor, Alabama, as a long-term confined disposal area to contain fine-grained maintenance dredging from the harbor (1), it was found that site feasibility was contingent on the ability to construct approximately 457 linear m (5000 linear ft) of retaining embankment across both ends and along the south shore of Pinto Pass, a sedimented channel used in the Civil War period for access to the harbor. A highly variable alluvial soil profile existed along the proposed dike alignment, and approximately 50 percent of the alignment was in the intertidal zone and had water depths of 0.2-0.5 m (0.5-1.5 ft) under mean tidal [El. 0 m (mean sea level)] conditions. Geotechnical exploration was limited by the generally soft surface conditions, which restricted equipment mobility, but the data obtained indicated that the foundation soils consisted of very soft, highly plastic clays and loose clayey fine sands and silts to a depth of approximately 12 m (40 ft) below the ground surface, where dense clean sand was encountered. The unconsolidated, undrained shear strength of the cohesive materials was 2.4-7.2 kPa (50-150 lbf/ft^2), and standard penetration test N-values were 0-5 along much of the alignment.

A multipurpose embankment was required, first to El. 2.4 m (8 ft) for initial containment and then to act as a preload fill to increase the foundation strength for further periodic embankment raising to El. 7.6 m (25 ft) during the next 20 years.

BASIS FOR USE OF FABRIC REINFORCEMENT

Initial calculations indicated that an embankment could be constructed to approximately El. 0.9 m (3 ft) without bearing failure of the foundation. Conventional alternatives for constructing the embankment to El. 2.4 m included preloading and staged construction, use of lightweight construction material, and end-dumping displacement. Nonengineering considerations dictated that the embankment be constructed in less time than was estimated for the preloading and staged construction alternative, and the use of lightweight construction material was not suitable because this would reduce the effectiveness of the embankment as a preload fill for future raising. End-dumping displacement is the procedure normally used by the U.S. Army Engineer District, Mobile (MDO) to construct embankments on soft soil. Sufficient quantities of relatively clean fine sand were available at nearby locations for construction of a displacement section. However, based on previous experience with Mobile Harbor soil conditions, it was estimated that the volumetric ratio of below ground to above ground material required would be approximately three to one for displacement construction. Use of this quantity of fill material would be expensive, and the relatively large lateral displacements produced might have disturbed pipelines, utility lines, roadways, and a bridge located adjacent to the proposed embankment alignment. It was also doubtful that the quality control during the displacement operation would be sufficient for the construction of a satisfactory base section for future embankment raising.

After the potentially applicable conventional engineering alternatives had been eliminated, it was proposed that a floating section be constructed by using geotechnical fabric (also called civil engineering fabric and filter cloth) as tensile reinforcement, placed transverse to the dike alignment between the soft foundation and the embankment material. The fabric reinforcement would hold the embankment together and prevent rotational foundation failures or lateral splitting until sufficient consolidation occurred in the soft foundation to support the embankment, i.e., the fabric would temporarily carry the difference between the embankment weight and the foundation bearing capacity.

Analysis of the proposed embankment-raising sequence by using consolidated, undrained shear test data for the foundation indicated that, if the initial embankment to El. 2.4 m could be constructed without failure, the foundation strength would increase such that the next raise increment [that to El. 3.7 m (12 ft)], could be placed without foundation failure and, once pore pressures from this raising dissipated, a second raising could be conducted, and so on. Fabric reinforcement would be needed only for initial construction, and long-term fabric durability was important. In addition to the higher probability of successful initial construction, the use of fabric reinforcement was postulated to result in a cost saving of 40-60 percent, because of the reduced volume of fill needed (1).

Thus, MDO decided to construct a 244-m (800-ft) long embankment test section along the proposed dike alignment, across the south end of Pinto Pass. This test section would verify the fabric-reinforcement concept and allow refinement of design and construction procedures for the remaining 1280 m (4200 ft) of embankment. A relatively clean, poorly graded fine sand [100 percent passing the 2.00-mm (U.S. no. 10) sieve, 83 percent passing the 425-µm (U.S. no. 40) sieve, and 2 percent passing the 150-µm (U.S. no. 100) sieve, uniformity coefficient of 1.3] available nearby would be used as embankment fill.

DESIGN OF EMBANKMENT TEST SECTION

The geometric configuration of the test section was controlled by the base section size needed to obtain stable side slopes for future raised sections, and consisted of an embankment with a 3.7-m-wide crest at El. 2.4 m (8 ft) and 10:1 (horizontal:vertical) side slopes, resulting in a section 52.4 m (172 ft) wide at El. 0. Potential failure modes for the embankment were investigated (2) and are shown conceptually in Figure 1. Analysis of the failure modes shown in Figure 1 indicated that the fabric must have a minimum uniaxial tensile strength of 17.5 kN/m (100 lbf/in) of width at not more than 10 percent elongation and a minimum ultimate strength of 39 kN/m (225 lbf/in) of width. The 10 percent elongation criterion was selected to limit the average lateral spreading to ±5 percent. Also, the coefficient of soil-fabric friction should be at least equal to the friction angle ($\phi = 30°$) for the fill sand in a loose relative density condition.

In addition to the fabric strength and frictional re-

Figure 1. Potential failure modes of fabric-reinforced embankments: (a) sliding wedge failure of embankment, (b) local bearing failure of soft foundation, (c) excessive settlement before stable bearing conditions can be achieved, and (d) insufficient fabric anchorage during embankment deformation.

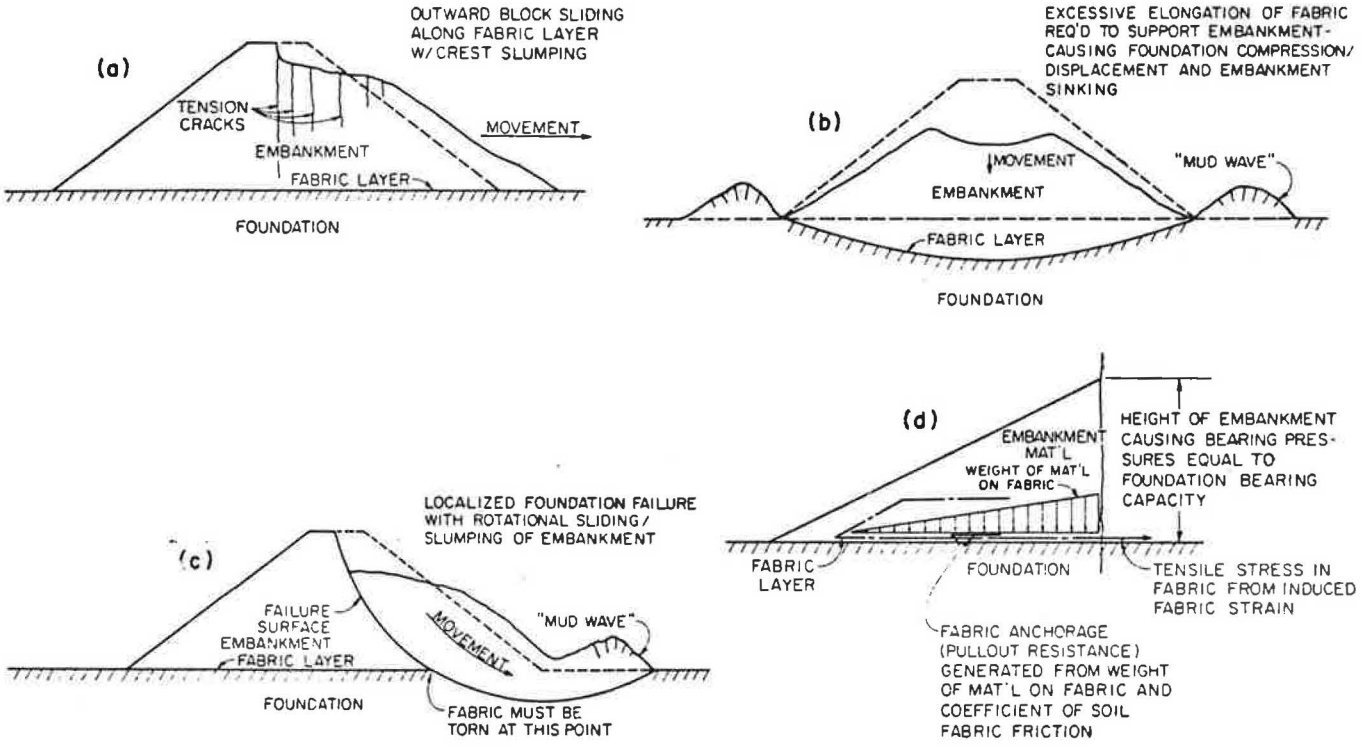

Figure 2. Proposed construction sequence for embankment cross section.

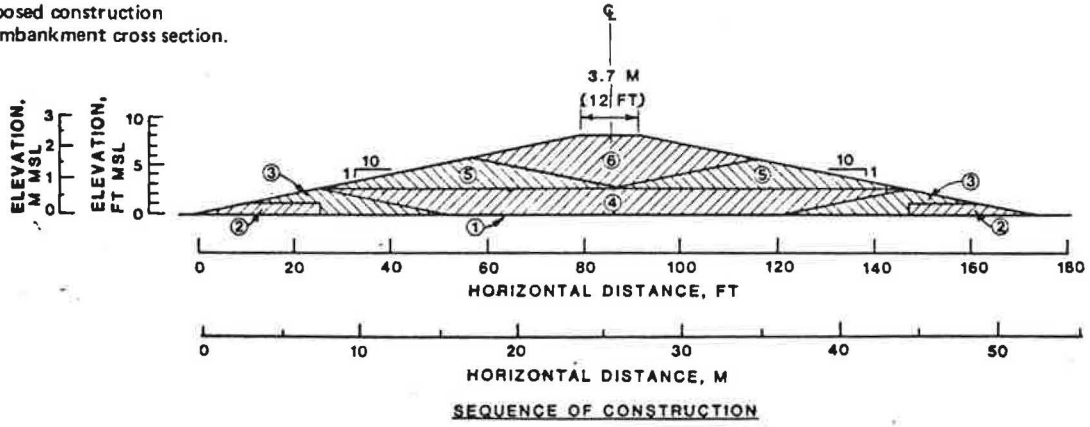

SEQUENCE OF CONSTRUCTION

① LAY GEOTECHNICAL FABRIC IN CONTINUOUS TRANSVERSE STRIPS, SEW STRIPS TOGETHER.
② END DUMP ACCESS ROADS AND LAP FABRIC OVER TOP.
③ CONSTRUCT OUTSIDE SECTIONS TO ANCHOR AND STRETCH FABRIC.
④ CONSTRUCT FIRST CENTER SECTIONS TO ANCHOR FABRIC.
⑤ CONSTRUCT SECOND CENTER SECTION.
⑥ CONSTRUCT CENTER SECTION.

quirements, a sequential construction scheme was developed that placed balanced forces on the soft foundation and provided proper fabric anchorage along the toes of the embankment before the placement of fill along the centerline. The construction sequence is shown in Figure 2, and the failure-mode analysis and construction details are described in detail elsewhere (2).

Selection of Fabric Reinforcement

Since few data were available concerning properties of geotechnical fabric for use as tensile reinforcement in embankment construction, test procedures were developed and a test program was carried out on 27 commercially available geotechnical fabrics (3). Four fabrics—Nicolon 66475, Nicolon 66186, Polyfilter-X, and Advance (Laurel) Type 1—satisfied initial modulus and ultimate strength requirements. Tensile stress-strain data for the four fabrics are shown in Figure 3, and laboratory test data for them are summarized in Table 1.

A plan and profile of the embankment test section, including fabric placement locations, is shown in Figure 4.

Figure 3. Stress-strain data for geotechnical fabrics meeting desired tensile strength criteria.

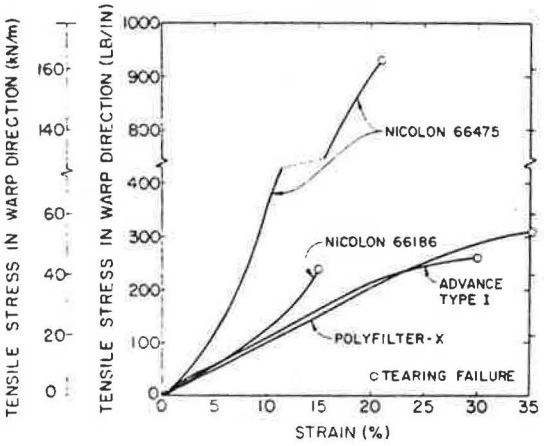

Table 1. Laboratory test data for the fabrics.

Fabric	Tensile Stress* (kN/m of width)	Ultimate Tensile Stress (kN/m of width)	Design Soil-Fabric Friction Angle† (°)	Creep Tendency	Wet Strength Loss
Nicolon 66475	63.4	158.0	30	Nil	Nil
Nicolon 66186	19.1	39.6	30	Nil	Nil
Polyfilter-X	18.0	54.5	30	Moderate	High
Advance Type 1	18.9	44.1	30	High	Moderate

Note: 1 kN/m = 0.175 lbf/in.
* At 10 percent ε.
† In a loose relative density condition, sand-sand friction angle = 30° and sand-fabric friction angles = 29°-31°, i.e., shear failure occurred in the sand just above the sand-fabric interface.

Construction Considerations

The key to successful completion of soft-ground engineering projects is the selection of appropriate construction equipment that will maintain mobility on soft soils. Based on previous U.S. Army Corps of Engineer research (4), small dozers [maximum 17-kPa (2.5-lbf/in^2) ground pressure] were selected for fill placement. Previous work in fabric-reinforced haul-road construction on soft soils (5) has indicated that a double-fabric-layer reinforced haul road along the outer edges of an embankment can carry loaded 7.6-m^3 (10-yd^3) tandem-axle dump trucks.

The most critical construction operations are those related to placement and sewing of fabric, as they are hand-labor intensive. In this project, the fabric [provided in 5.5- and 5-m (18- and 16.4-ft) wide strips] was to be placed on the soft foundation (with and without a working table), unrolled transverse to the alignment, and sewed to previously placed fabric. The newly placed fabric would then be covered by approximately 0.3 m of fill and the outside edges lapped back into the embankment and covered to provide a haul road for dump-truck delivery of fill. The types of equipment required for construction of the test section and their estimated work quantity were computed (2); the estimated cost of test section construction, excluding fabric, was $119 000.

Test Section Instrumentation

To monitor behavior during construction and to allow evaluation of test section performance, five settlement plates and eight Cassagrande piezometers were installed at each station in the embankment. The settlement plates

Figure 4. Plan and profile of embankment test section.

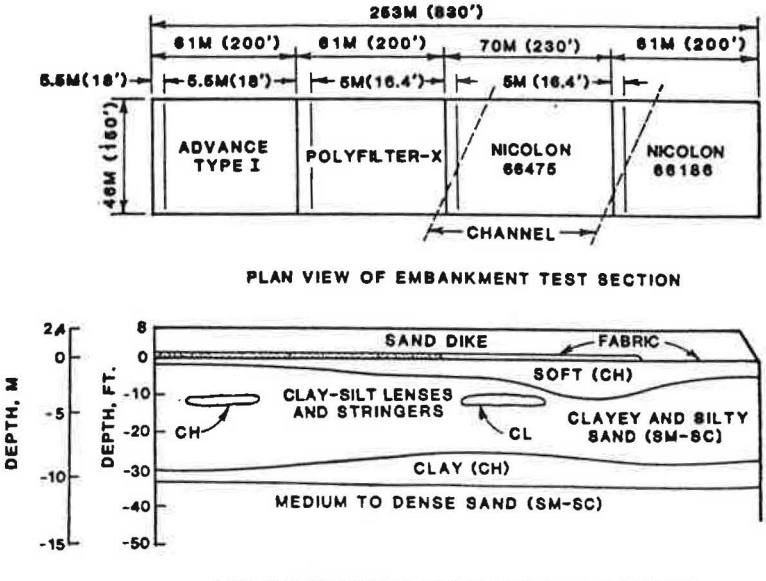

were installed on the fabric immediately after placement, and the piezometers were installed on the alignment centerline and at the outside third point (alternating left and right at each station) to depths of 1.5, 3, 6, and 9 m (5, 10, 20, and 30 ft) below the surface, as soon as dike construction had progressed to the point where a drill rig could maintain mobility. Settlement plate risers were used to measure vertical settlement and horizontal displacement during and after embankment construction (6).

Figure 5. Covering outside edges of the fabric with sand fill.

Figure 6. Lapping fabric back into embankment.

Figure 7. Unsatisfactory working table near channel.

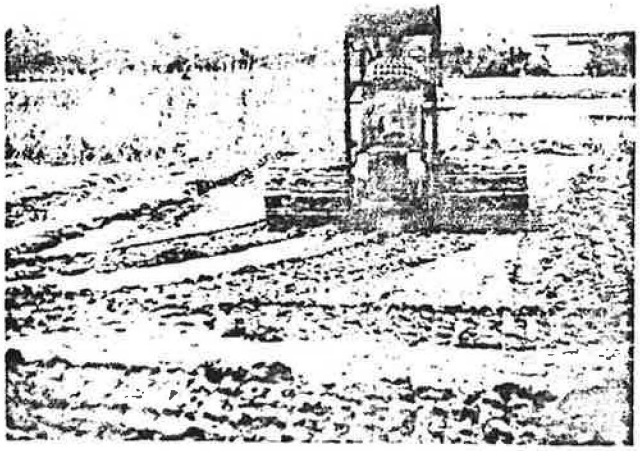

Test Section Construction

Construction of the test section began in November 1978. The initial construction sequence called for placement of the fabric on a 0.3-m-thick working table placed on existing foundation and vegatation. Once the working table was placed, 5.5-m-wide strips of, first Advance Type 1 and then Polyfilter-X, fabric were brought to the leading edge of the embankment, unrolled transverse to the dike alignment, sewed to the previous strip, and spread on the working table. The fabric was then covered with approximately 0.3 m of sand (see Figure 5), and the outside edge was lapped back and covered to anchor the fabric and provide a two-layer reinforced haul road along each side of the embankment (see Figure 6). It was necessary to accomplish these operations relatively quickly. If the working table was left in place overnight,

Figure 8. Unrolling fabric on top of existing fabric strip.

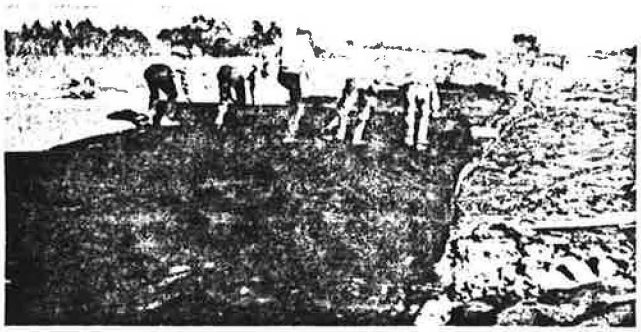

Figure 9. Sewing new fabric strip to existing strip.

Figure 10. Surface appearance of strip on top of mud wave.

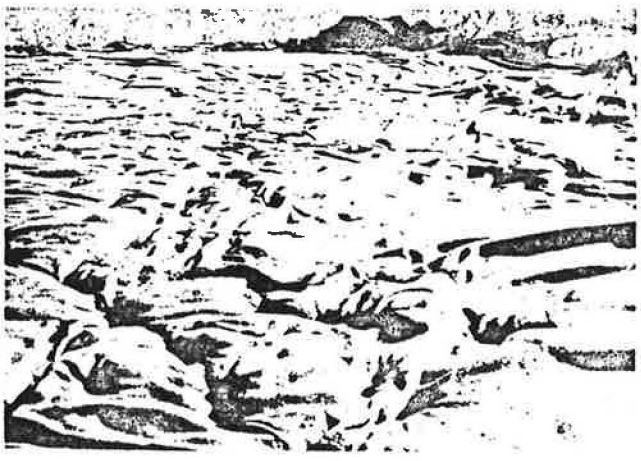

Figure 11. Appearance of strip after placement of sand fill.

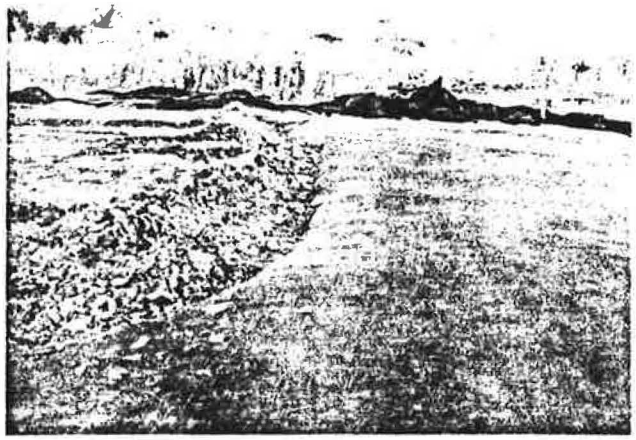

Figure 12. Gap caused by tensile failure of thread holding fabric strips together.

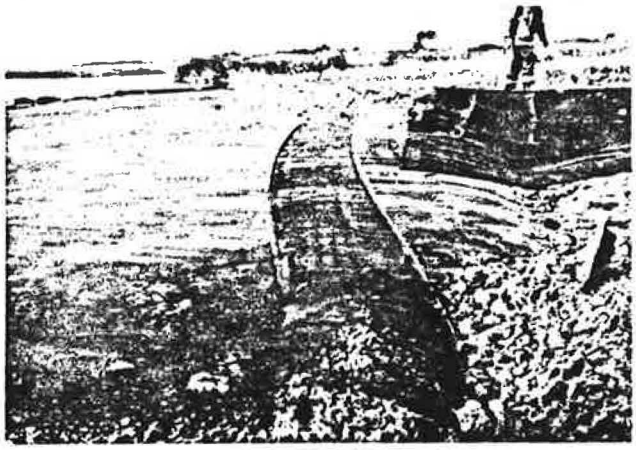

Figure 13. Placing fabric directly on foundation.

Figure 14. Aerial view of completed embankment test section: looking east.

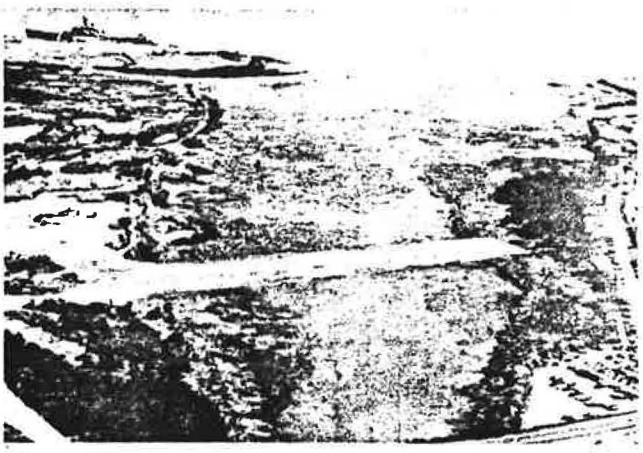

excess pore pressures generated in the foundation would saturate the sand and cause quick conditions and restrict dozer mobility.

Placement of the working table went smoothly until approximately 122 linear m (400 linear ft) of fabric had been laid along the alignment. Both the Advance Type 1 and the Polyfilter-X fabrics were placed on a sand working table. However, as the leading edge of the embankment approached the Pinto Pass channel, no vegetative root mat was available and the dozers could not maintain sufficient mobility to construct a satisfactory working table (see Figure 7). At this point, one transverse strip of Nicolon 66475 fabric was placed on the last portion of the completed working table, and placement of the subsequent fabric across the channel was carried out by "working on the mud wave". As the dozers pushed sand cover onto a newly laid fabric strip, a shallow mud wave was created underneath the fabric and pushed out under its leading edge. This mud wave raised the fabric approximately 0.5 m in elevation, i.e., above high tide level. Workmen then unrolled a transverse strip of fabric on top of the existing fabric, as shown in Figure 8, sewed the two strips together, as shown in Figure 9, and pushed and shoved the new strip of fabric off the leading edge of the existing fabric strip onto the top of the forward portion of the foundation mud wave. This operation left the surface of the fabric rather wrinkled and, as shown in Figure 10, footprints of laborers walking on the fabric were also evident. However, once dozer placement of sand cover on the fabric was reinitiated, the forward-moving mud wave stretched the fabric and removed all wrinkles, as shown in Figure 11. A new fabric strip was then unrolled, and the process was repeated. During one of the early mud-wave-displacement fabric-stretching operations, the thread holding two adjacent pieces of fabric together failed in tension, causing the gap shown in Figure 12. This gap was covered with another strip of fabric and the fabric-sewing operations were modified to use 0.45-kN (100-lbf) test nylon thread, which gave a seam strength greater than the fabric strength.

Once the stronger thread was placed in service, no further seam failures occurred and the operation progressed across the channel. Two sections of Nicolon 66186 were also placed by using the mud-wave-displacement technique. The mud wave subsided against the other bank of the channel, and the remaining sections of Nicolon 66186 were laid directly on the foundation without using a working table, as shown in Figure 13, to evaluate the effect of this modification on embankment behavior.

Construction of the test section was completed in January 1979. An aerial view of the completed test section is shown in Figure 14, and a typical cross section is shown in Figure 15. [More detail concerning construction operations is available elsewhere (6).]

Figure 15. Construction details.

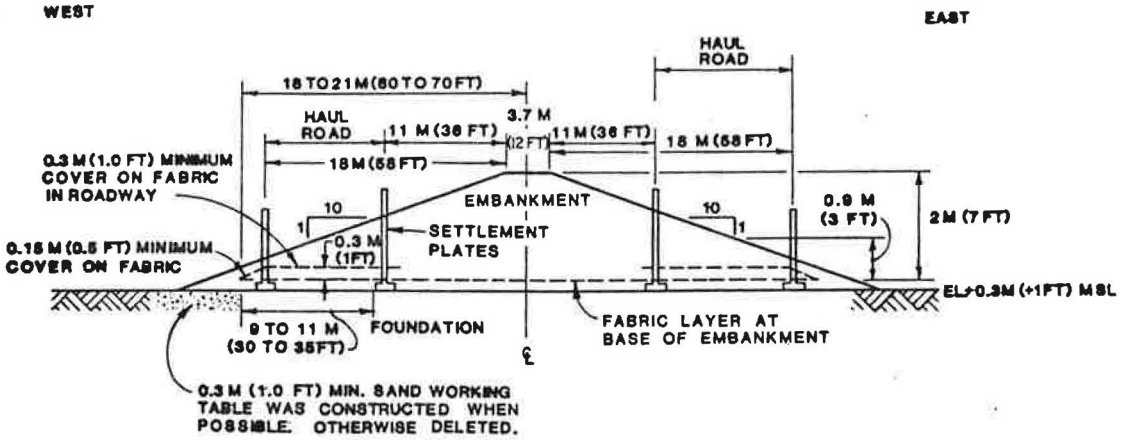

Figure 16. Settlement profiles: stations 5+00 and 6+00.

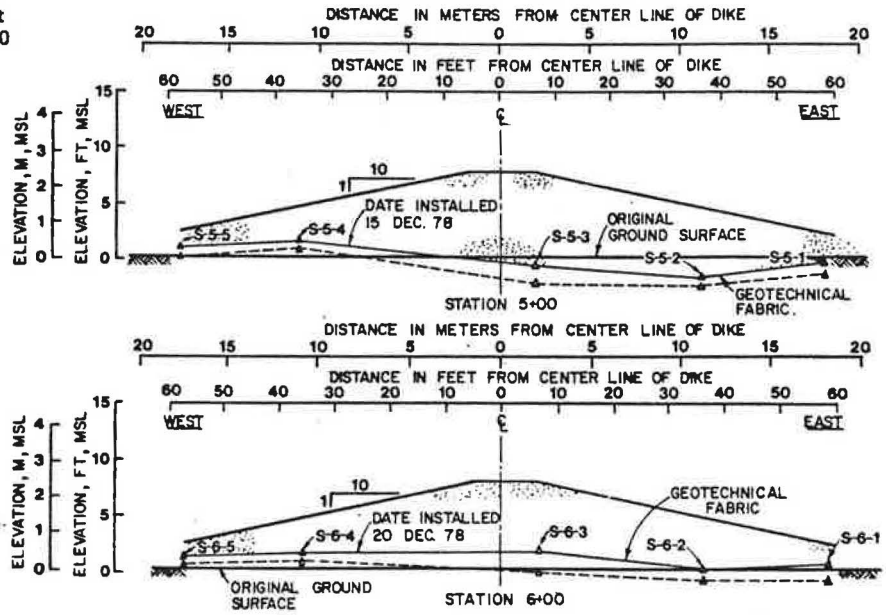

POSTCONSTRUCTION EVALUATION AND ASSESSMENT

The test section was finished to design width and grade without lateral splitting or rotational foundation bearing failure, despite foundation excess-pore-pressure levels of 4.3 m (14 ft) for the 2.4-m-high embankment. Computations (6) indicated essentially zero effective stress conditions in the foundation materials. Foundation displacements produced by completion of the embankment to El. 2.4 m were less than 0.3 m throughout the alignment. As of July 1979, vertical foundation consolidation was less than 0.3 m except at stations 5+00 and 6+00, in the center of the Pinto Pass channel, where settlements of approximately 0.5 m had occurred, and pore pressures had dissipated to 15 percent or less of their maximum values. Settlement profiles at stations 5+00 and 6+00 are shown in Figure 16. The settlements are approximately half the values predicted from consolidation theory. Examination of Figure 15 shows two other interesting details: The fabric elevation, when placed and covered, was somewhat higher than the original ground surface because of the mud-wave-displacement technique used for fabric stretching. As a result, the final fabric elevations after settlement are reasonably close to the original ground surface. Also, the foundation settlements are more nearly uniform than would be predicted from classical settlement theory. The less-than-expected and more nearly uniform settlements encountered transverse to the alignment may have been caused by internal arching of the embankment material, which would tend to develop a more nearly uniform soil pressure on the foundation.

Lateral embankment spreading was minimal at all locations except stations 5+00 and 6+00 in the Pinto Pass channel. At these locations, approximately 1.2 m (3.8 ft) of lateral spreading occurred, concentrated within the center 27-m (90-ft) width of the embankment. The outside portions of the embankment, located between the exterior and first interior settlement plates, moved laterally in essentially intact condition. This may have been caused by trucks using the space between the rows of settlement plates as a haul road. In the center 27-m-wide portion of the embankment, the elongation caused an average strain of 4 percent in the fabric. Comparison of this field-condition strain and the stress-strain behavior of Nicolon 66475 fabric shown in Figure 3 indicates that a fabric tensile stress of approximately 14.6 kN/m (1000 lbf/ft) of width was developed. This value is in relatively close agreement with the 16.8 kN/m (1150 lbf/ft) of width theoretical lateral active earth pressure at the embankment centerline. Thus, the fab-

ric stress is somewhat less than that necessary to maintain stability against rotational foundation bearing failure, and it may be tentatively concluded that, had the fabric not been present, the embankment would have failed by lateral splitting.

The only significant fabric elongation measured was from lateral spreading. Total fabric elongation from bearing and consolidation settlement was considerably less than 0.5 percent. From a speculative viewpoint, the tendency for the embankment to fail by horizontal spreading, as hypothesized in Figure 1a, is counterbalanced by the tendency for it to fail by excessive centerline displacement, as hypothesized in Figure 1c. Thus, the effects of the two conditions on embankment deformation are in opposition, and the net effect may have been to somewhat nullify each other and produce a relatively uniform settlement profile over the embankment cross section.

After construction, the outside edges of the fabric were exposed by excavation at several locations and this fabric was not found to be in a stressed condition. Thus, the hand-labor-intensive operation of lapping the outside edges of the fabric back into the embankment to provide additional anchorage was probably unnecessary. Advantages exist for construction of a double-fabric-layer reinforced haul road along each outer edge of the embankment, but this requirement could probably be satisfied more efficiently by unrolling a second strip of fabric parallel with the alignment and covering this strip to provide required haul-road characteristics. [More detail concerning postconstruction evaluation of the test section is available elsewhere (6, 7).]

CONSTRUCTION COSTS

The estimated cost for test-section construction, exclusive of fabric, was approximately $119 000, but the actual cost was only $108 000. Approximately 16 700 m^2 (20 000 yd^2) of fabric was used. Fabric bid prices should not be considered representative because of the relatively small quantities involved but were $1.46/$m^2$ ($1.22/$yd^2$) for Advance Type 1, $1.57/$m^2$ ($1.31/$yd^2$) for Polyfilter-X, $2.69/$m^2$ ($2.25/$yd^2$) for Nicolon 66186, and $4.17/$m^2$ ($3.49/$yd^2$) for Nicolon 66475. Total cost for the test section, including fabric and reef shell used to surface the haul road to the borrow area, was approximately $154 500. Approximately 15 200 m^3 (20 000 yd^3) of sand fill were estimated, and 17 500 m^3 (23 000 yd^3) of fill were actually hauled and placed along the alignment. Of the $108 000, approximately $93 000 was used in earthwork-related operations; the remaining costs were related to fabric placement and sewing. Dividing the total cost of earthwork operations by the volume of material transported gives a unit cost of material placement, spreading, semicompaction, and finish grading of $5.31/$m^3$ ($4.05/$yd^3$). This cost is reasonable for material movement in soft-ground engineering situations in which the size of digging, hauling, and spreading equipment is limited. More detail on construction costs is available elsewhere (6).

CONCLUSIONS

Fabric-reinforced construction techniques are based on the concept that low foundation strength and point-to-point foundation variability can be compensated for by use of geotechnical fabrics that have more easily predicted engineering properties. The design concepts and construction procedures involved are relatively simple and based on application of logical engineering principles rather than on detailed mathematical analyses. Based on the results of the test program summarized in this paper, the following may be concluded:

1. Use of geotechnical fabrics to provide transverse tensile reinforcement is a technically feasible method of rapidly constructing embankments on foundations too soft to support the unreinforced embankment without failure.
2. If procedures are used that provide essentially balanced loading on the foundation and that cover the outside edges of the fabric to provide suitable anchorage before placement of the interior embankment fill, construction of fabric-reinforced embankments by using available low-ground-pressure dozer equipment and conventional dump-truck material hauling is operationally practical.
3. Compared with conventional end-dumping displacement methods, fabric-reinforced embankment construction appears particularly cost-effective. The additional construction costs of purchase and placement of fabric are more than recovered by the savings in fill required to construct the above-ground embankment cross-section.
4. Although specific situations will dictate exact fabric strength requirements, high-tensile-strength, high-deformation-modulus fabrics should prove most suitable for embankment reinforcement.
5. There appears to be no particular advantage to constructing a working table before fabric placement, as long as the ground surface is reasonably level. When the mud-wave-displacement method of fabric stretching is used, the longitudinal seam strength should be equal to or greater than the fill-direction tensile strength of the fabric.

ACKNOWLEDGMENT

We gratefully acknowledge the support of the U.S. Army Engineer District, Mobile, Alabama, and the Dredging Operations Technical Support Project of the U.S. Army Engineer Waterways Experiment Station, Vicksburg, Mississippi.

REFERENCES

1. T. A. Haliburton, P. A. Douglas, and J. Fowler. Feasibility of Pinto Island as a Long-Term Dredged-Material Disposal Site. U.S. Army Engineer Waterways Experiment Station, Vicksburg, MS, Miscellaneous Paper D-77-3, Dec. 1977.
2. T. A. Haliburton; Haliburton Associates. Design of Test Section for Pinto Pass Dike, Mobile, Alabama. U.S. Army Engineer District, Mobile, AL, June 1978.
3. T. A. Haliburton, C. C. Anglin, and J. D. Lawmaster. Selection of Geotechnical Fabrics for Embankment Reinforcement. U.S. Army Engineer District, Mobile, AL, May 1978.
4. W. E. Willoughby. Assessment of Low-Ground-Pressure Equipment for Use in Containment Area Operations and Maintenance. U.S. Army Engineer Waterways Experiment Station, Vicksburg, MS, Technical Report D-77-8, Nov. 1977.
5. T. A. Haliburton, J. Fowler, and J. P. Langan. Perimeter Dike Raising with Dewatered Fine-Grained Dredged Material at Upper Polecat Bay Disposal Area, Mobile, Alabama. U.S. Army Engineer Waterways Experiment Station, Vicksburg, MS, Miscellaneous Paper D-78-3, Dec. 1978.
6. J. Fowler. Analysis of Fabric-Reinforced Embankment Test Section at Pinto Pass, Mobile, Alabama. Graduate College, Oklahoma State Univ., Stillwater, Ph.D. thesis, July 1979.

7. T. A. Haliburton. Evaluation of Construction Procedure for Fabric-Reinforced Embankment Test Section, Pinto Pass, Mobile Harbor, Alabama. U.S. Army Engineer Waterways Experiment Station, Vicksburg, MS, March 1979.

Publication of this paper sponsored by Committee on Embankments and Earth Slopes.

Notice: The Transportation Research Board does not endorse products or manufacturers. Trade and manufacturers' names appear in this paper because they are considered essential to it.

Planning Slope Stabilization Programs by Using Decision Analysis

Duncan C. Wyllie, N. R. McCammon, and W. Brumund

Maintenance funds are rarely sufficient for all needs, and this requires that decisions be made as to the most effective allocation of these funds. In the case of slope stabilization, these decisions will be based on the frequency and location of failures, the consequences of failures (i.e., the cost of accidents), and the cost of stabilization. Decision analysis is a simple but useful tool to determine the most cost-effective stabilization program. The expected costs of slope failures are calculated for different stabilization programs, and these costs are added to the costs of the stabilization work to determine the expected total cost. The program that has the minimum total cost is likely to be the most cost effective. An example of the use of decision analysis is given that shows the variation in expected total cost for rockfalls along a section of highway for no stabilization work, a limited scaling program, and a more-comprehensive ditching, scaling, and bolting program. It is shown that the frequency of rockfalls must be substantially reduced before there is any significant reduction in the cost of accidents and that this requires an extensive stabilization program. The example also illustrates how the probability values used in the decision analysis can be related to the design of the stabilization measures.

It is often necessary in transportation engineering to determine the optimum allocation of the limited funds available to maintain slopes in acceptably safe condition. These decisions are rarely straightforward because the likely types of failure are varied, the consequences are diverse, and their occurrences are difficult to predict. This paper describes the use of decision analysis, a simple but effective tool, for the analysis of the impact of different stabilization programs on the expected cost of slope failures.

Recent applications of decision analysis in engineering include the selection of safe routes for the transportation of hazardous materials (1) and surveys carried out to assess the safety of dams (2). In this paper, the focus is on the optimization of a maintenance program for a series of highway or railway rock cuts that have a history of rockfalls, some of which have interrupted traffic and caused accidents. The costs of these events and of different stabilization programs are estimated, and these costs and the probabilities of rockfalls occurring are used to calculate the expected costs of rockfalls under alternative maintenance-program scenarios. This information shows which stabilization program is more cost effective. Probability analysis can then be used to ensure that the probability of failure of the stabilized slope is consistent with the probability used in the decision analysis.

PRINCIPLES OF DECISION ANALYSIS

Decision analysis is a technique in which the consequences of all of the events that might occur in a particular situation are evaluated. Probabilities are assigned to events that occur by chance, and the costs of those events are determined. This information is then used to calculate the expected costs of different courses of action, which can be used as a guideline in making decisions.

The first task in decision analysis is to draw a decision tree that shows all possible events. In this paper, rockfalls from highway cuts are considered, although the same approach can be used on railroad cuts. On the tree, events that occur as a result of a decision are distinguished from events that occur by chance. The decision point in this analysis is whether or not to carry out a stabilization program. Once this decision has been made, regardless of what has been decided, a chance event will occur; that is, the slope will be either stable or unstable. Probabilities can be assigned to each of these events and, because they are mutually exclusive, the sum of probabilities at each chance point is 1.0.

Establishment of realistic probabilities for different events requires both experience and sound judgment. This is particularly true for rare events; experimental evidence shows that people tend to overestimate the likelihood of their occurrence (3). The best method for establishing probabilities is to study existing records and modify them where necessary to suit local conditions.

The next task is to assign the total costs to society (e.g., maintenance, injury, business losses, traffic delays) of each of the events at the tips of the decision tree and to determine the costs of stabilization at appropriate decision points. If the cost of an event cannot be expressed in terms of a single value, it can be expressed as a probability distribution in which all the costs within the range are given probabilities of occurrence. Summation of the area under the probability distribution curve will give the expected cost of the event. The determination of costs usually involves the cooperation of the owner, who is also likely to provide useful input on the structure of the decision tree and the assignment of probabilities.

The final task in the analysis is that known as averaging out and folding back (4) each branch of the tree. The product of cost and probability, summed over all events at a particular chance point, gives the expected cost. This procedure is started at the tips of the branches and worked back to the decision point. If the objective of the analysis is to determine the least

costly option, the path that has the least expected cost is selected.

DATA COLLECTION FOR DECISION ANALYSIS

The purpose of decision analysis is to assist in predicting the outcome of future events, and the reliability of the prediction will be greater if reliable data on past events are available and if the mechanism and causes of failure are thoroughly understood.

In the cause of rockfalls from slopes adjacent to a highway or a railway (see Figure 1), three types of information are required:

1. If a record of rockfalls exists, the locations, frequencies, and consequences of these falls should be summarized and these data used to estimate the probabilities with which such events occur. It is unlikely, however, that there will be sufficient records to establish the complete rockfall population from which to calculate true probabilities. Therefore, it may be necessary to make appropriate modifications based on judgment and experience to the calculated probabilities. For instance, the records may have been collected during a period when the winters were more severe than usual and frost action produced an unusually large number of rockfalls. In such a case, the probability should be adjusted downward.
2. The impact of rockfalls on traffic should be studied to determine the average costs of different classes of events. For example, the costs of a delay caused by a major rockfall would be due to the interruption to traffic, removal of the rock, and repairs to the slope and the pavement. In the case of an impact, costs will result from damage to the car, injury to or death of its occupant(s), and damage to the pavement. Even when there is neither a delay nor an impact, it may still be necessary to remove the rockfall and perform repairs. In addition, there are indirect costs such as the lost wages of those injured, engineering studies of stability conditions, and legal fees in the event of a court case.
3. The physical and geological characteristics of the slopes should be studied to determine the causes of failure and whether further falls are likely. One possibility is to evaluate the stability conditions for each slope on a numerical point rating from very high to very low probability that a rockfall will occur. The detailed information should include the length and spacing of the natural fractures in the rock, their strength characteristics and orientation with respect to the slope face, groundwater pressures, and whether heavy blasting has caused damage to the rock behind the face (5).

Figure 1. Rockfall conditions on cut slope.

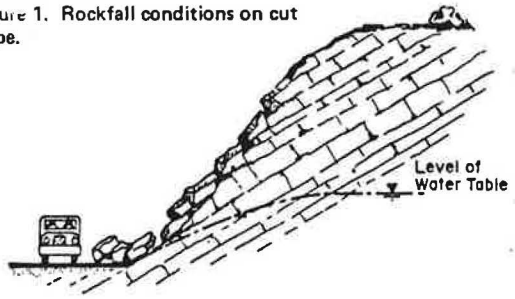

APPLICATION OF DECISION ANALYSIS

To illustrate the use of decision analysis, consider the case where a number of unstable slopes above a major highway have experienced frequent rockslides. A decision is required on whether a preventive stabilization program to reduce the likelihood of future slides is economically justified and, if so, how much money should be spent.

An examination of the length of highway where the rockfalls have been occurring shows that, on a 1.5-km-long section of essentially constant geological characteristics, there are a number of potentially unstable slopes. Rockfalls have been occurring because the slopes were cut at 45°, which undercuts the bedding planes that dip at about 30° toward the highway. In addition, groundwater pressures exist within the slope (Figure 1).

The first step in the decision analysis is to draw a decision tree to show the range of conditions expected (see Figure 2). The first point in the tree is the decision point for the three alternative courses of action. These are

1. No stabilization,
2. Option 1—expenditure of $6000/0.1-km segment

Figure 2. Decision analysis: existing stability condition.

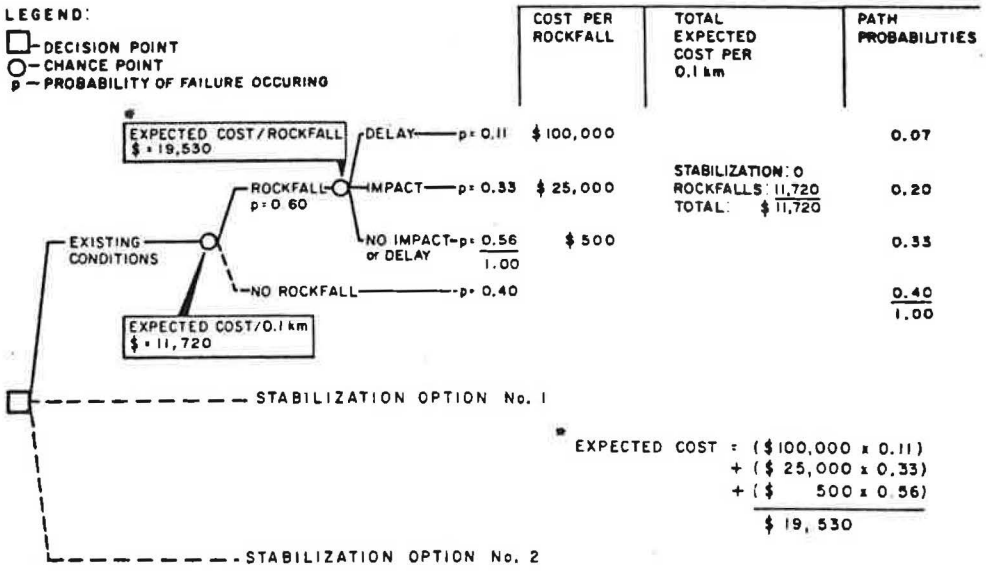

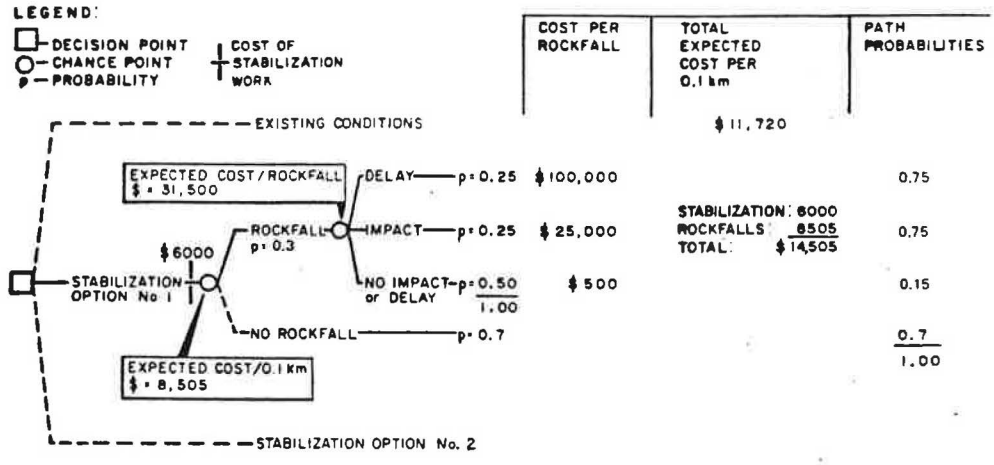

Figure 3. Decision analysis: stabilization option 1.

of highway for removal of loose rock from the face, and

3. Option 2—expenditure of $10 000/0.1-km segment of highway to install tensioned rock anchors and to excavate a ditch and construct a gabion wall along the toe of the slope.

Whichever course of action is taken, the same events can take place, although the probabilities of their occurrence will differ if the stabilization program is effective. Thus, the structures of the trees are identical for each of the three options. The events that can occur at the first chance point are either

1. A rockfall takes place or
2. The slope is stable and no rockfall takes place.

If a rockfall does occur, then one of three types of events can take place at the second chance point:

1. There is a delay,
2. There is an impact, or
3. There is neither an impact nor a delay, but there may be some damage to the highway.

The probabilities of these events occurring per 0.1-km segment of highway can be estimated by dividing the expected number of rockfalls by 15, i.e., the number of 0.1-km segments in 1.5 km of highway. For example, if nine rockfalls have occurred on this 1.5-km section, then the probability of a rockfall occurring on a given 0.1-km segment is 9/15 or 0.6, and the probability of no rockfall occurring on that segment is (1 - 0.6) or 0.4. This probability unit can then be used to compare the expected rockfalls over other sections of highway that have the same geology.

To calculate the expected cost of rockfalls in the future, probabilities of future rockfalls and their consequences are calculated from the existing rockfall conditions by assuming that the instability problem will be similar in the future to what it has been in the past (although some allowance might be made for increases in traffic). If, of the nine rockfalls that have occurred, one caused a delay (p = 1/9 or 0.11), three caused an impact (p = 3/9 or 0.33), and five caused neither a delay nor an impact (p = 5/9 or 0.56), then the probabilities can be assigned as shown in Figure 2. Path probabilities are then calculated by multiplying the probability along each path on the tree. This gives the overall probability of an event occurring if a previous event has occurred with a certain probability (4).

Average costs for the three types of events for the case of a heavily used highway that has a high proportion of commercial traffic are estimated (6) to be as follows:

Type of Event	Cost ($)
Delay	100 000
Impact	25 000
Damage to highway only	500

Finally, these probabilities and costs are averaged out and folded back to determine the expected cost of rockfalls per 0.1-km segment. For no stabilization, this cost is calculated to be $11 720. The objective of the stabilization work is thus to reduce the probability of failure so that the expected cost of rockfalls plus the stabilization cost is less than $11 720.

The first stabilization option consists of removing loose rock from the slopes. This option is estimated to cost $6000/0.1-km segment; from experience, this will approximately halve the number of rockfalls. The probabilities are calculated by assuming that four rockfalls will occur in the same time interval as in the no-stabilization option of which one will be a delay, one an impact, and two will cause no delay (see Figure 3). (It should be noted that, because probabilities of occurrences have been rounded to whole numbers, small differences in path probabilities will have no significance.)

Calculation of the probabilities of these events shows that, although the probabilities of the impact and no-delay events have been considerably reduced from existing conditions, the path probability of a delay occurring is essentially unchanged. This is reasonable because the stabilization work has done nothing to improve the stability of the overall slope and rockfalls can still be expected to occur. Calculation of the expected costs by using these probabilities and the same costs for each type of event as before shows that the expected cost of rockfalls per 0.1-km segment of highway is $8505. This plus the stabilization cost of $6000/0.1-km segment gives a total expected cost of $14 505. This cost is greater than the existing cost of rockfalls, which means that a scaling program is not economically justified.

The second stabilization option consists of excavating at the toes of the unstable slopes to form a ditch, constructing a gabion wall to catch small rockfalls, and installing tensioned rock anchors where necessary to prevent large rockfalls (see Figure 4). It is estimated that this option will cost $10 000/0.1-km segment of highway. The ditch, however, is designed to prevent small rockfalls from reaching the highway so that the probability of impact and no-impact events will be very low.

Figure 4. Illustration of stabilization program.

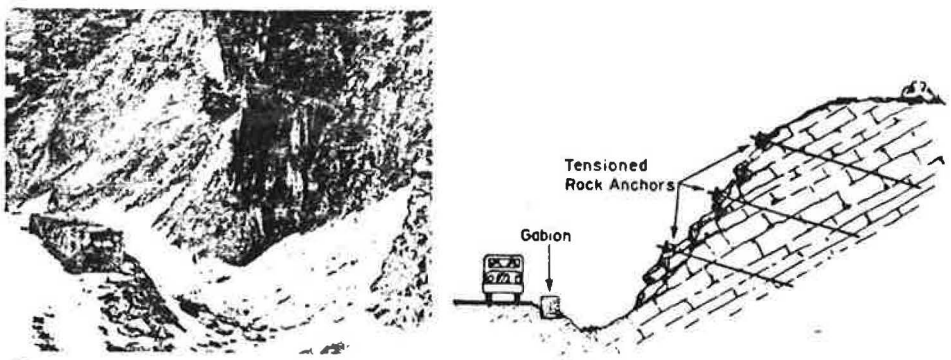

Figure 5. Decision analysis: stabilization option 2.

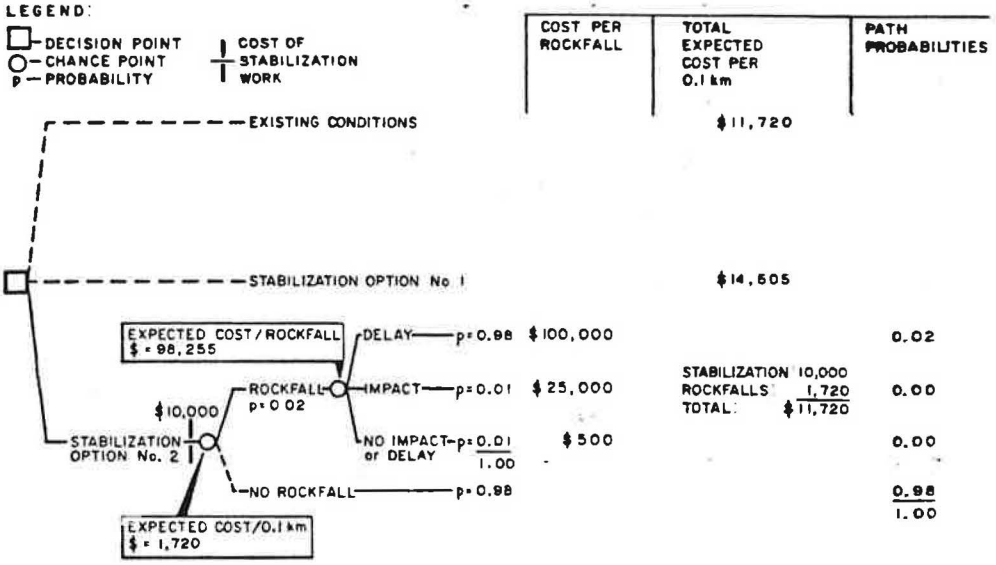

Figure 6. Definition of parameters used in stability analysis.

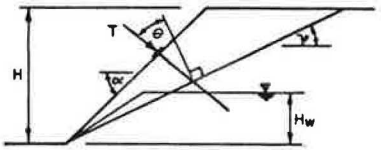

The installation of rock anchors will reduce the probability of a large rockfall occurring that would cause a delay. For the stabilization option to be economically justified, the expected cost of stabilization and rockfalls must be less than the existing cost of $11 720/0.1-km segment of highway. As shown in Figure 5, this expected cost will be achieved if the probability of a delay is less than 0.0175 (approximately 0.02). The required probability is calculated from the required expected cost by working from left to right through the tree.

The design of the rock-bolting program to achieve this level of probability of failure can be carried out by using probability analysis in conjunction with standard factor-of-safety (FOS) analysis. In this way, it is possible to relate the consequences of failure to the amount of stabilization work carried out.

PROBABILITY ANALYSIS

A probability analysis can be used as a guideline in the objective selection of an appropriate FOS. This analysis takes account of the variability and lack of definition in the parameters used. Furthermore, this probability of failure can then be used in the decision analysis to examine the consequences of failure. If the consequences are unacceptable, then the decision can be made to take action to reduce the probability of failure to a level that has an acceptable consequence.

Alternatively, the design of stabilization measures can be carried out on the basis of a selected FOS. This is a somewhat subjective selection and may not be consistent from case to case. Usually, a sensitivity analysis is also carried out to determine which factors have the greatest effect on the FOS. If the definition of the more-sensitive factors is uncertain, then a further subjective decision is made to increase the FOS.

The following example shows how a probability analysis, in conjunction with the decision analysis, can be used to select an appropriate FOS for the stabilization work. One method of calculating the probability of failure of a rock slope is as follows.

The stability of a slope is dependent on the relative magnitudes of two forces—a displacing force (D) that acts to cause failure and a strength (or resisting) force (R) that acts in the opposite direction. The difference between the two forces (R - D) is the margin of safety and is positive when the slope is stable and negative when the slope is unstable. The ratio of the two forces (R/D) is the FOS and is greater than 1.0 when the slope is nominally stable. In the case of a planar type, the

Figure 7. Normal distributions used in calculation of probability of failure.

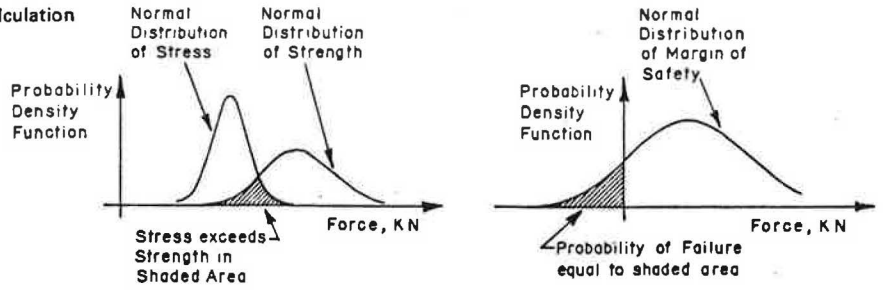

two forces are calculated by using Equations 1 and 2.

$$R = (W \cos\psi + T \cos\theta - U)\tan\phi \quad (1)$$

$$D = (W \sin\psi - T \sin\theta) \quad (2)$$

where W = weight of sliding block, U = water pressure action on failure plane, and α, H_w, ψ, T, and θ are defined in Figure 6 and have the values given below.

Parameter	Value	Estimated SD	Comments
Friction angle (α) (°)	41	5	Determined from rock texture and surface roughness, cohesion = 0
Height of water table (H_w) (m)	3.3	1.5	Variation in peak spring water levels (determined by piezometer measurements)
Dip of bedding planes (ψ) (°)	30	2.5	Determined by dip measurements made during surface geological mapping
Bolt tension per linear meter of slope (T) (kN)	120	10	Actual load (which is less than design load due to anchor relaxation)
Bolt angle (ϕ) (°)	16	3	Variation due to changes in rock surface

Because of the variable properties of rock, it is rarely possible when calculating these forces to define the magnitudes of parameters used in the analysis precisely, and it is more realistic to express their magnitudes in terms of ranges of values. One of the most convenient expressions for variability is the normal distribution. This is a bell-shaped curve that is symmetrical about the mean value and has a width that is defined by the standard deviation of the sample. An important property of the normal distribution is that the area under the curve between any two values on the horizontal axis represents the probability of a sample occurring within that range (7).

If all parameters used in the calculation of the resisting and displacing forces are independent and can be expressed as normal distributions, these can be combined by appropriate methods (8) to obtain the normal distributions of the two forces. If the two curves are plotted on the same figure and intersect at some point (as shown in the left-hand side of Figure 7), then D > R and the probability of failure of the slope is equal to the shaded area shown on the right-hand side of Figure 7. Alternatively, Monte Carlo techniques can be used to combine different types of distributions (8).

The probability of failure can be calculated by subtracting the two distributions to obtain the distribution of the margin of safety, i.e., the area under the curve to the left of the vertical axis. These calculations can be performed on a programmable pocket calculator.

If the parameters used in the analysis have little variation, then the distribution curve for the margin of safety will be narrow and only a slight increase in the strength will be required to produce a significant decrease in the probability of failure.

To illustrate the application of probability analysis in the design of stabilization measures, consider the slope discussed in the decision analysis above. Here, for the stabilization program to be economically justified, it is necessary to reduce the probability of failure by approximately 70 percent, i.e., from 0.07 to 0.02. The first step is to calculate the probability of failure and the factor of safety of the existing slope. Rock anchors are then added progressively, and the probability of failure is calculated until it is reduced by about 70 percent. For example, consider a 15-m-high slope cut at 45° and having the parameters shown above.

The probability of failure of this slope is 0.34 (FOS = 1.2) and must be reduced (by 70 percent) to 0.10. If two rock bolts are installed, the probability of failure will be 0.18 (FOS = 1.47), and if three rock bolts are installed the probability of failure becomes 0.12 (FOS = 1.63). Thus, the required improvement to the stability of the slope can only be achieved by adding three bolts rather than two (which is an insignificant additional cost).

CONCLUSIONS

Decision analysis can be used as a guideline in making rational decisions when there are several courses of action available. This approach offers the following advantages over subjectively made decisions:

1. Decision analysis encourages decision makers to scrutinize their problems as a whole as well as to evaluate the interactions among various facets of their problems.
2. The systematic approach helps communication. It allows each expert to give testimony about his or her area of expertise.
3. Systematic examination of the value of information in a decision context helps evaluation of what information is important.
4. Analysis distinguishes the decision maker's preference for consequences, including attitudes toward risky situations.
5. The methodology of decision analysis is useful as a mediating device in situations in which the advisors to a decision maker disagree about an appropriate course of action.

ACKNOWLEDGMENT

We express our appreciation to J. C. Collings of De Leuw Cather (Canada) for reviewing the traffic engineering aspects of this study.

REFERENCES

1. J. E. Acton. Assessment of Hazards Associated with Highway Engineering. Proc., Institute of Civil Engineers, Vol. 64, Part 1, Aug. 1978, pp. 381-391.
2. J. R. Benjamin. Applied Statistical Decision Theory for Dam Construction. Presented at Conference on Dam Safety, Stanford Univ., Palo Alto, CA, 1978.
3. S. O. Russell. Civil Engineering Risks and Hazards. British Columbia Professional Engineer, Jan. 1976.
4. H. Raiffa. Decision Analysis. Addison-Wesley, Reading, MA, 1970.
5. E. Hoek and J. W. Bray. Rock Slope Engineering, 2nd ed. Institute of Mining and Metallurgy, London, 1977.
6. S.-M. Chin. Cost as a Criterion for Evaluating Highway Level of Service. ITE Journal, Aug. 1978.
7. E. Kreyszig. Advanced Engineering Mathematics, 2nd ed. Wiley, New York, 1967, Section 18.10.
8. Pit Slope Manual: Chapter 5—Design. Canada Center for Mineral and Energy Technology, Department of Energy, Mines, and Resources, Ottawa, Canada, 1977.

Publication of this paper sponsored by Committee on Exploration and Classification of Earth Materials.

Abridgment

Advantages of Founding Bridge Abutments on Approach Fills

D. H. Shields, J. H. Deschenes, J. D. Scott, and G. E. Bauer

A set of controlled experiments has been carried out in which the ultimate bearing capacity at various locations within a granular approach fill for a spill-through bridge abutment was measured. It was shown that existing design procedures for spread-footing-supported abutments in approach fills are unduly conservative, and it is recommended that the experimentally determined bearing-capacity values be used as the basis for design.

Footing foundations would be competitive in cost with piled foundations for spill-through bridge abutments if the design bearing pressure for footings near slopes could be increased. That is, if the allowable bearing pressures could be located closer to the end slope of the approach fill, the resulting bridge length would be comparable to that of a bridge having a pile foundation.

Current bearing-capacity limits are based on theoretical considerations. This paper describes a set of controlled experiments in which the ultimate bearing capacity at various locations within a granular approach fill was measured. It was found that the theoretical approach seriously underestimates the capacity of footings close to the crest of a slope. Present indications are that piles can be omitted from existing spill-through abutment design, and the abutments can be placed directly on select, well-compacted gravel at lower cost. A concomitant benefit is that a footing-supported abutment and fill will settle as a unit; this will eliminate the maintenance cost often associated with bridge approaches that settle while the bridge itself does not.

In 1978, an actual underpass structure was built to a new design based on the tests reported here. The behavior of the structure is being monitored, and its performance will be compared with that of the corresponding model.

DEFINITION OF THE PROBLEM

Generally, one distinguishes two basic types of abutments—the retaining and the spill-through. In a retaining abutment, the approach fill is contained within the vertical abutment wall and the wing walls, whereas in the spill-through abutment, the approach fill is self-supporting and the bridge appears to rest on the fill near the top of the end slope. In fact, in the majority of cases, the bridge does not rest on the fill but is, instead, supported on piles that extend down through the fill to the natural soil or rock.

Why Use Piles?

Economics plays a large role in the design of bridges, in particular in the design of fairly routine highway and railway bridges of the overpass type. Based on present design practices, the economic advantage is nearly always in favor of founding spill-through abutments on piles rather than on spread footings. Generally, the bridge on spread footings is longer than the bridge on piles and the spread-footing alternative requires a fairly large zone of more-expensive, compacted select fill.

To design a spread footing for a spill-through abutment, the designer must resolve the dilemma of determining the probable ultimate capacity and settlement of the footing. At present, there are at least eight bearing-capacity theories that engineers can use, and all eight purport to take into account the effects of the proximity of the sloping face of the approach fill. The problem is that all eight give different answers.

Most of the theories are applicable only to a footing located right at the crest of the slope; only two—those of Meyerhof (1) and Giroud (2)—treat the general problem of the capacity anywhere within a slope and also use acceptable analytical techniques. Because it is unlikely that a designer would locate an abutment footing right at the crest at the end slope of the approach fill, Meyerhof's and Giroud's theories are the most widely used for design. Even then, the difference between the two theories can be considerable—particularly in dense material within the region close to the crest of the slope.

Figure 1. Basis for cost comparison.

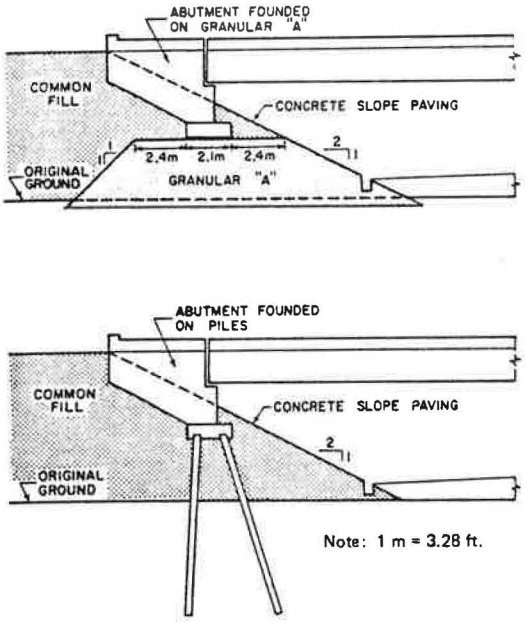

Table 1. Cost comparison for abutment footings: typical highway underpass structure.

Ontario Location	On Piles ($/bridge)	On Spread Footing ($)		Saving ($/bridge)
		Per Cubic Meter of Fill	Per Bridge	
Southwest	17 900	10.80	16 650	1 250
East	16 400	5.25	8 800	7 600
Central	16 950	7.85	12 300	4 650
North	20 000	3.90	7 000	13 000

Notes: 1 m³ = 1.31 yd³.
Costs in 1976 Canadian dollars (1.00 1976 Canadian dollar = 1.01 1976 U.S. dollars).

Figure 2. Locations of test footings.

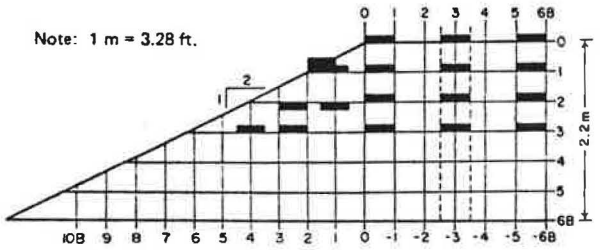

A New Look at the Footing Alternative

If experimental proof were available to show that existing design procedures for spread-footing-supported abutments in approach fills are unduly conservative, what economic benefit would there be in choosing spread footings over piles? This question can be approached as follows: Consider the possibility that a spread footing could be designed to carry an abutment located at the exact position of a pile-supported abutment; this would mean that the bridge length and thus cost would be the same. Consider also the possibility that the width of the footing would be equal to the width of the pile cap; this means that the abutments themselves would be the same, and they would cost the same. Thus, comparison of the costs of pile- and footing-supported abutments will be limited to comparing the cost of the piles and their installation with the cost of the select granular zone under the footing. The two systems compared are shown in Figure 1. The piled foundation is made up of thirty-eight 32.4-cm (12.8-in) outside-diameter, 9-m (30-ft) long, steel tube piles, each designed to carry 22.7 Mg (25 tons), and the spread-footing foundation is a 3.4-m (10-ft) thick zone containing approximately 1150 m^3 (1500 yd^3) of granular A. The cost-comparison results are shown in Table 1 (this comparison makes allowance for the fact that common fill would be required for the piled foundation so that the cost for granular A shown is the difference in cost between granular A and common fill).

The conclusions that can be drawn from this are that

1. In all cases, there is a saving in selecting the spread-footing foundation and
2. The magnitude of the saving depends on the cost of granular fill at the bridge location.

If longer piles were required to reach the bearing stratum or if cheaper gravel could be used (or both), the savings would be even greater.

Another advantage of using spread footings to carry bridge abutments in approach fills is that the bridge and the fill will settle together, and there will be no bump such as occurs when the abutment and the fill settle differentially. Of course, a settling abutment may not be desirable for a multispan continuous bridge structure.

PROVIDING THE PROOF

Given the worthwhile savings that could result from a change in spread-footing design practice, the Ontario Ministry of Transportation and Communications and the geotechnical group at the University of Ottawa conducted large-scale experiments to measure the bearing capacity of spread footings adjacent to a 2:1 slope of granular material—the standard design slope of the ministry. Two test series were envisioned—one series in compact material and another series in dense material. A grid of 12 footing locations was chosen for the tests (see Figure 2), and it was decided to make the footings long in comparison with their width to simulate an infinitely long, continuous strip footing in the tests.

Previous research (3) on footings on flat ground had indicated that a 300-mm (1-ft) wide footing is the minimum that can be used on granular soil to simulate a full-scale footing. This dimension controlled the size of the bin that was required in which to perform the tests. The actual bin (or sand box) is 15 m (50 ft) long, 2 m (6.6 ft) wide, and 2.2 m (7 ft) high, but it is divided into two equal-length bins 7.5 m (25 ft) long to facilitate material storage between tests. The width of the sand box was arbitrarily fixed at six times the width of the footing; because the footing stretched from one side of the bin to the other, the sides of the bin were made rigid so that the soil could move only in plane strain. The length of the test was ample to allow full development of the failure zone from under the footing out into the slope. [The test arrangement is described in detail by Shields and others (4).]

To overcome the potential error due to friction on the sides of the box, the footing was made in three equal parts or segments.

The next decision that had to be made was the choice of the granular material. Ideally, granular A should have been chosen but, because each test required moving 40-50 Mg of material, making obvious that mechanical handling would be required, and the equipment to pick up,

Figure 3. $N_{\gamma q}$ contours for dense sand.

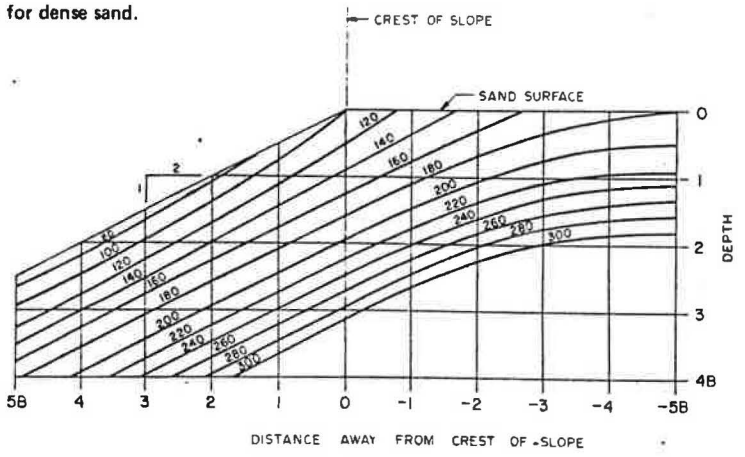

Figure 4. New (1978) bridge design.

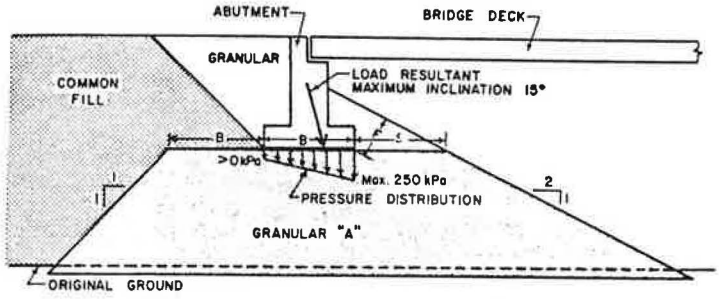

s depends on minimum frost depth F.

Note: 1 kPa = 6.89 lbf/in^2.

transport, and deposit the material in a controlled fashion could handle only sand, a crushed quartz sand was chosen to simulate the granular A. Tests showed that the quartz sand had a lower strength (lower angle of internal friction) and was more compressible (lower Young's modulus) than either crushed stone granular A or crushed gravel granular A at the same relative density. This meant that the footing tests on the sand would give results that were conservative with respect to the performance on gravel.

Test Procedure

Increments of load were applied to the footing until failure was reached. Each of the three footing sections was loaded independently, but all sections were forced into the sand at the same rate. The load on the middle section was recorded, as was the amount of settlement of the footing under each load.

Measurements were also made of the movement of the surface of the sand.

Test Results

Because the test results would have to be scaled up from the 300-mm-wide footing used in the sand box to field size [typically 1.8-4.6 m (6-15 ft)], the test results are presented in terms of $N_{\gamma q}$ contours, where $N_{\gamma q}$ = experimental bearing-capacity factors. Figure 3 shows the experimental results for dense sand. These results do not agree with either Meyerhof's or Giroud's theoretical values.

DESIGN RECOMMENDATIONS

For the present, it is recommended that the experimental $N_{\gamma q}$ values be used empirically as the basis for the design of abutment footings in approach fills. It seems, therefore, that bridge lengths can be comparable for both pile- and footing-supported abutments and that the economic advantages of footings will in fact be realized.

The bridge structure built in 1978 to the new specifications is shown in Figure 4. The movement of the structure is monitored, as is the overall settlement behavior of the approach fill. The structure is instrumented to measure the distribution of bearing pressures on the foundation and the earth pressures on the vertical surfaces. One goal is to ascertain the actual direction and location of the resultant force on the foundation.

As a cautionary note, it must be noted that many spill-through abutments act partly as retaining walls; the resulting horizontal earth pressures lead to foundation loads that are inclined and eccentric. A series of tests have recently been completed in the sand box to determine the reduction in bearing capacity that is brought about by inclining the load 15° to the vertical, and size effects have been studied by carrying out tests in which a 600-mm (2-ft) wide footing was used.

ACKNOWLEDGMENT

The financial support of the National Research Council of Canada, which enabled the test facility to be built and maintained, is gratefully acknowledged. GKN Keller (Canada) Limited donated the sand spreader. The project was financed by the Ontario Ministry of Transportation and Communications. J. Keen of the ministry supplied the cost estimates for the comparison between footing and pile foundations.

REFERENCES

1. G.G. Meyerhof. The Ultimate Bearing Capacity of Foundations on Slopes. Proc., 4th International

Conference on Soil Mechanics and Foundation Engineering, London, England, Vol. 2, 1957, pp. 301-332.
2. J. P. Giroud and Tran-Vo-Nhiem. Force Portante d'une Fondation sur une Pente. Annals d'Institute Technique Bâtiment et des Travaux Publiques: Serie—Théorie et Methodes de Calcul, Paris, No. 142, 1971.
3. Y. Lebegue. Essais de Fondations Superficielles sur Talus. Proc., 8th International Conference on Soil Mechanics and Foundation Engineering, Moscow, U.S.S.R., Vol. 4.3, 1973, p. 313.
4. D. H. Shields, J. D. Scott, G. E. Bauer, and A. Barsvary. Bearing Capacity of Foundations near Slopes. Proc., 9th International Conference on Soil Mechanics and Foundation Engineering, Tokyo, Japan, June 1977.

Publication of this paper sponsored by Committee on Foundations of Bridges and Other Structures.

Pile Design and Installation Specification Based on Load-Factor Concept

G. G. Goble, Fred Moses, and Richard Snyder

The use of load-factor procedures for the design of bridge superstructures is expanding rapidly. However, substructure design is still based exclusively on allowable stress methods. This paper presents an approach to load-factor design for pile foundations. The load factors suggested follow the current American Association of State Highway and Transportation Officials recommendations, while the resistance factors recommended are based on the capacity-determination methods and the construction control procedures used. Actual values are selected to be consistent with currently used procedures where they are available. The proposed specification can provide a framework for the use of more-appropriate resistance factors as they become available from ongoing research.

About two decades ago, dramatic changes began to occur in structural design philosophy. Before that time, structural designers sought to develop structural systems that would resist the effects of expected load applications with no structural distress. This was achieved by requiring that the stresses calculated by an elastic analysis of the structure when subjected to the expected design or working load not exceed some accepted, allowable stress. These allowable stresses were usually defined either explicitly or implicitly as a fraction of the yield or ultimate strength of the material involved. The fact that the loads were statistically distributed with substantially different probabilities of occurrence of different types of loads was ignored. Design loads were developed, and their effects on the structure were analyzed deterministically.

There are clear advantages to this approach. The structure is subjected to an elastic analysis, and the limit on allowable stresses is placed well below the elastic region, so it can be expected that, even though the structural engineer is primarily concerned with the design of a structure having sufficient strength, many serviceability questions will be satisfied indirectly. For instance, in such an approach, one can expect that deflections will be tolerable and acceptable. The structure is subjected to elastic analysis and, therefore, indirectly deflections are controlled.

Another important but less understood advantage of an elastic-analysis-and-working-stress approach is that there is a clear and direct redesign process available to the structural engineer. Those portions of the structure that are found in the analysis to be overstressed can be increased in size while parts of the structure where stresses are less than the allowable can be decreased in size. This approach provides a simple redesign algorithm.

There are also important disadvantages to working-stress design. For instance, a statically indeterminate structure that has a high degree of redundancy will have a different factor of safety to collapse than will a statically determinate structure. When such structures are designed by working-stress procedures, the actual factor of safety (FOS) for a particular structure can vary considerably. Because the loads that must be carried by the design can come from a variety of sources, the accuracy and reliability of the determination of their magnitude can vary widely. Likewise, our ability to predict the behavior of various types of structural elements varies, as does the consequence of failure (the collapse of a column is usually more serious than is a beam failure). There are other considerations that motivate the change in practice. For instance, the behavior of reinforced concrete members does not satisfy working-stress analysis because of time-dependent and inelastic deformations.

On the other hand, if working-stress analysis is completely abandoned for an exclusively strength-design-based procedure, then difficulties can arise with other performance aspects of the structure. For example strength evaluation procedures completely neglect questions of deflection.

In summary, traditional working-stress design procedures have come under criticism because they do not recognize the statistical distribution of loads and the nondeterministic character of structural-element strength. These factors, together with considerations of the varying consequences of failure for different element types, all point to the need for design procedures that will produce factors of safety that include these consequences.

One solution is the procedure known as limit-state design or load-and-resistance-factor design. This procedure deals directly with the questions involved in structural design. The structure is designed to satisfy requirements of strength and serviceability, both directly and separately. By serviceability in structural design,

we are referring to such considerations as deflection, long-term deformation, vibration, and corrosion control.

Strength considerations are solved directly by specifying the FOS of component behavior. This FOS, however, can vary because the method recognizes that, under different conditions, different FOSs are appropriate. For instance, if the magnitude of the load applied to a structure is well known, then it is reasonable to use a smaller FOS than that used when the load magnitude is variable.

Other factors that affect such design procedures include considerations of the reliability of member performance. For example, the flexural behavior of an underreinforced concrete beam can be accurately predicted and, furthermore, the member will show a substantial deflection before it loses the capability of carrying a small amount of increasing load. It gives a strong warning of impending failure. On the other hand, in a reinforced-concrete column, the same material will exhibit less ductility and give much less warning of failure. It is appropriate that the FOS in the first case be smaller than that in the second. An example of this development is the American Concrete Institute (ACI) ϕ-factor for different concrete elements. This kind of an approach to design is particularly well suited to the design of pile foundations. In fact, it may be well suited to all kinds of foundations, although only pile foundations will be discussed here.

Let us consider one further problem currently faced by the structural designer when he or she approaches the design of either a pile-supported foundation or a spread footing. As elements are proportioned, usually from the top of the structure downward, the loads are collected and carried along. At the base of the structure, the foundation loads are collected. However, these loads, which are derived from the structural design, will be in the form of a factored load to be applied to the ultimate strength of the foundation. But current practice requires that soil limitations be handled in terms of working loads, and so working loads appropriate to the design of this particular element must be assembled. After the allowable soil loads imposed by the foundation engineer are satisfied, the design of the footing element itself must be accomplished by using a load-and-resistance-factor procedure. This approach is not only inconvenient but also lacks philosophical clarity. It means, for example, that a footing is proportioned for loads that are above the values permitted for the foundation soil.

The problem is further complicated by the fact that, during the evaluation of the strength of a pile foundation, the foundation engineer will probably determine the ultimate capacity of an individual pile. He or she or the structural engineer will then assign a rather arbitrary FOS. Traditionally, for well-controlled designs, this number is approximately two. In current practice in the United States, however, it varies widely. Surely, it should be related to the procedures that are used in design and construction control.

In this paper, the framework for a design specification for pile foundations is proposed that avoids the inconvenience of dealing with both factored and working loads and, at the same time, provides a more-rational approach for dealing with pile design. The specification used as the framework is the American Association of State Highway and Transportation Officials (AASHTO) bridge design specification.

The definition of FOS has been rather loosely used in working-stress design. The designer generally defines the FOS as the structural strength divided by the working load. In the context of load-factor-based design, the nomenclature must be used more carefully. The structural strength is actually not so easily defined. This is also true for pile performance where we do not yet have a generally accepted procedure for evaluating even the results of a static load test. In the remainder of this paper, the term FOS will refer specifically to the ratio between the defined or nominal element strength and the working load.

This specification, as is the case for most load-factor design procedures, divides the FOS into two parts. The first part is the factor that is applied to each design load. It is usually expressed as a constant appropriate to the particular type of load multiplied by the nominal load in question; a much larger factor is used for live loads because their intensities and load effects are not as accurately predicted as is the dead-load effect. The other portion of the FOS is used to reduce the predicted or nominal strength of a structural element and is based on an evaluation of the accuracy with which this element capacity can be predicted, the variability of the element capacity, the warning of failure that it will give, and the consequences of failure.

Thus, serviceability conditions are handled directly in load-factor design procedures. This specification divides the problem of determining an acceptable pile design into three separate considerations: strength, serviceability, and driveability. In the context of pile foundations, serviceability refers to such factors as long-term settlements, corrosion, and other such considerations. These factors, although frequently difficult to analyze, are very important in pile design.

One reason for the low allowable stresses that are enforced on some types of piles is the consideration that sometimes they cannot be installed to higher working loads due to driving difficulties. It seems unrealistic to limit allowable stresses in all piles because some of them cannot be installed for those stresses. Driveability should be evaluated as a separate consideration.

DESIGN FOR STRENGTH

The selection of a pile design based on strength considerations involves ensuring that the applied load is less than the pile strength. Because both the load and the strength show a statistical variation, the purpose of the FOS is to ensure that the probability that the strength will be less than the load is sufficiently small. This requirement is summarized in Figure 1. Figures 1a and 1b illustrate hypothetical distributions of load and strength (normal distribution assumed). When these curves are superimposed (Figure 1c), the crosshatched area is related to the portion of the cases where failure will occur (the load is less than the strength). Figure 1d shows the effect of increased variability. Even though the average strength is the same in both cases, the probability of failure will be greater for the case having the greater variability.

In the AASHTO bridge code, the load expression is currently defined in load-factor form as

$$U = 1.3 [D + (5/3 L)] \quad (1)$$

where U = factored load, D = actual dead load, and L = working live load. (The AASHTO bridge design specification also contains additional ultimate-load equations that must be satisfied, and Equation 1 is in a more-complex form, but these complicating details will not be discussed here.)

In foundation design for bridges, the contribution of the dead load is usually the dominant influence. Therefore, the foundation loads can be approximated by

$$U = 1.3D \quad (2)$$

Figure 1. Effect of variability of distribution of load and strength on frequency of failure.

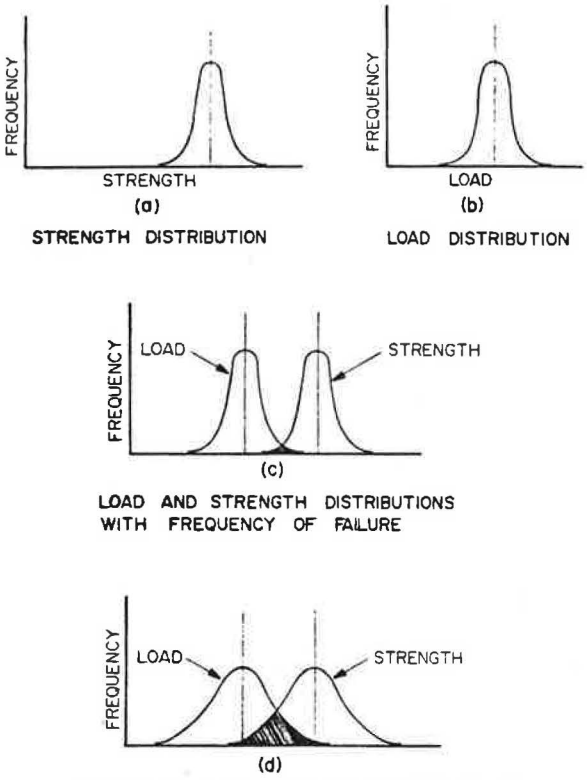

To ensure adequate safety against failure, the nominal ultimate strength of the pile (R') must be reduced by a strength safety factor (ϕ). Thus,

$$R = \phi R' \quad (3)$$

where ϕ = resistance factor (in the AASHTO specification, this is called the capacity-modification factor) and R' = nominal ultimate strength. A design is acceptable if

$$R > U \quad (4)$$

Because the factors to be applied to the load are already specified, it is only necessary to determine appropriate values for ϕ. Consider the ways in which a pile can fail. First, it can fail due to structural failure (an infrequent occurrence) and, second, it can fail by penetration into the ground. In the first case, values of ϕ have already been defined for columns in specifications such as the ACI building design specification; a value of 0.7 seems appropriate when applied to piles. Further refinement of this value for particular pile types will probably be necessary.

The establishment of ϕ for the second failure mode is more difficult. In order that ϕ be related to the variability of the pile strength, it should be dependent on the means used to establish pile capacity, the variability of the soil, and the construction control procedures used. Six different procedures now in use can be defined.

1. Case-method analyzer with static load test: One of the initial production piles is driven to the required ultimate capacity as determined by the case method analyzer (1), making allowance for the estimated setup or relaxation. Blow counts are recorded. After a wait time sufficient to allow the pore water pressure to dissipate, a static load test is performed to failure. After completion of the static load test, the pile is restruck and tested by the case-method analyzer, and the blow count is again recorded. The dynamic record is examined for pile damage (2), and any necessary adjustments are made in the driving criteria. Additional pile tests are made by the case method analyzer.

2. Static load test: One of the initial production piles is driven to the required ultimate capacity as determined by wave equation analysis, making allowance for estimated setup or relaxation. Blow counts are recorded. After a wait time sufficient to allow the excess pore water pressure to dissipate, a static load test is performed to failure. Any necessary adjustments are made in the driving criteria by using the wave equation analysis. Additional piles are proof-load-tested statically to the specified ultimate capacity.

3. Case-method analyzer: One of the initial production piles is driven to the required ultimate capacity as determined by the case-method analyzer, making allowance for the estimated setup or relaxation. Blow counts are recorded. After a wait time sufficient to allow the excess pore water pressure to dissipate, the pile is restruck and tested by the case-method analyzer, and the blow count is again recorded. The dynamic record is examined for pile damage, and any necessary adjustments are made in the driving criteria. Some additional piles are tested by the case-method analyzer.

4. Wave equation analysis: The driving criteria are set by wave equation analysis, making allowance made for setup or relaxation. Blow counts are recorded. After a wait time sufficient to allow the excess pore water pressure to dissipate, selected piles are restruck, and the blow count is carefully measured at the beginning of the restrike.

5. Analysis based on soil data (static analysis): The required depth of penetration is set by an appropriate static analysis based on soil boring data. The piles are driven to that penetration independent of blow count.

6. Dynamic formula: The driving criteria is set by use of the dynamic formula, making allowance for setup or relaxation. The formula is written without a safety factor. Blow counts are recorded. After a wait time sufficient to allow the excess pore water pressure to dissipate, selected piles are restruck, and the blow count is carefully measured at the beginning of the restrike.

It is difficult to derive rational values for ϕ because sufficient data are not available for a thorough, systematic analysis. The table below presents recommended values together with total FOSs that exist when used with the AASHTO load factors, assuming dead load (1.30) is dominant.

Inspection Class	Uniform Soil		Variable Soil	
	ϕ	Total FOS	ϕ	Total FOS
1	0.70	1.86	0.70	1.86
2	0.65	2.00	0.60	2.17
3	0.55	2.36	0.55	2.36
4	0.45	2.89	0.45	2.89
5	0.35	3.71	0.35	3.71
6	0.22	5.91	0.22	5.91

These values were selected by correlating the FOS with current practice. Therefore, inspection class 2 has a total factor of safety of 2.0 (assuming dominant dead loads). This case is judged to be the currently widely used and well-established practice. The use of a dynamic formula gives the traditional FOS of 6.0. The other values were established by interpolation.

DESIGN FOR SERVICEABILITY

Serviceability considerations are very important in pile foundation design. Of primary interest are long-term deformations (settlements). Reliable and accurate settlement computations for pile foundations are very difficult to make. They must be made by using nominal loads, and they should be calculated independently of strength evaluations. Other serviceability limitations (for example, durability) tend to involve subjective judgment and are not directly related to structural considerations. (Further discussion of serviceability considerations is beyond the scope of this paper.)

DESIGN FOR DRIVEABILITY

In the past, attempts have been made to place simple limitations on some pile and driving system parameters to ensure that critical driving stresses are not exceeded. The question of tension stresses induced in concrete piles during easy driving is of particular concern. The most common approach has been the arbitrary limitation of pile-ram weight ratios. These limitations have been shown to be inadequate and even incorrect (3).

It may be possible to solve the problem by using closed-form solutions of the one-dimensional wave equation, but this has not yet been done. The most reliable approach is the use of a wave equation computer program. However, the program must properly model the driving system, and proper input data must be used.

If a wave equation analysis is used, the next question that arises is the determination of acceptable values for dynamic driving stresses. Because this is a short-term load that can be controlled, it is reasonable to approach closely to the failure stress. Furthermore, the only consequence of failure during installation is that a pile must be replaced (providing that proper inspection methods are being used).

Allowable driving stresses for steel and prestressed concrete piles are usually given in terms of yield stress (Fy) and 28-day cylinder strength (f'_c), respectively.

Material	Allowable Stress
Steel	$0.85F_y$
Concrete	
Compression	$0.8f'_c$
Tension	$3(f'_c)^{1/2}$

COMMENTS AND DISCUSSION OF PROCEDURE

The load-factor design procedure is now the dominant method for structural design, and its use is increasing. However, it has not yet been used for foundation design, even though it fits well philosophically with the methods of foundation design, particularly for deep foundations. The AASHTO bridge design specification load-factor expressions were used in organizing this specification. Of course, other codes could have been used equally well, since they all have the same general form.

Other construction control procedures can be inserted into this framework, and improvements in the state of the art can be readily incorporated. Proper and reasonable ϕ factors must be used. The use of such a procedure may encourage the assembly of additional pile load test data (to failure) so that improved ϕ factors can be determined.

One of the important attractions of the procedure described in this paper is that the cost trade-off of improved field testing and construction control can be directly evaluated. Thus, the engineer can show the owner the advantages of improved engineering on large jobs.

The field-testing and construction-control procedures are not described in detail because those aspects are beyond the scope of this paper. It should be noted that emphasis is placed on restrike testing. This procedure is one of the most important tools for improving pile-capacity analysis. It is usually quite inexpensive to perform and will probably justify increased capacities. On the other hand, one of the most dangerous problems is the relaxation of pile capacity, which can be detected by restrike testing.

One of the principal advantages of the load-factor philosophy is the separation of strength and driveability considerations. At present, allowable stresses in steel and timber piles are held at a low level because sometimes such piles cannot be driven to higher capacities due to excessive driving stresses. The two problems are quite unrelated and should be separated and dealt with independently.

Pile foundation design specifications have remained essentially unchanged for several decades. During this same time, structural design codes and procedures have undergone a gradual change to greater rationality and realism. The procedures suggested in this paper will accomplish the same thing for pile foundation design.

ACKNOWLEDGMENT

A portion of the work discussed in this paper was sponsored by the Federal Highway Administration. However, this agency has not adopted these procedures and does not necessarily support the opinions expressed here.

REFERENCES

1. G. G. Goble, G. E. Likins, and F. Rausche. Bearing Capacity of Piles from Dynamic Measurements. Ohio Department of Transportation, Columbus, March 1975.
2. F. Rausche and G. G. Goble. Determination of Pile Damage by Top Measurements. Presented at ASTM Symposium on Behavior of Deep Foundations, Boston, MA, June 1978.
3. G. G. Goble, G. E. Likins, and K. Fricke. Driving Stresses in Concrete Piles. Prestressed Concrete Institute Journal, Vol. 21, No. 1, Jan.-Feb. 1976.

Publication of this paper sponsored by Committee on Foundations of Bridges and Other Structures.

Prediction of Shear Strength of Sand by Use of Dynamic Penetration Tests

Harry M. Coyle and Richard E. Bartoskewitz

Texas cone penetrometer tests were conducted at six sites in the middle and upper Texas gulf coast region. The soils tested were cohesionless and included poorly graded sands and silty sands. The direct-shear test method was used to determine the effective angle of internal shearing resistance of the soils, and an empirical relationship was used to obtain standard penetration test values from the measured Texas cone penetrometer test data. The standard penetration test N-values of fine and silty saturated sands were corrected to account for the development of pore pressures during driving. Both the Texas cone and the standard penetration test N-values were correlated with the shear strengths and with the effective angles of internal shearing resistance of the sands. The new correlations were compared with existing correlations commonly used in the geotechnical profession, and it was found that the currently used relationships between the N-value and the effective angle of internal shearing resistance are a lower bound for these test data.

Soil sounding or probing consists of forcing a rod into the soil and observing the resistance to penetration. According to Hvorslev (1), "variation of this resistance indicates dissimilar soil layers, and numerical values of this resistance permit an estimate of some of the physical properties of the strata." The oldest and simplest form of soil sounding consists of driving a rod into the ground by repeated blows of a hammer. The penetration resistance in this dynamic test is defined as the number of blows (N) that produces a penetration of 1 ft.

In the United States, the most commonly used dynamic penetration test is the standard penetration test (SPT). The results of the SPT can usually be correlated with the pertinent physical properties of a sand. Meigh and Nixon (2) have reported the results of various types of in situ tests at several sites and have concluded that the SPT gives a reasonable, if not somewhat conservative, estimate of the allowable bearing capacity of a fine sand. Gibbs and Holtz (3) have found that a definite relationship exists between the N-value as determined from the SPT and the relative density of a sand. A relationship between the N-value and the effective angle of shearing resistance, which has become widely used in foundation design procedures in sands, has been reported by Peck, Hanson, and Thornburn (4).

The Texas State Department of Highways and Public Transportation (TSDHPT) currently uses a penetration test similar to the SPT for investigation of foundation materials encountered in bridge-foundation exploration work. The penetration test is especially useful in investigations in cohesionless soils because of difficulties in obtaining undisturbed samples for laboratory testing. According to the Texas foundation manual (5), "the design of foundations in cohesionless soils is generally based upon visual classification and penetrometer test data." The Texas cone penetrometer (TCP) test consists of dropping a 756-N (170-lbf) hammer 0.61 m/blow (2 ft/blow) to drive a 7.6-cm (3.0-in) diameter cone that is attached to the end of the drill pipe. The details of the cone penetrometer are shown in Figure 1. The penetrometer is first lowered tc the bottom of the bore hole and driven 12 blows to seat it in the soil. Then, the penetrometer test is started and the number of blows (the N-value) required to produce the next 1 ft of penetration is recorded.

The objective of the study reported in this paper was to develop an improved correlation between the N-value (in blows per foot) obtained by using the TCP test or the SPT and the drained shear strength of a cohesionless soil. Correlations were developed for two types (as defined by the Unified Soil Classification system) of soils:

1. SP—poorly graded sands, gravelly sands, and little or no fines and
2. SM—silty sands and poorly graded sand-silt mixtures.

SAMPLING PROGRAM

Correlating shear strengths with penetration test N-values requires that undisturbed sand samples be collected and penetration tests be carried out at corresponding depths at the same test site. This requires a sampling procedure in which a relatively large number of samples can be recovered and tested with minimal disturbance.

Previously used methods for collecting undisturbed samples of cohesionless soils were investigated first. Methods such as solidification of the lower end of the sample by chemical injection or freezing (6) and solidification of the sand before sampling by asphalt injection or by freezing the soil by the use of a cooling mixture in auxiliary pipes (1) do not always produce undisturbed samples and are very elaborate and expensive. Also, according to Bishop (7), mechanical core retainers, such as that used in the Denison sampler, cause excessive disturbance in clean sands.

With the aid of personnel from TSDHPT, a sampling apparatus similar to a small-diameter Shelby tube sampler was developed. This sampling device (see Figure 2) consists of a thin-walled sampler that has a coupling head to adapt the sampler to the drilling rod. A check valve in the coupling head allows the drilling fluid to escape while the sample tube is lowered to the bottom of the borehole and prevents the water pressure in the drilling rod from forcing the sample out of the sampler during extraction. Two vent holes above the check valve allow the drilling fluid to drain from the drilling rod while the sample tube is being extracted from the bore hole.

The sample tubes were made of either stainless or galvanized steel and had an outside diameter of 44.09 mm (1.736 in) and a wall thickness of 1.91 mm (0.075 in). For minimum disturbance (1), it is preferable that area ratio of the sampler not exceed 10-15 percent as computed by using Equation 1:

$$\text{Area ratio} = \text{volume of displaced soil/volume of soil} = (D_w^2 - D_e^2)/D_e^2 \quad (1)$$

where D_w = outside diameter of sample tube and D_e = inside diameter of sample tube. The area ratio of the chosen sampler was 20 percent, very close to this limit. In a preliminary field study, the 254-mm (10-in) and 305-mm (12-in) diameter samplers were found to permit the best recovery.

The borings were made by using a truck-mounted Failing 1500 rotary-core drilling rig. As the hole ad-

Figure 1. Details of Texas cone penetrometer.

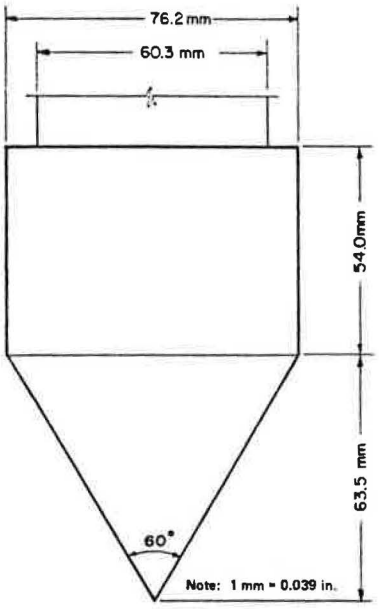

Figure 2. Cross section of sampling apparatus.

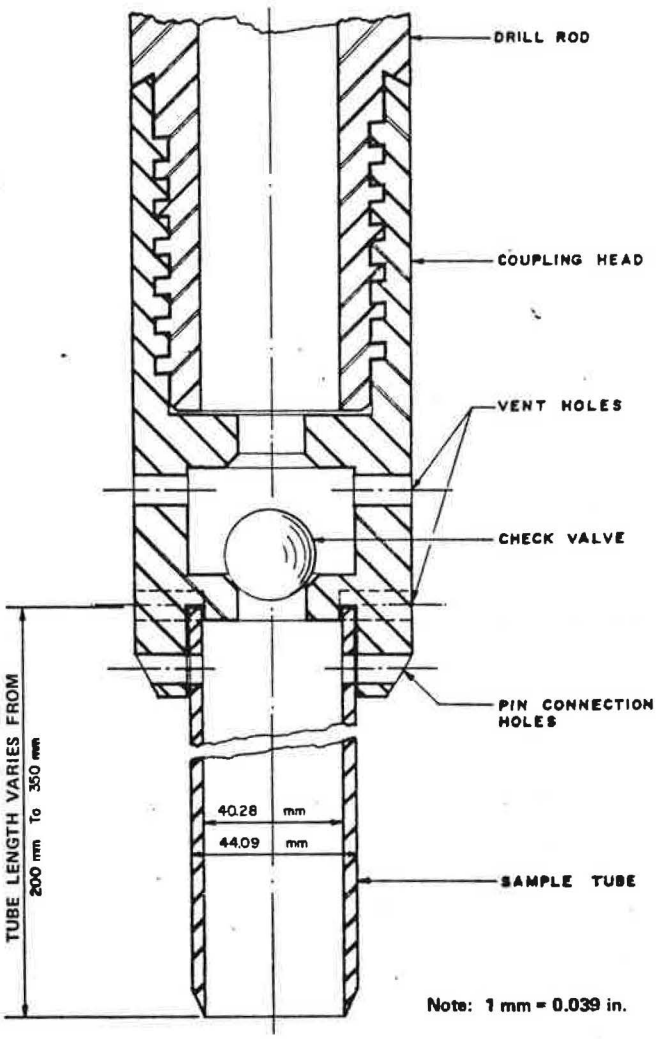

vanced through cohesive material, continuous Shelby tube samples were taken and selected samples were kept for visual observation and unit weight determination. Once the sand stratum from which the undisturbed samples were to be taken was encountered, cuttings were removed by washing through the Shelby tube. The small-diameter sampler and coupling head were then attached to the drilling rod. The sampler was pushed in a rapid continuous motion by a hydraulically powered pull-down. After extraction from the bore hole, the sampler was removed from the coupling head and the cuttings at the top of the sample tube were observed. Any indication of overpushing was recorded, along with the depth of the sample and its visual classification. The sample tube was then sealed on each end, covered with paraffin, and packaged for transportation to the soils laboratory.

TEST PROGRAM AND SITES

The test program was conducted by a TSDHPT soil investigation team in cooperation with Texas Transportation Institute personnel. Standard practices of field investigation as described in the foundation manual (5) were followed. The purposes of the field investigation were to

1. Establish the location of the groundwater table,
2. Obtain a soil description by visual inspection of samples,
3. Obtain TCP N-values, and
4. Obtain undisturbed samples for laboratory testing.

After the undisturbed sand samples were obtained, the TCP test was performed at corresponding depths at each test site. The penetrometer tests were conducted in new boreholes located not more than 3.05 m (10 ft) from the holes from which the soil samples had been obtained.

Because the boreholes were advanced by using a 76-mm Shelby tube sampler, samples of the cohesive soils could be kept for determination of their unit weight whenever there was an indication of change in soil properties. The unit weights and moisture contents were determined from the Shelby tube samples in the conventional manner. The Unified Soil Classifications, moisture contents, and total unit weights of the cohesionless soils were determined from the small-diameter samples. To determine the Unified Soil Classification, mechanical sieve analysis and Atterberg limits were conducted.

Five test sites were investigated and eight borings were made during the period of September 1974-August 1975. [Complete laboratory and field data for these sites are reported elsewhere (8).] One additional test site was investigated and one boring was made during the period of September 1975-August 1976. [Laboratory and field data for this site are reported elsewhere (9).] The test sites investigated in 1974-1975 were located in Brazos County near College Station (sites A, B, and C) and in Harris County near Houston (sites D and E). The test site investigated in 1975-1976 was located in Nueces County near Corpus Christi (site F).

Typical boring logs for two of the test sites are shown in Figures 3 and 4. Figure 3 shows the log of boring no. 3 at test site A, where the soil was essentially all sand. (Because the penetration resistance is defined in terms of U. S. customary units, SI units are not given for this quantity and the depth below ground at which it is measured in Figures 3, 4, 7, and 8 and in Table 1.) Figure 4 shows the log of boring no. 1 at test site D, where alternating layers of clay and sand occurred. Overall, penetration tests were conducted at depths of 1.8-21.4 m (6-70 ft), and N-values ranged from 20 to 330 blows/m (6 to 100 blows/ft).

Figure 3. Log of boring 3: site A—TX-30.

DEPTH, FEET	SOIL SYMBOL	SAMPLE	DESCRIPTION OF STRATUM	UNIFIED CLASSIFICATION	PERCENT PASSING NUMBER 200 SIEVE	MOISTURE CONTENT, PERCENT	TOTAL UNIT WEIGHT, kN PER CU M	THD PENETROMETER TEST N VALUE, BLOWS PER FT
			Note: 1 m = 3.28 ft; 1 kN/m³ = 6.4 lbf/ft³.					
5			BROWN LOOSE SILTY SAND	SM	15.0	5.1	15.5	6
8					10.9	6.0	16.3	6
10					—	6.5	15.9	20
13				SP-SM	11.5	11.9	16.6	20
15					—	21.0	19.4	—
16			TAN AND LIGHT GRAY STIFF SILTY CLAY					

Figure 4. Log of boring 1: site D—Woodridge Road.

DEPTH, FEET	SOIL SYMBOL	SAMPLE	DESCRIPTION OF STRATUM	UNIFIED CLASSIFICATION	PERCENT PASSING NUMBER 200 SIEVE	MOISTURE CONTENT, PERCENT	TOTAL UNIT WEIGHT, kN PER CU M	THD PENETROMETER TEST N VALUE, BLOWS PER FT
			Note: 1 m = 3.28 ft; 1 kN/m³ = 6.4 lbf/in³.					
10			TAN AND LIGHT GRAY PLASTIC CLAY WITH CALCAREOUS NODULES			12.1	21.0	
						17.7	20.7	
						21.5	20.1	
						21.5	20.0	
				SM	34.1		19.6	22
20			TAN FINE SILTY SAND					
				SP-SM	12.7	24.7	19.4	48
				SP-SM	5.8	21.6	19.2	33
						27.5	18.7	
30			TAN AND LIGHT GRAY STIFF TO VERY STIFF SILTY CLAY WITH CALCAREOUS NODULES			13.9	21.6	
						18.5	21.1	
						31.1	19.3	
			WHITE FINE SILTY SAND	SM	24.9	20.4	21.2	30
40						16.0	20.9	
			TAN AND LIGHT GRAY STIFF TO PLASTIC CLAY			16.2	21.0	
						17.4	20.8	
						18.4	21.0	
						17.2	20.9	
50			LIGHT GRAY FIRM SILTY SAND	SPSM	11.7	22.6	19.7	80
				SM	20.7	27.6	18.8	68

LABORATORY INVESTIGATION

The purpose of the laboratory investigation was to determine the drained shear strength of the cohesionless samples. The direct shear test was used to determine the effective angle of shearing resistance which, in turn, was used to calculate the drained shear strength. First, cuttings were removed from both ends of the sample, and the total unit weight of the sample remaining in the tube was determined. Then the sample tube was placed in the extrusion device shown in Figure 5, and the direct shear box was inverted and placed over the tube. The sample was extruded into the box until the end plates made contact with the restraining pins in the base of the shear box. The samples were trimmed by using a 0.02-mm (0.001-in) thick trimming device. The box was then removed from the extrusion device and placed upright in the direct shear loading apparatus for testing.

The test setup used for the drained direct shear tests to determine the angle of shearing resistance is shown in Figure 6. A normal stress was applied on plane a-a through the loading frame by a constant-speed motor that turned the lower half of the shear box while the upper half was held in place by a horizontal arm and thus caused a relative motion between the two halves. The force required to hold the arm was determined by readings on a proving ring. The shearing force was increased until the sample failed along plane a-a. Three tests were performed at normal stresses of 69, 138, and 207 kPa (10, 20, and 30 lbf/in^2). The shear strength of the sample corresponding to each normal stress was determined by dividing the maximum force required to shear the sample by the cross-sectional area of the sample. A failure envelope was then plotted by using the shear stresses at failure and the corresponding normal stresses. The angle of shearing resistance (ϕ') is the angle between the failure envelope and the horizontal.

In this test, it is necessary to use a strain rate that allows drainage during testing. As noted by Means and Parcher (10), a number of investigators have shown that the strength of a soil tested in the laboratory depends "to a remarkable extent upon the rate and duration of loading employed in the test." In his text (11), Lambe states that "rapid shear of saturated (cohesionless) soil may throw stresses into the pore water, thereby causing a decrease in strength of a loose soil or an increase in the strength of a dense soil." A sample of silty sand [21 percent passing the 75-μm (no. 200) sieve] from test site E was used to investigate the effect of the rate of loading, and it was found that varying the strain rate from 0.002 to 0.13 mm/min (0.0001 to 0.005 in/min) resulted in a difference in the angle of shearing resistance of only 1°. Thus, a strain rate of 0.13 mm/min was considered suitable to allow drainage and thereby prevent pore pressure from building up.

Unit weights of both small-diameter and standard Shelby tube samples were determined. In general, samples taken at approximately equal depths had unit weights that were in very close agreement, independent of the method of sampling. At test sites where several consecutive small-diameter samples were taken, consistency in the unit weights was observed. This consistency was especially noticeable at test site E where an obviously dense material (N > 100) was encountered; for this test site, the three samples tested had unit weights (determined from the small-diameter samplers) of 21.49-21.62 kN/m^3 (136.8-137.6 lbf/ft^3), These two factors—the independence of the unit weights from the method of sampling and the consistency of the unit weights at each test site—indicate that the unit weights determined from the small-diameter samplers are of acceptable accuracy.

The shear strength at depths corresponding to the depths at which penetrometer tests were conducted was determined by using the general Mohr-Coulomb relationship:

$$s = c' + \sigma_n' \tan \phi' \quad (2)$$

Figure 5. Cross section of extrusion assembly.

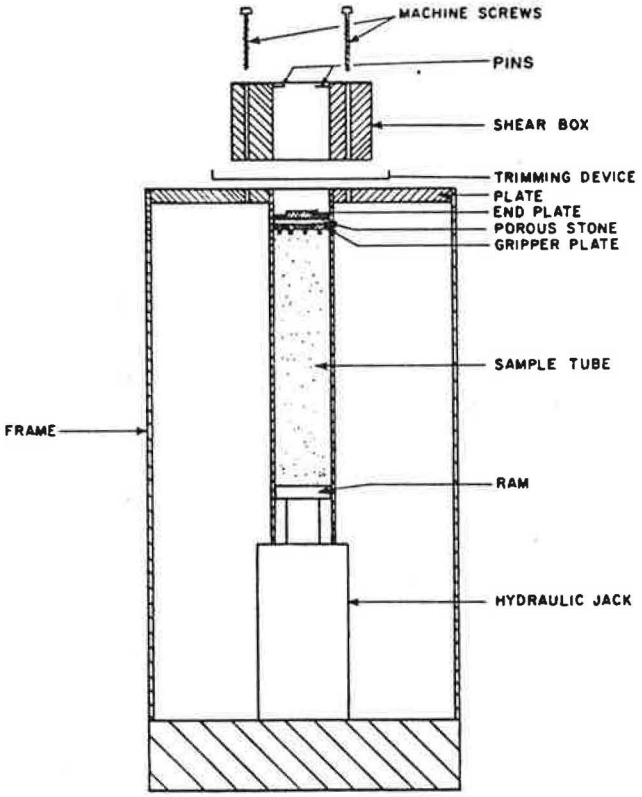

Figure 6. Direct shear equipment.

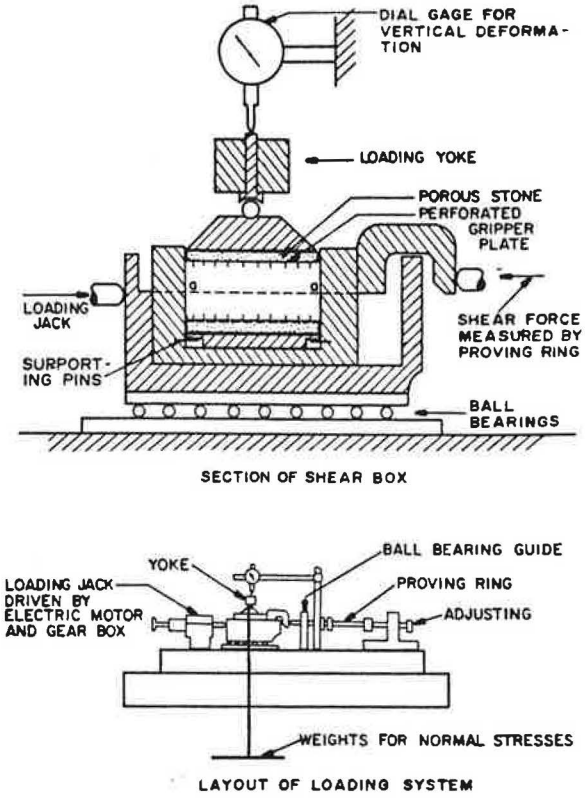

where

s = effective shear strength of soil,
c' = effective cohesion,
σ_η' = effective normal stress, and
ϕ' = effective angle of shearing resistance.

For drained tests conducted on cohesionless soils, $c' = 0$, and therefore

$$s = \sigma_\eta' \tan \phi' \quad (3)$$

The normal stress at a point above the groundwater level is equal to the overburden pressure (p), which is calculated by using the relationship:

$$\sigma_\eta = p = \gamma h \quad (4)$$

where

σ_η = normal stress,
γ = unit weight of soil, and
h = depth below ground surface.

The stress below the groundwater level, however, must be calculated by using the effective overburden pressure (p'). If it is assumed the pore-water pressure is hydrostatic, this can be expressed as

$$p' = (\gamma - \gamma_\omega)h \quad (5)$$

where γ_ω = unit weight of water and h = depth below the groundwater level. The shear strength is then calculated by combining the overburden pressure (based on averaged unit weights for the soil strata) contributed by each soil stratum above and below the groundwater level with the effective angle of shearing resistance as in Equation 3.

For various depths at test sites A and D, typical average unit weights, angles of shearing resistance, shear strengths calculated by using these data and information about the position of the groundwater level, and corresponding N-values are summarized in Figures 7 and 8, respectively.

DEVELOPMENT OF CORRELATIONS

The relationship between TCP test N-value (N_{TCP}) and ϕ' for sand used by the TSDHPT is represented by the solid curve shown in Figure 9 (5). As can be seen from this figure, this relationship forms a lower bound for the data obtained in this study, although the scatter in the data does not warrant the establishment of a new curve. However, the current relationship is apparently conservative.

Based on the data shown in Figure 10, Touma and Reese (12) have proposed the following general relationship between N_{TCP} and the SPT N-value (N_{STP}):

$$N_{SPT} = 0.5 N_{TCP} \quad (6)$$

where N_{SPT} and N_{TCP} are both expressed in blows per foot.

Bowles (13) recommends the use of Equation 7 for very fine or silty saturated sand (below the water table) if the measured penetration number (N) is greater than 15:

$$N'_{SPT} = 15 + (1/2)(N_{SPT} - 15) \quad (7)$$

where N'_{SPT} = adjusted penetration number and N_{SPT} = measured penetration number. Equation 7 is based on the assumption that N_{SPT} is approximately 15 when the in

Figure 7. Summary of shear strength data: boring 3—site A.

DEPTH	SYMBOL	SAMPLE	DESCRIPTION OF STRATUM	AVERAGE TOTAL UNIT WEIGHT, kN PER CU M	ANGLE OF INTERNAL SHEARING RESISTANCE, DEGREES	DRAINED SHEAR STRENGTH, kPa	THD PENETRATION TEST, BLOWS PER FT
			Note: 1 m = 3.28 ft; 1 kN/m³ = 6.4 lbf/ft³; 1 kPa = 0.145 lbf/in².				
1-5			BROWN LOOSE SILTY SAND	15.5	34.5	18	6
5-10				16.3	30	19	6
10-13				15.9			20
13-16				16.6	36.5	31	20
16-18			TAN AND LIGHT GRAY STIFF SILTY CLAY				

Figure 8. Summary of shear strength data: boring 1—site D.

DEPTH	SYMBOL	SAMPLE	DESCRIPTION OF STRATUM	AVERAGE TOTAL UNIT WEIGHT, kN PER CU M	ANGLE OF INTERNAL SHEARING RESISTANCE, DEGREES	DRAINED SHEAR STRENGTH, kPa	THD PENETRATION TEST, BLOWS PER FT
			Note: 1 m = 3.28 ft; 1 kN/m³ = 6.4 lbf/ft³; 1 kPa = 0.145 lbf/in².				
10			TAN AND LIGHT GRAY PLASTIC CLAY WITH CALCAREOUS NODULES	20.5			
20			TAN FINE SILTY SAND	19.6	41	82	22
				19.4	40	92	48
				19.2	43	110	33
30			TAN AND LIGHT GRAY STIFF CLAY WITH CALCAREOUS NODULES	21.4			
				19.3			
40			WHITE FINE SILTY SAND	21.2	37.5	122	30
			TAN AND LIGHT GRAY STIFF TO PLASTIC CLAY	20.9			
50			LIGHT GRAY SILTY SAND	19.7	41	169	80
				18.8	38.5	155	68

situ void ratio equals the critical void ratio of the soil. Also, in fine-grained materials, the coefficient of permeability is so low that the change in pore pressure created by the expansion of the soil impedes penetration by the split spoon and thus increases the penetration number.

In this study Equation 6 was used to evaluate the N_{SPT} values for each N_{TCP} value obtained from all study test sites and, where appropriate, Equation 7 was used to determine the adjusted N-value (N'_{SPT}). The N-values

Figure 9. Relationship between TCP test N-value and effective angle of shearing resistance for SP, SM, and SP-SM soils.

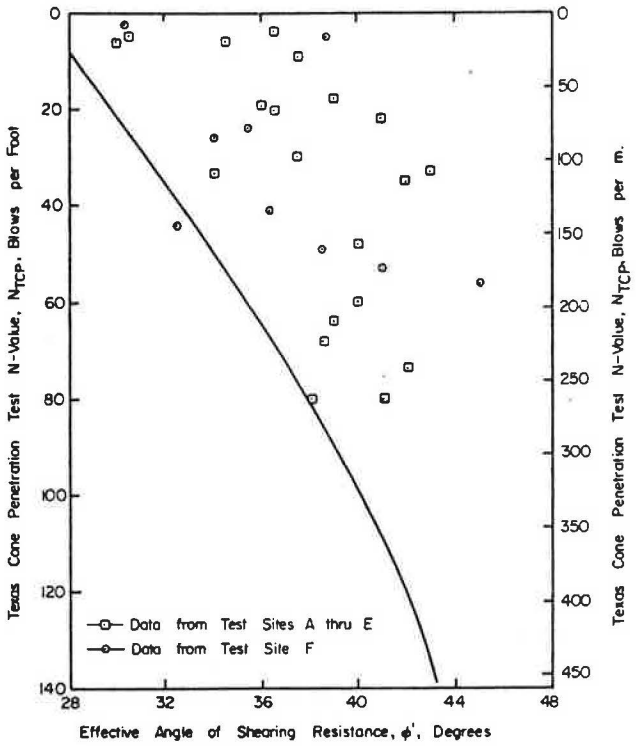

and the other significant study data are given in Table 1. The relationship between N_{SPT} and ϕ' (which is widely used for foundation design in sands) given by Peck, Hanson, and Thornburn (4) is shown by the solid curve in Figure 11. A plot of N'_{SPT} values versus the ϕ' values obtained in this study is shown in Figure 12; it would appear that the dashed curve is a more accurate lower bound for the relationship. However, the dashed curve can only be used with the adjusted N-value (N'_{SPT}).

It has been shown that the shear strength of a cohesionless soil depends on the angle of shearing resistance and the normal pressure acting on the failure plane. Means and Parcher (10) have reported that the factors affecting the angle of shearing resistance are degree of density, void ratio or porosity, particle size and shape, gradation, and moisture content. Because the resistance to penetration is also reported to be affected by these same factors and especially by the normal pressure, a relationship should exist between penetration resistance and shear strength.

The effect of shear strength on penetration resistance has been verified by several workers. According to DeMello (14), "The shear resistance is the principal parameter at play in resisting penetration." Desai (15) concluded that shear strength was one of the main factors affecting penetration resistance. Jonson and Kavanagh (16) have summarized their findings by stating that the resistance to penetration is a function of the shearing resistance of the soil.

A plot of the drained shear strength (s) versus the corresponding N_{TCP} value is shown in Figure 13. Least-squares statistical analysis was used to develop a constant of proportionality for the two soil parameters. The relationship can be expressed as follows:

$$s = 2.0N_{TCP} \quad (8)$$

The coefficient of correlation for this relationship is

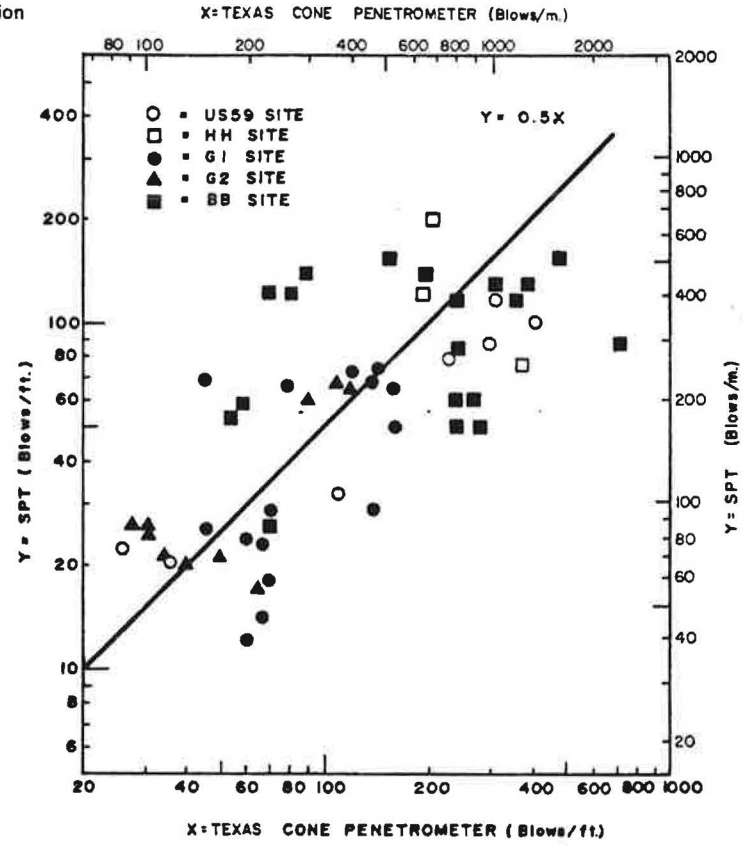

Figure 10. Correlation between standard penetration and TCP test N-values in sands.

Table 1. Summary of N-values, effective angles of shearing resistance, and drained shear strengths.

Test Site	N-Value (blows per foot) N_{TCP}	N_{SPT}	N'_{SPT}	ϕ'(°)	s (kPa)	Test Site	N-Value (blows per foot) N_{TCP}	N_{SPT}	N'_{SPT}	ϕ'(°)	s (kPa)
A	35	18	17	42.0	39.4	D	80	40	28	41.0	169.2
A	60	30	23	40.0	43.1	D	68	34	25	38.5	164.9
A	4	2	2	36.5	20.3	E	64	32	24	39.0	113.3
A	5	3	3	31.5	20.0	E	80	40	28	38.0	173.9
A	9	5	5	37.5	29.4	E	74	37	26	42.0	198.9
A	6	3	3	34.5	17.9	F	5	3	3	38.7	18.2
A	6	3	3	30.0	19.1	F	2	1	1	31.3	22.6
A	20	10	10	36.5	30.9	F	41	21	18	36.3	46.9
B	33	17	16	34.0	41.5	F	53	27	21	41.0	64.6
C	19	9	9	36.0	42.3	F	49	25	20	38.5	65.5
C	18	9	9	39.0	61.0	F	26	13	13	34.0	61.1
D	22	11	11	41.0	81.9	F	24	12	12	35.5	70.4
D	48	24	20	40.0	92.0	F	44	22	19	32.5	67.1
D	33	17	16	43.0	110.4	F	56	28	22	45.0	113.0
D	30	15	15	37.5	122.4						

Note: 1 kPa = 0.145 lbf/in².

$r^2 = 0.67$. Equation 8 can be used to predict the drained shear strength of these sands if N_{TCP} is known.

A correlation between s and N_{SPT} was also developed. Equation 6 was used to convert the measured values of N_{TCP} into the appropriate values of N_{SPT}. The plot of s versus N_{SPT} is shown in Figure 14. The relationship can be expressed as follows:

$$s = 3.9N_{SPT} \quad (9)$$

The coefficient of correlation for this relationship is also $r^2 = 0.67$.

If Equation 7 is used to adjust the N_{SPT} values where the soil conditions warrant, a correlation can be developed between s and N'_{SPT}. The plot of s versus N'_{SPT} is shown in Figure 15. The relationship can be expressed as follows:

$$s = 5.0N'_{SPT} \quad (10)$$

The coefficient of correlation for this relationship is $r^2 = 0.64$. Therefore, the use of N'_{SPT} did not lead to an improved correlation.

FACTORS AFFECTING PENETRATION RESISTANCE

A number of workers have investigated the factors affecting resistance to penetrometer penetration. Although many variables are involved, a certain amount of agreement exists as to the major ones affecting resistance to penetration in sands. Desai (15), in an effort to present a rational analysis of the penetration phenomenon, stated that "The driving of the cone would cause an upward displacement of the subsoil till a certain depth or surcharge

pressure is reached which will not permit such displacement." He concluded that density, structure, depth, and groundwater table will have significant effects on resistance. In a study of the SPT in sands, Gibbs and Holtz (3) concluded that "The overburden pressures were found to have the most pronounced and consistent effects on the penetration resistance values." Schultz and Knausenberger (17) report that "Dynamic penetrometers react very sensitively to any changes of compactness or grain size."

The consensus seems to be that unit weight, particle size, moisture content, and overburden pressure are the major factors affecting resistance to penetration in sands. This opinion is substantiated by the summary of the con-

Figure 11. Relationship between standard penetration test N-value (N_{SPT}) and effective angle of shearing resistance for SP, SM, and SP-SM soils.

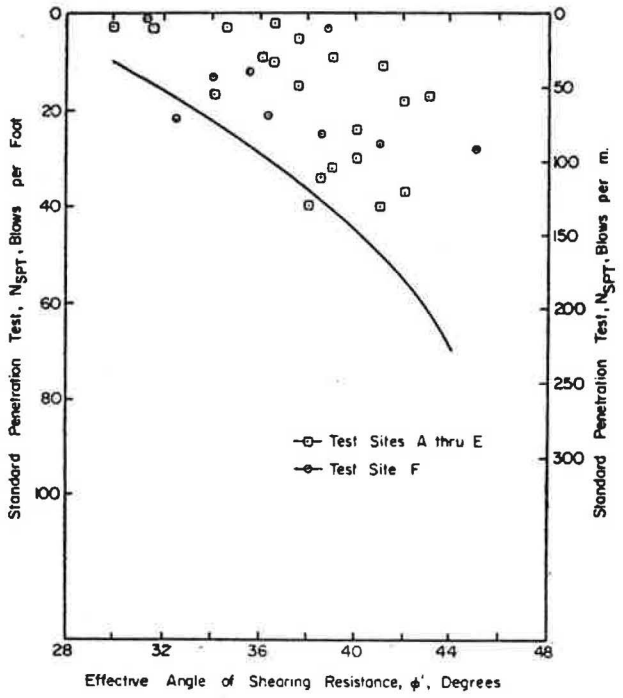

Figure 12. Relationship between standard penetration test N-value (N'_{SPT}) and effective angle of shearing resistance for SP, SM, and SP-SM soils.

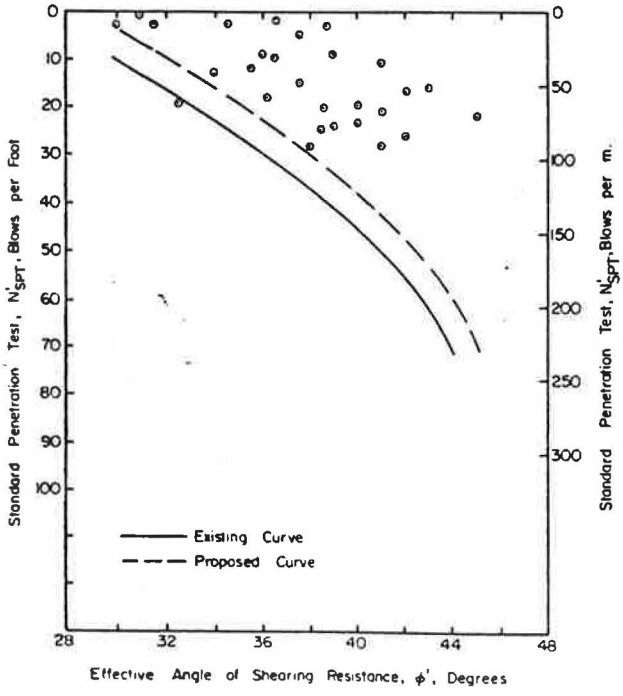

Figure 13. Relationship between drained shear strength and resistance to penetration (N_{TCP}) for SP, SM, and SP-SM soils.

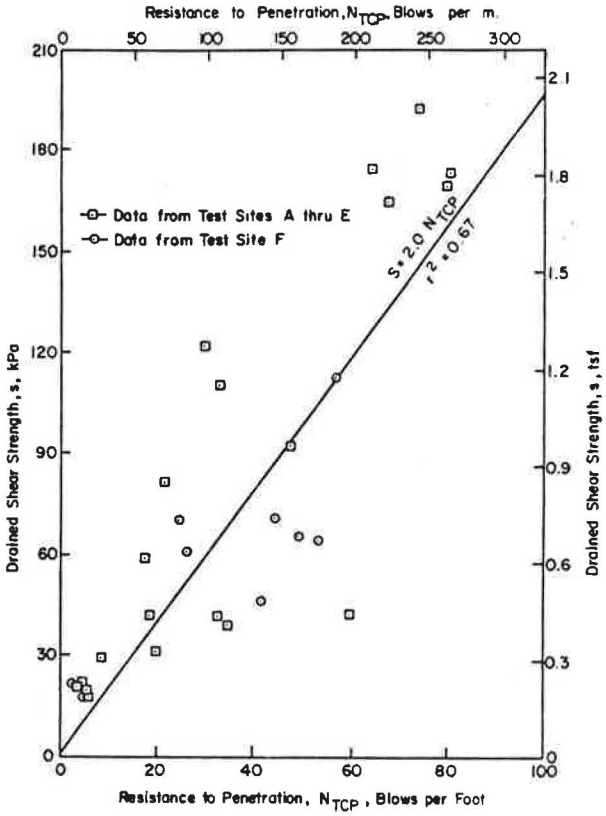

Figure 14. Relationship between drained shear strength and resistance to penetration (N_{SPT}) for SP, SM, and SP-SM soils.

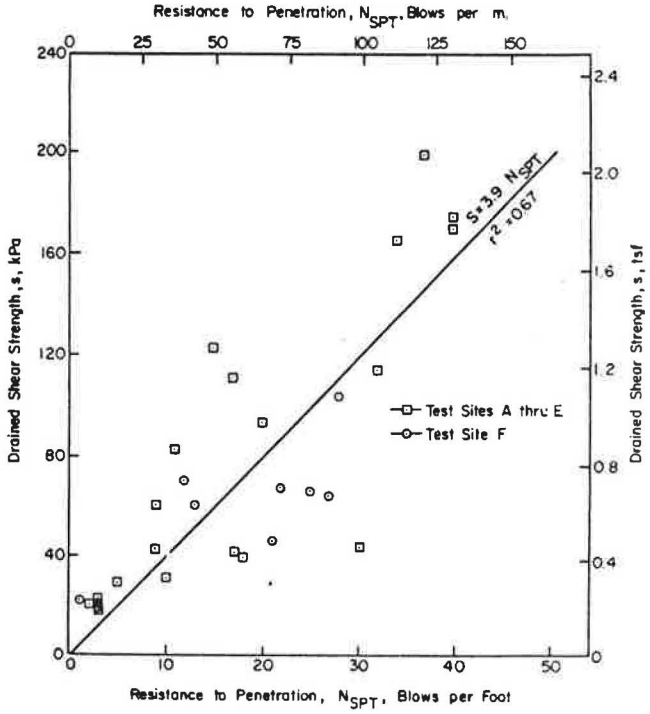

Figure 15. Relationship between drained shear strength and corrected resistance to penetration for SP, SM, and SP-SM soils.

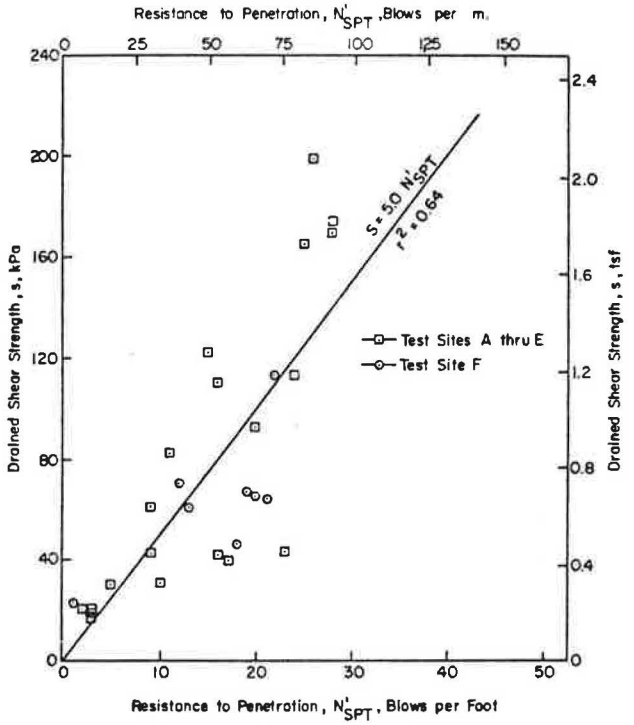

clusions of 21 workers given by Bodarik (18); although there is not complete agreement concerning the factors that have the most effect, there is general agreement concerning what factors affect the resistance to dynamic penetration in sands.

The effect of overburden pressure on penetration resistance is probably best explained by Bodarik, who states that

> The stress caused by the weight of the overburden presses the particles together and greatly delays their displacement during penetration. Since compressive forces in sands are transmitted from grain to grain through points of contact, increases in earth pressures, even in loose sands, cause an appreciable increase in density and affect the results of the sounding.

Some field observations have confirmed the effect of overburden pressure on the results of the SPT. Fletcher (19) reported that the removal of 4.6 m (15 ft) of overburden from a sand deposit will "relieve pressure noticeably and thus affect the N-value at shallow depths by underestimating relative density and hence the bearing capacity." Attempts have been made by various workers [for example, Bowles (13)] to correct the N-value at shallow depths to include the effect of overburden. Gibbs and Holtz (3) have shown that "for two cohesionless soils of the same density, the one with the greatest overburden pressure has the higher penetration number." Several cases were observed in this study where N-values increased with increasing overburden pressure. However, variations in other factors may also have affected the resistance to penetration.

Terzaghi and Peck (20) have suggested that, in loose, very fine or silty sands below the groundwater level, positive pore-water pressures might develop in the soil due to dynamic application of the load and the low permeability of the soil. According to Sanglerat (21), "These positive pore-water pressures would reduce the shearing resistance of the soil which opposes the penetration of the sampling spoon; hence, the standard penetration value of these loose soils would decrease upon submergence." On the other hand, for dense, very fine or silty sands, the penetration test might induce negative pore-water pressures that would increase the resistance to penetration and thus increase the N-value. The effect of the groundwater level was noted at two test sites in this study. In neither case could a definite conclusion be drawn concerning the effect of the groundwater level on the N-value because of the variations in other factors that affect the resistance to penetration. However, an increase was observed in the resistance to penetration of relatively loose materials below the water table, which is not in agreement with the statement made by Terzaghi and Peck.

Another factor thought to have a major effect on the resistance to penetration is particle-size distribution. According to Desai (15), "Grain size distribution has a considerable effect on the penetration resistance for a given relative density." Because it has been shown (3, 22) that penetration resistance can be related to relative density and relative density is a function of particle size, it can be concluded that particle size does have an effect on penetration resistance. A sand composed of a large amount of gravel, according to Desai, will have a relatively low resistance to penetration, because the round gravel will act like ball bearings and thus reduce friction and penetration resistance considerably. Sands that have a large amount of fine material will experience positive or negative pore-water pressures (depending on the state of compactness), which will result in increases or decreases in the N-values. In natural sand deposits where the particle-size characteristics are not uniform, the effect of particle size is not so easily determined. As in the case of unit weights, it is suspected that the particle size will affect the N-value, but this effect is not obvious. Several situations were encountered in this study in which the penetrated soil had a large percentage of material passing the 75-μm (no. 200) sieve and correspondingly high N-values. However, other factors (such as overburden pressure, position of the groundwater table, and unit weight) were not constant among these situations and, thus, the cause of the increased N-value could not be attributed to any one factor.

CONCLUSIONS

The relationship between the drained shear strength and the resistance to penetration of cohesionless soils was studied by the use of new techniques in sampling and testing. The following conclusions are made:

1. The TCP test N-value (N_{TCP}) and the drained shear strength (s) of poorly graded and silty sands (SP, SM, and SP-SM) can be correlated by using Equation 8.
2. For the same sands, the SPT N-value (N_{SPT}) and the adjusted SPT N-value (N'_{SPT}) can be correlated with the drained shear strength (s) by using Equations 8 and 9, respectively.
3. The relationship between the effective angle of shearing resistance (ϕ') and the N_{TCP} currently used by the TSDHPT was found to be a lower bound for the data obtained in this study.
4. A widely used relationship between ϕ' and N_{SPT} was found to be a lower bound for the data obtained in this study; a new lower-bound curve was developed based on the relationship between ϕ' and N'_{SPT}.
5. Other factors that might affect penetration resistance in a cohesionless soil (e.g., overburden pressure, unit weight, particle-size characteristics, and position of the groundwater level) were also con-

sidered in this study, but no correlations or trends were established. Rather, it is shown that, in a field study such as this, control of individual factors is not possible. Therefore, because individual factors cannot be separated, it is probable that interaction occurs and a combination of several factors actually affects the resistance to penetration.

ACKNOWLEDGMENT

We gratefully acknowledge the support and assistance of the Texas State Department of Highways and Public Transportation and the Federal Highway Administration, whose cooperative sponsorship made this study possible. George D. Cozart and Franklin J. Duderstadt did much of the field work and analysis reported in this paper in partial fulfillment of the requirements for the M. S. degree at Texas A&M University, College Station. The contents of this paper reflect our views; we are responsible for the facts and the accuracy of the data presented herein. The contents do not necessarily reflect the official views or policies of the Federal Highway Administration. This paper does not constitute a standard, specification, or regulation.

REFERENCES

1. M. J. Hvorslev. Subsurface Exploration and the Sampling of Soils for Civil Engineering Purposes. Engineering Foundation, New York, 1949.
2. A. C. Meigh and I. K. Nixon. Comparison of In Situ Tests for Granular Soils. Proc., 5th International Conference on Soil Mechanics and Foundation Engineering, Paris, France, Vol. 1, 1961.
3. H. J. Gibbs and W. G. Holtz. Research on Determining the Density of Sands by Spoon Penetration Testing. Proc., 4th International Conference on Soil Mechanics and Foundation Engineering, London, England, Vol. 1, 1957, pp. 35-39.
4. R. B. Peck, W. E. Hanson, and T. H. Thornburn. Foundation Engineering, 2nd ed. Wiley, New York, 1974, p. 310.
5. Foundation Exploration and Design Manual, 2nd ed. Bridge Division, Texas Highway Department, Austin, July 1972.
6. F. E. Falquist. New Methods and Techniques in Subsurface Exploration. Journal of the Boston Society of Civil Engineers, Vol. 23, 1941, p. 144.
7. Q. W. Bishop. New Sampling Tool for Use in Cohesionless Sands Below Ground Water Level. Geotechnique, Vol. 1, No. 2, Dec. 1948, p. 125.
8. G. D. Cozart, H. M. Coyle, and R. E. Bartoskewitz. Correlation of the Texas Highway Department Cone Penetrometer Test with the Drained Shear Strength of Cohesionless Soils. Texas Transportation Institute, Texas A&M Univ., College Station, Res. Rept. 10-2, Aug. 1975.
9. F. J. Duderstadt, H. M. Coyle, and R. E. Bartoskewitz. Correlation of the Texas Cone Penetrometer Test N-Value with Soil Shear Strength. Texas Transportation Institute, Texas A&M Univ., College Station, Res. Rept. 10-3F, Aug. 1977.
10. R. E. Means and J. V. Parcher. Physical Properties of Soils. Charles E. Merrill Books, Inc., Columbus, OH, 1963.
11. T. W. Lambe. Soil Testing for Engineers. Wiley, New York, 1951, p. 93.
12. F. T. Touma and L. C. Reese. The Behavior of Axially Loaded Drilled Shafts in Sand. Center for Highway Research, Univ. of Texas at Austin, Res. Rept. 176-1, Dec. 1972.
13. J. E. Bowles. Foundation Analysis and Design. McGraw-Hill, New York, 1968, p. 125.
14. V. F. B. DeMello. The Standard Penetration Test. Proc., 4th Pan American Conference on Soil Mechanics and Foundation Engineering, San Juan, PR, Vol. 1, 1971.
15. M. D. Desai. Subsurface Exploration by Dynamic Penetrometers, 1st ed. S. V. R. College of Engineering, Surat (Gujarat), India, 1970.
16. S. M. Jonson and T. C. Kavanagh. The Design of Foundations for Buildings. McGraw-Hill, New York, 1968.
17. E. Schultz and H. Knausenberger. Experiences with Penetrometers. Proc., 4th International Conference of Soil Mechanics and Foundation Engineering, London, England, Vol. 1, 1957.
18. G. K. Bodarik. Dynamic and Static Sounding of Soils in Engineering Geology. Israel Program for Scientific Translations, Jerusalem, 1967.
19. G. F. A. Fletcher. Standard Penetration Test: Its Uses and Abuses. Journal of the Soil Mechanics and Foundation Engineering Division, Proc., ASCE, Vol. 91, No. SM4, Jan. 1956, pp. 67-75.
20. K. Terzaghi and R. B. Peck. Soil Mechanics in Engineering Practice, 2nd ed. Wiley, New York, 1967.
21. G. Sanglerat. The Penetrometer and Soil Exploration. Elsevier, New York, 1972, p. 246.
22. K. Drozd. Discussion of Penetration Test. Proc., 6th International Conference on Soil Mechanics and Foundation Engineering, Montreal, Vol. 3, 1965, pp. 335-336.

Publication of this paper sponsored by Committee on Foundations of Bridges and Other Structures.

Prediction of Permanent Strain in Sand Subjected to Cyclic Loading

Rodney W. Lentz and Gilbert Y. Baladi

The trend toward ever-increasing axle loads on highways and airport pavements requires that new methods for pavement design and rehabilitation be developed. This paper introduces a simple and economical procedure whereby permanent strain in sand subjected to cyclic loading can be characterized by using stress and strain parameters from the universally accepted static triaxial test. To develop the procedure, duplicate samples were tested by using both a static triaxial apparatus and a closed-loop electrohydraulically actuated triaxial system. The dynamic test results

were normalized with respect to parameters obtained from the corresponding static test. The normalized cyclic-principal-stress difference showed a unique relationship to the normalized accumulated permanent strain that was independent of moisture content, density, and confining pressure. Benefits to be gained by use of such a simplified procedure include significant saving of laboratory time and energy, as well as reduced equipment and personnel costs. Also, practicing engineers are more likely to accept the use of rational design methods if they have available a simple test procedure to characterize material behavior.

The trend toward ever-increasing axle loads on highway and airport pavements has revealed the inadequacy of the currently used empirical methods for the design of flexible pavements. These methods are usually based on correlating pavement performance with some empirical test (such as the California bearing ratio or stabilometer measurements) that categorizes material strength or on the use of limiting subgrade-strain criteria derived from elastic-layer theory (1). Such methods lack the ability to predict the amount of deformation that will occur after a given number of load applications when the loading exceeds the range for which performance data are available. Because soil behaves in a nonlinear fashion, performance under higher levels of loading cannot be extrapolated from performance at lower load levels.

Several rational methods of pavement design have been proposed to overcome this deficiency. These methods are usually quasi-elastic (elastic theory is used to predict stresses, and permanent strains are determined by repeated-load laboratory tests) (1). Other methods combine viscoelastic theory with laboratory testing (2, 3). To be useful, these methods must have the capability of predicting the cumulative permanent deformation that will occur as a consequence of traffic loading, which requires the development of an adequate method for characterization of permanent strain (3, 4). Further, these methods should be simple and economical and not require complicated or expensive new equipment or testing procedures. This paper describes such a method.

BACKGROUND INFORMATION

The parameters reported to affect the accumulation of permanent strain in cohesionless materials include number of load repetitions, stress history, confining pressure, stress level, and density (1, 3, 5-9).

The effect of the number of load repetitions on permanent strain has been studied by several investigators, some of whom have indicated that the relationship is a straight line on a semilogarithmic plot (6) and others that it is a straight line on a log-log plot (1). The effect of stress history is reported to be a significant reduction in the amount of permanent strain experienced under subsequent loading (8). It has been reported that, for a given difference in cyclic principal stress, increasing the confining pressure decreases the permanent strain (5, 6, 9). For a constant confining pressure, the permanent strain after a given number of load cycles has been found to depend directly on the magnitude of the principal-stress difference (5, 6). It has been shown that curves of cyclic stress versus permanent strain are analogous to static stress-strain curves (6) and that they can be described by using hyperbolic functions developed for static test results (10, 11). A reduction in density has been shown to cause an increase in permanent strain accumulation (6, 12).

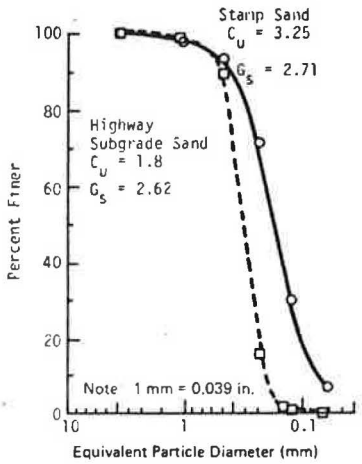

Figure 1. Particle-size distribution curves: highway subgrade and stamp sands.

TESTING PROCEDURE AND EQUIPMENT

The material used in the testing program was a uniform medium sand typical of that found in the northern half of Michigan. For verification purposes, a few tests were also conducted on samples of a fine stamp sand (crushed rock from a stamp mill). Particle-size distribution curves for both materials are shown in Figure 1; the results are described in greater detail elsewhere (13).

Drained, cyclic triaxial tests were run on 51-mm (2-in) diameter by 137-mm (5.4-in) long samples compacted moist. Identical samples were tested under drained, static triaxial conditions to obtain stress-strain curves for use in normalizing the dynamic test results. For both the static and the dynamic tests, loads were measured by using a load cell mounted directly beneath the sample base, and deformation was measured by using a linear variable differential transformer mounted across the length of the sample (14). The loading system consisted of a closed-loop electrohydraulic actuator operated in the load-controlled mode. The cyclic triaxial tests used a sinusoidal wave form having a frequency of 1 Hz and were conducted to at least 10 000 cycles. Three levels of confining pressure (σ_3) and two levels of density were used. For each combination of these variables, several levels of cyclic principal stress difference (σ_d) were used. Because stress history has a large influence on permanent strain, each combination of variables required a new sample.

The static triaxial tests were performed by using the triaxial cell used for the dynamic tests. Loads were applied gradually in increments of approximately 10 percent of the estimated sample strength [as suggested by Bishop and Henkel (15)] by using the electrohydraulic actuator. As the failure stress was approached, the size of the load increment was reduced to allow for a reliable determination of strength. Each load increment was maintained until the rate of strain had become very small before the deformation reading was recorded, a procedure that was expected to produce the same stress-strain curve as would conventional constant-strain-rate triaxial equipment.

TEST RESULTS

The samples for the cyclic triaxial tests were compacted moist to 99 percent of the maximum dry density as determined by AASHTO T180, and the tests were run at confining pressures of 34.5, 172.4, and 344.8 kPa (5, 25, and 50 lbf/in^2). The change in permanent strain is large during the first few cycles of load but then gradually decreases. Thus, the data can conveniently be presented as plots of permanent strain versus logarithm of number of load cycles that, as shown in Figure 2 for the results obtained for σ_3 = 34.5 kPa, can be approximated by straight lines. A least-squares technique can

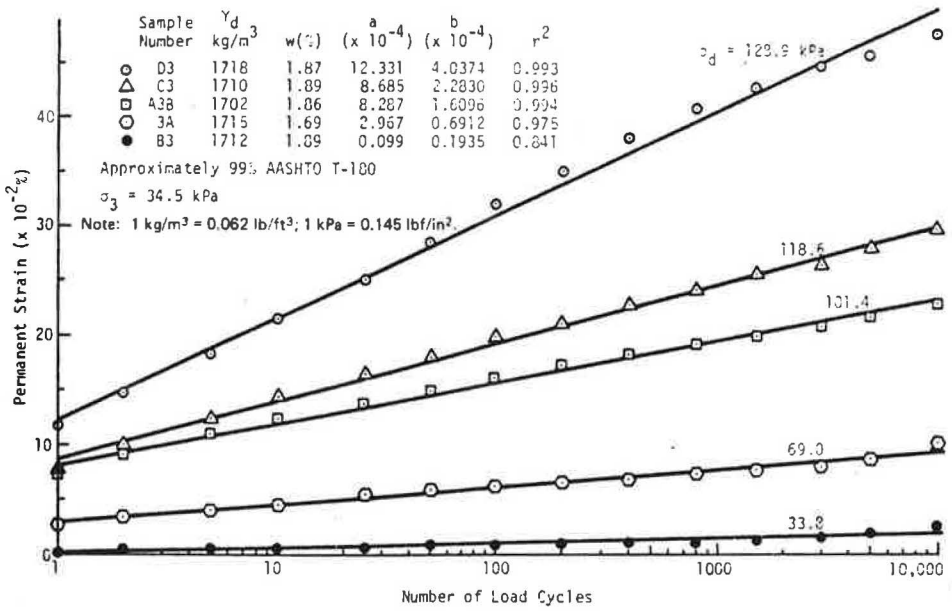

Figure 2. Effect of cyclic-principal-stress difference and number of load cycles on permanent strain at constant confining pressure: highway subgrade sand.

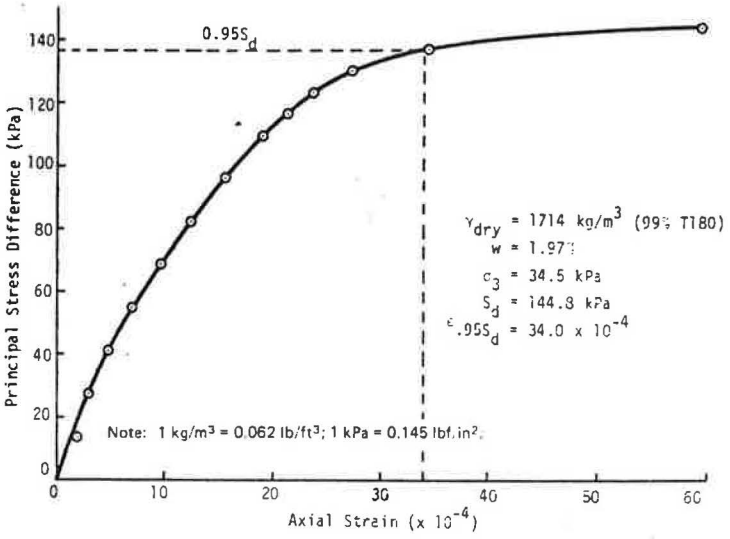

Figure 3. Relationship between static stress and axial strain: highway subgrade sand.

then be used to determine the best-fit straight line through each set of data. The equations of the lines have the form

$$\epsilon_p = a + b \ln N \quad (1)$$

where

ϵ_p = accumulated permanent strain,
N = number of load repetitions, and
a and b = regression constants.

The constant a represents the permanent strain occurring during the first cycle of load, and the constant b represents the rate of change in permanent strain with increasing number of load repetitions.

Typical results of a static triaxial test are shown in Figure 3.

DISCUSSION OF RESULTS

The results of the cyclic tests can be presented in the form of plots of σ_d versus ϵ_p at any given N. This was done for three values of σ_3 and N = 10 000 (see Figure 4). This figure makes the significant effect of σ_3 obvious.

Thus, the effect of σ_3 and/or σ_d on the static strength was studied by normalizing the value of σ_d for each cyclic test by dividing it by the peak strength (S_d) of an identical sample tested at the same value of σ_3 under static triaxial conditions (see Figure 5). This normalizing procedure draws the curves closer together and reduces, but does not eliminate, the total effect of σ_3. This, however, suggests the possibility that normalizing the permanent strain to some reference strain obtained in the static triaxial test could eliminate the effect of σ_3. The criteria for such a reference strain value are that (a) it should contain the plastic deformation characteristics of the sand under the given test conditions and (b) it must be a well-defined value that can be reproduced by different operators. Based on these criteria, the static strain at 95 percent of peak strength ($\epsilon_{0.95S_d}$) was selected as the reference value. At this load, a large amount of the total strain is permanent and thus represents the plastic characteristics of the material. However, the curve is still rising steeply enough so that the strain value is well defined. The method for determination of $\epsilon_{0.95S_d}$ is illustrated by the dashed lines in Figure 3; each combination of σ_3, moisture, and sample density will require a separate static stress-strain curve to obtain the normalizing parameters (S_d and $\epsilon_{0.95S_d}$).

When the cyclic permanent strains shown in Figure 5 were normalized by dividing by $\epsilon_{0.95S_d}$, the curves collapsed to produce a single curve as shown in Figure 6, which also shows additional normalized results for samples at a lower density. It should be noted that, although the points plotted in Figure 6 represent samples tested at three different confining pressures and two densities, the data can be reasonably represented by a single curve. The significance of this is that this curve and the results of a static triaxial stress-strain test allow the prediction of the permanent strain after 10 000 cycles at any level of cyclic-principal-stress difference.

Because it has been shown (6, 16) that cyclic stress-permanent strain curves can be described by hyperbolic functions, a least-squares procedure was used to determine the best-fit hyperbolic curve for the data shown in Figure 6.

To verify that this curve applies to material other than the subgrade sand used in the testing program, several tests were performed on the crushed stamp sand, which had a finer gradation than the subgrade sand, as well as a different mineralogical composition and a much more angular particle shape. Due to its particle shape, at the same effort, the stamp sand compacted to a much lower density than the subgrade sand. Cyclic and static triaxial tests were performed on samples of stamp sand at confining pressures of 34.5 and 172.4 kPa, and the data were normalized by using the procedure described above. The results, which are shown by the solid squares and solid circle in Figure 6, indicate that the procedure may be applicable to a range of cohesionless materials.

Figure 4. Relationship between cyclic-principal-stress difference and permanent strain at N = 10 000.

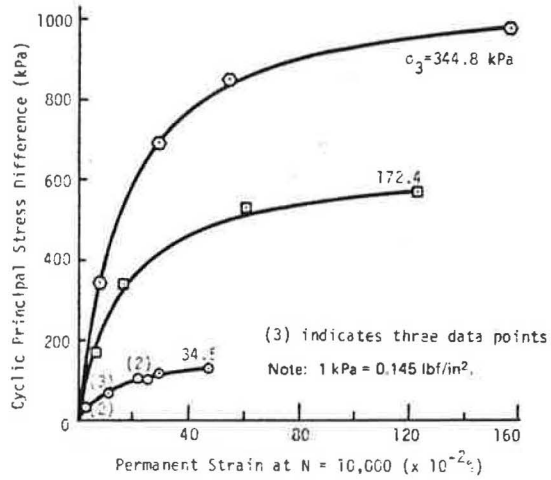

Figure 5. Relationship between normalized cyclic-principal-stress difference and permanent strain at N= 10 000.

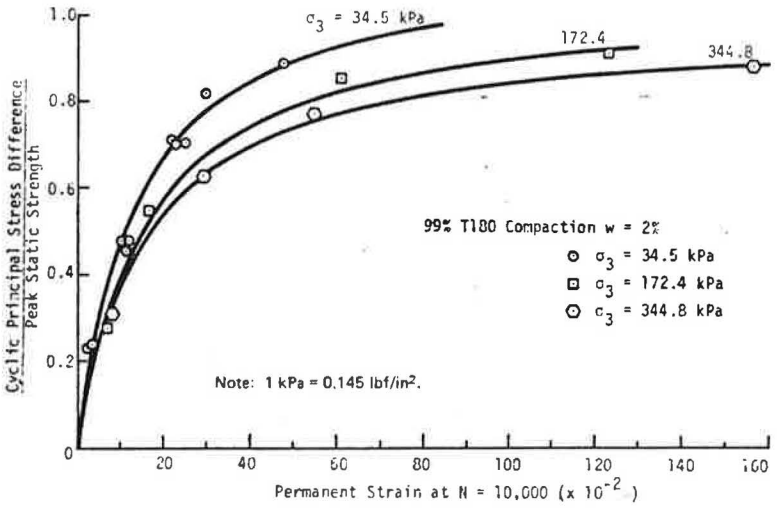

Figure 6. Relationship between normalized cyclic-principal-stress difference and normalized permanent strain at N = 10 000.

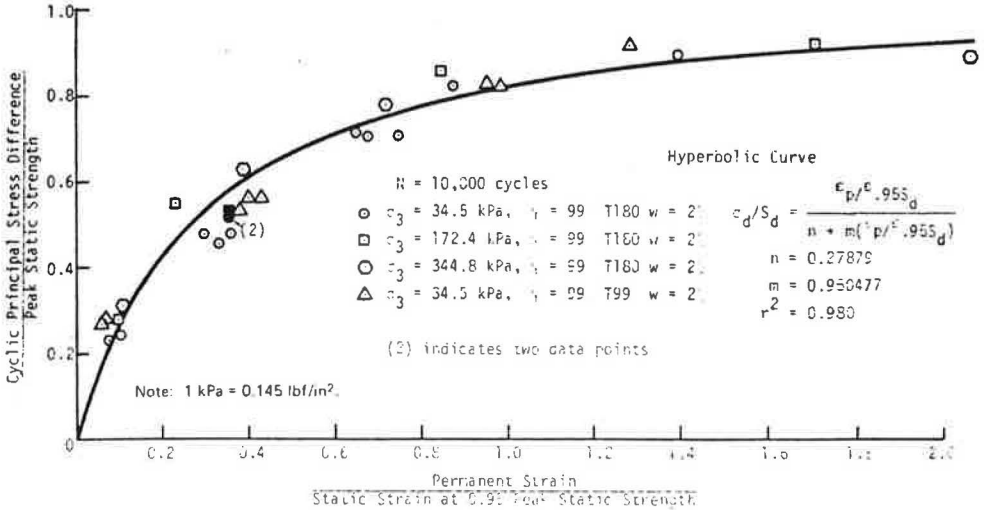

BENEFITS TO PRACTICING ENGINEERS

In practice, the use of the material characterization procedure described in this paper could result in significant saving of laboratory time and obviate the need for expensive testing equipment. Also, rational pavement design methods that require characterization of permanent strain behavior are more likely to gain quick acceptance by practicing engineers if a simple test method is available.

Work is continuing on the development of a general constitutive equation that will require only the stress-strain results from static triaxial tests to predict accumulated permanent strain after any number of load cycles. Also, applicability to a wider range of subgrade soils, including cohesive ones, is being tested.

CONCLUSION

This paper has presented a simple procedure for characterizing the permanent strain behavior of cohesionless subgrade material by using stress-strain curves obtained from static triaxial tests. More research is needed to extend the procedure to a wider variety of subgrade materials and to develop a general constitutive equation for predicting permanent strain.

The adoption of this procedure in practice will save both laboratory time and money in meeting material characterization needs.

REFERENCES

1. E. J. Yoder and M. W. Witczak. Principles of Pavement Design, 2nd ed. Wiley, New York, 1975.
2. W. J. Kenis. Predictive Design Procedure: A Design Method for Flexible Pavements Using the VESYS Structural Subsystem. Proc., 4th International Conference on the Structural Design of Asphalt Pavements, Ann Arbor, MI, Vol. 1, 1977, pp. 101-130.
3. W. L. Huffered and J. S. Lai. Analysis of N-Layered Viscoelastic Pavement Systems. Federal Highway Administration, Rept. FHWA-RD-78-22, 1978, pp. 224. NTIS: PB 282 578.
4. P. S. Pell and S. F. Brown. The Characteristics of Materials for the Design of Flexible Pavement Structures. Proc., 3rd International Conference on the Structural Design of Asphalt Pavements, London, England, 1972, pp. 326-342.
5. J. R. Morgan. The Response of Granular Materials to Repeated Loading. Proc., 3rd Conference of the Australian Road Research Board, Sydney, Vol. 3, Part 2, 1966, pp. 1178-1191.
6. R. D. Barksdale. Laboratory Evaluation of Rutting in Base Course Materials. Proc., 3rd International Conference on the Structural Design of Asphalt Pavements, London, England, 1972, pp. 161-174.
7. Y. T. Chou. Engineering Behavior of Pavement Materials: State of the Art. U.S. Army Engineer Waterways Experiment Station, Vicksburg, MS, Tech. Rept. S-77-9, 1977.
8. I. V. Kalcheff and R. G. Hicks. A Test Procedure for Determining the Resilient Properties of Granular Materials. Journal of Testing and Evaluation, Vol. 1, No. 6, 1973, pp. 472-479.
9. S. F. Brown. Repeated Load Testing of a Granular Material. Journal of the Geotechnical Engineering Division, Proc., ASCE, Vol. 100, No. GT7, July 1974, pp. 825-841.
10. J. M. Duncan and C. Y. Chan. Nonlinear Analysis of Stress and Strain in Soils. Journal of the Soil Mechanics and Foundation Engineering Division, Proc., ASCE, Vol. 96, No. SM5, Sept. 1970, pp. 1629-1653.
11. R. L. Kondner and J. S. Zelasko. A Hyperbolic Stress-Strain Formulation for Sands. Proc., 2nd International Pan-American Conference on Soil Mechanics and Foundation Engineering, Sao Paulo, Brazil, Vol. 1, 1963, pp. 289-324.
12. I. V. Kalcheff. Characteristics of Graded Aggregates as Related to Their Behavior Under Varying Loads and Environments. Presented at Conference on Graded Aggregate Base Materials in Flexible Pavements, Oak Brook, IL, National Crushed Stone Assn., Washington, DC, 1976.
13. R. W. Lentz. Permanent Deformation of Cohesionless Subgrade Material Under Cyclic Loading. Department of Civil Engineering, Michigan State Univ., East Lansing, Ph.D. dissertation, 1979.
14. R. W. Lentz and G. Y. Baladi. Simplified Procedure to Characterize Permanent Strain in Sand Subjected to Cyclic Loading. Proc., International Symposium on Soils Under Cyclic and Transient Loading, Swansea, Wales, 1980.
15. A. W. Bishop and D. J. Henkel. The Measurement of Soil Properties in the Triaxial Test, 2nd ed. Edward Arnold, Ltd., London, England, 1962.
16. C. L. Monismith, N. Ogawa, and C. R. Freeme. Permanent Deformation Characteristics of Subgrade Soils Due to Repeated Loading. TRB, Transportation Research Record 537, 1975, pp. 1-17.

Publication of this paper sponsored by Committee on Soil and Rock Properties.

Rock-Slope Stability on Rail Transportation Projects

C. O. Brawner

This paper summarizes the factors that contribute to instability of rock slopes, outlines methods of control of instability, and describes examples of instability and stabilization. The factors that contribute to instability of rock slope include geologic conditions, groundwater, climatic conditions, blasting effects, train vibration, and earthquakes. The methods of control considered include (a) stabilization by excavation or resloping, drainage, surface stabilization, and construction of support systems; (b) protection; and (c) construction of warning systems.

In recent years, there has been a gradual increase in traffic through the western mountain regions of Canada and the United States. For example, traffic on the Canadian Pacific Railway in western Canada has almost doubled since 1968.

Much of the railway is constructed in rough, mountainous terrain, and many high soil and rock cuts exist. It might be expected that, because most of the cuts on the railway are from 50 to more than 100 years old, the slopes would now be stable. However, the increases in frequency, weight, and length of trains in the past decade have increased the vibrational stresses in the trackside slopes. As a result, unless rock-slope stabilization programs are carried out, rockfalls and slope failures will occur more frequently and be more severe.

A number of recent rock-slope failures have caused train derailments and loss of life. The courts in Canada no longer accept rockfalls and slides as acts of God. Such events are considered to be predictable and controllable.

Fortunately, our understanding of rock mechanics and rock-slope stability has increased greatly in the past 15 years (1-4). It is now economically and practically feasible to locate potential areas of rock instability and to develop rational and practical programs to improve stability.

This paper summarizes the factors that contribute to instability of rock slopes, outlines methods of control of instability, and describes examples of instability and stabilization.

FACTORS THAT INFLUENCE THE STABILITY OF ROCK SLOPES

Rock-slope stability is influenced by many factors. Any program selected for stabilization must take into consideration the cause of instability, the delays that will be created during the stabilization program, and the cost of stabilization.

The assessment of stability must be based on the geologic, hydrologic, climatic, topographic, rail traffic, and environmental conditions at the specific site. Frequently, geologic conditions are the most important factor and, because such conditions frequently differ greatly over short distances, each rock slope must be investigated individually.

1. Geologic conditions: Rock that is sound or has randomly oriented joints that are discontinuous over short distances will stand vertically for considerable height. For example, for a soft intact rock, vertical slopes of up to 1200 m (4000 ft) should exist. In nature, vertical slopes of this magnitude are unusual. Weaknesses in the rock—faults, shears, joints, bedding planes, zones of weathering, hydrothermal alteration, and such—control the maximum height and angle at which the slope will be stable. When weaknesses exist, the most important factor is the orientation and dip of the discontinuity relative to the orientation of the slope face. The most serious type of problem is that of weaknesses or combinations of weaknesses that dip out of the slope. If the shear strength along the discontinuity is exceeded, failure will occur. The shear strength is influenced by the roughness along the discontinuity and the presence of weak material (fault gouges, altered infills, calcite stringers, and such).

2. Groundwater: The frictional force developed along a potential failure surface is proportional to the normal force acting on that surface. If water pressure exists in the discontinuity, the normal force is reduced by that pressure. If the water table is near to the ground surface, the factor of safety of a rock slope is about 35 percent less than if the slope is well drained.

3. Climatic conditions: The major effects of the weather on slope stability (other than changes in groundwater levels) are due to the combination of freeze-thaw and wet-dry cycles and to chemical alteration. When water accumulates in a crack and freezes, the expansion force can be sufficient to develop raveling and rockfalls. Thus, instability is normally greatest during the freeze-thaw and snowmelt periods in the spring.

4. Blasting effects: The excavation techniques used for transportation construction up until 5-10 years ago gave little consideration to the effects of blasting on the rock. The amount of explosive detonated at one time should be controlled to minimize particle acceleration forces. This can be done by using delay fuses. Recently developed preshear and cushion techniques allow rock slopes to be excavated to steeper inclinations that have lower long-term maintenance requirements. Figure 1 presents a comparison of the effects of blasting technique. The slope in the upper portion of the picture was excavated by using a controlled preshear technique, while that in the lower portion was excavated by a mass-volume technique in which widely spaced, heavily loaded holes were used.

5. Vibration: Vibrational stresses caused by train traffic can lead to rockfalls and slope failures. The frequency and magnitude of the vibration influence the stability. Unit trains have more uniform frequencies, and the increasing length of these trains increases the length of time during which the vibration occurs. Replacement of wooden ties by concrete ties, which transmit more of the vibration to the roadbed, tends to increase the amount of rockfall.

6. Earthquakes: Much of the western portion of North America is in an earthquake zone of moderate to high potential. The current state of the art does not allow accurate prediction or warning of earthquakes. Earthquakes can cause major slides in rock; for example, an earthquake having a magnitude of 7.5-8.5 on the Richter scale caused a slide on the Madison River in West Yellowstone, Montana, and one having a magnitude of 3.2 caused a slide 16 km (10 miles) east of Hope, British Columbia, on Highway 3.

Types of Rock Instability

It is essential to define the types of failure that present the greatest hazard to a transportation facility. The types of instability and their associated causes are summarized in Table 1.

Evaluation of Rock Stability

The evaluation of rock stability is most effectively done in two stages. In stage 1, the relevant geologic, topographic, climatic, hydrologic, and traffic data are gathered; a site inspection is made; and site mapping is carried out. Frequently, evaluation of these data obtained will be sufficient to assess stability.

When the initial study indicates a potential for large-scale failure or for a failure that could have serious consequences, more extensive (stage 2) investigation is usually necessary. This may include drilling boreholes and orienting the core by down-the-hole photography, borehole periscope, or other means. Direct shear tests on joints or infill material, determination of water pressure in the joints by the use of piezometers, and the performance of stability computations will often be required (4).

METHODS OF CONTROL

There are three approaches that can be used separately or in combination in the development of a realistic program to control stability:

1. Stabilization,
2. Protection, and
3. Warning systems.

The prime responsibility is to provide a practical degree of safety at a justifiable cost. It must be recognized that it is physically impossible to protect against all possible failures. It is not economical or practical to locate or predict all of the potentially unstable areas. The cost of providing 100 percent safety is extremely high.

Figure 1. Comparison of effects of different blasting procedures.

1. Stabilization: Stabilization of rock slopes is done where the cause and extent of the failure can be defined and the cost of the stabilization can be justified. A stabilization program must be based on a definitive site investigation. The types of stabilization procedures include (a) excavation or resloping, (b) drainage (surface and subsurface), (c) stabilization of the surface, and (d) support system (see Table 2).
2. Protection: Protection involves the prevention of rock from falling on the track. Where the volumes of falling rock are large and the volume of traffic is heavy, the use of expensive procedures (such as tunnels or rock sheds) can be justified. In other areas, slope or ditch treatment will frequently be sufficient.

One of the most effective protection procedures is the use of a deep inner-ditch catchment or, alternatively,

Table 1. Types and causes of instability.

Type of Instability	Frequency of Occurrence	Associated Causes
Rock slide	Rare	Geological weaknesses that bound large rock volumes dipping out of the slope; weathered rock; high water pressures; earthquakes; oversteepening of slope
Block or wedge failure	Infrequent	Geological weaknesses that bound blocks or wedges of rock; high water pressures; adverse climatic conditions; vibrations from blasting or traffic; earthquakes; root wedging
Rockfall	Frequent in steep blocky rock; infrequent in massive rock	Weathering; temperature changes; freezing and thawing; wetting and drying; water pressure in joints; root wedging; joints that dip out of the slope; traffic vibration; weak gouges in faults and shear zones that dip out of slope; poor blasting control
Running slope: boulders and talus	Frequent in areas of talus, till slopes, and coarse gravel slopes	Slopes that are cut steeper than the angle of repose; erosion that undercuts boulders or more resistant rock
Debris avalanche	Infrequent	Slides and trees that fall into gullies or are carried by water and snowslides; extreme snowmelt or rainfall
Slope erosion	Frequent in areas of high precipitation; more frequent on new construction	Heavy to very heavy precipitation or snowmelt on exposed slopes; slopes that are cut steeper than angle of repose; existence of fine-grained soils in slope

Table 2. Types of stabilization procedures for rock slopes.

Type of Stabilization	Example	Comments
Excavation	Scaling[a]	Applicable to rock faces that have infrequent, random-oriented geologic discontinuities; requires careful use of explosives as vibration may loosen other rocks
	Trimming[a]	May require removal of rock promontories or larger blocks by drilling and blasting; should have parallel drill holes wherever possible
	Slope flattening	Can be used where excessive rockfalls occur or where joints or bedding dip out of slope; requires benches wide enough to clean out as rock falling from above may bounce from debris-filled bench onto roadbed or track
Drainage	Runoff diversion	Should be used where water runs over the face; may require lining of ditches
	Subsurface drainage[b]	Commonly uses horizontal drain holes drilled into the slope on 3- to 8-m centers to distances of at least 12 m (but not more than one-fourth of the slope height); requires use of perforated plastic pipe if holes collapse and of insulation or heating if ice glaciers develop
	Ice glacier reduction	Uses horizontal drain holes to intercept slope-face seepage that will freeze; may require radiant heaters on poles to control the freezing
Surface stabilization	Shotcrete[c]	Can be used to minimize further slope-face deterioration and seal exposed joints; applicable to blocky slopes; requires that surface be cleaned and wetted before application and frequent drain openings be left; normally 5 cm thick
	Shotcrete plus wire mesh	Used where rock is very blocky and the blocks are small; size of wire mesh depends on rock conditions and slope height
	Dry rock wall on slope	Can be used where shallow rock or soil slopes are raveling to provide support; will be free draining
Support system	Buttresses[d]	Can be used to support large volumes of rock that would otherwise require excavation or where key rocks retain large volumes above; may require reinforcement or anchor grouting to the rock mass
	Rock bolts and cables[e]	Can be used to tie key rocks that, if removed, would undermine support for other rocks; should be tensioned and then grouted full length to develop long-term stability and to protect against corrosion; may be used in conjunction with shotcrete
	Rock dowels[f]	Can be grouted into drill holes located at toes of rock blocks to prevent sliding
	Bolted wire mesh	Can be used where large areas of rock face contain blocky jointed rock; requires corrosion-resistant mesh

Note: 1 m = 3.28 ft.
[a]See Figure 2. [b]See Figure 3. [c]See Figure 4. [d]See Figure 5a. [e]See Figure 5b. [f]See Figure 5c.

Figure 2. Scaling and trimming of rock face to improve stability.

catch walls can be constructed. One of the most efficient and economical types of wall is the gabion wall, which can be varied in height and is flexible under impact (see Table 3).

3. Warning systems: Warning systems are used where occasional falls are expected but the cost of protection or stabilization would not be justified.

The most commonly used warning system is the electric fence connected to the signal system. With this method, the probability that the locomotive engineer will have sufficient warning to stop in time is less than 100 percent. Also, if the fall occurs while the train is between signals, the engineer will not be warned, and those slides that are caused by train vibration will hit the train behind the locomotive. Radio transmitters connected to the fences increase the warning time.

In the winter, ice and snow frequently cause the wires to break or short-circuit. The use of combined heating and signal cable can reduce this problem. Considerable research is being carried out to improve warning systems. Programs include vibration meters, robot patrols, television monitoring, guided radar, and laser detection.

Figure 3. Drainage control: (a) horizontal drain installation and (b) installation of drain.

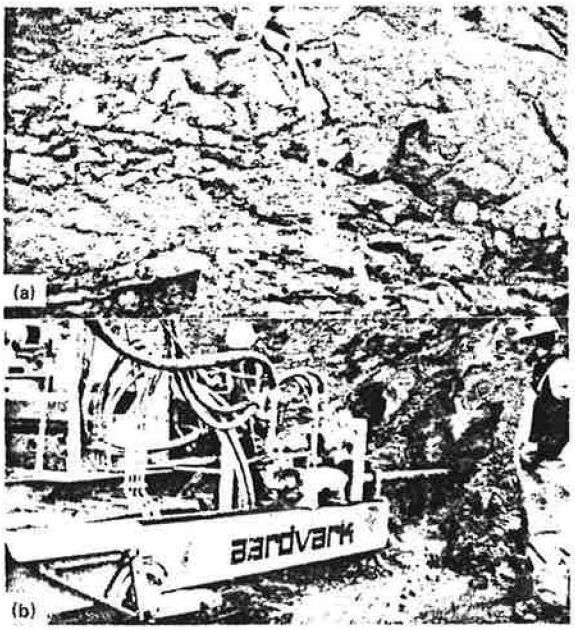

Figure 4. Shotcrete treatment to stabilize blocky rock slope above tunnel.

Figure 5. Support systems: (a) concrete buttress to support massive rock slab, (b) rock bolts to stabilize rock block, and (c) dowels concreted into shallow boreholes to resist sliding block.

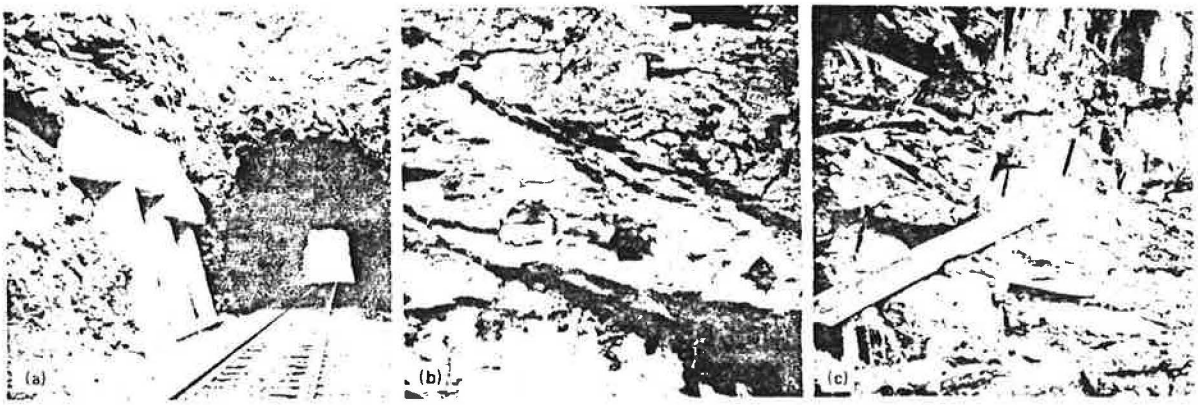

Table 3. Types of protection measures for rock slopes.

Type of Protection	Example	Comments
Slide sheds[a]		Can be constructed where slide or avalanche runs are well defined and slides occur frequently to carry debris over top of track
Tunnels		Can offer safe conditions where rock slopes are very irregular, steep, or dangerous; may require lining in faulted or adversely jointed rock and special drainage procedures if wet conditions are encountered
Relocation of alignment		Should be considered where slide conditions are severe
Slide channels and bridges		Can be constructed where slide tracks cross railway near track level
Slope treatment	Catch berms	Can be excavated along base of rock cliffs on talus, fill, or soil slopes to intercept rolling rock; must be wide enough for periodic cleaning
	Wire mesh blankets[b]	Can be draped over a slope that is raveling to control surface falls
Ditch treatment	Deeper ditches[c]	Can be used to catch rocks that roll or fall from above (§); should be cut vertical if this angle is stable; should be wide enough to be cleaned mechanically
Catch walls[d]		Are effective when located on inner side of ditch; should have vertical back faces; because concrete walls are rigid and may be damaged by large rocks, gabion walls, which are less expensive and more flexible, are preferred
Catch fences		Can be installed along inner ditches to catch rolling rock; for larger rocks, scrap rail can be welded horizontally; are costly to maintain
Debris fences		Can be constructed from steel rails in creeks and gullies that periodically carry debris, logs, brush, and such
Slide diversion channels		Can be constructed where slide channels exist and adjacent room is available to direct slides away from track

[a]See Figure 6. [b]See Figure 7. [c]See Figure 8. [d]See Figure 9.

Figure 6. Wooden and concrete rockslide sheds to carry frequent rockfalls over track.

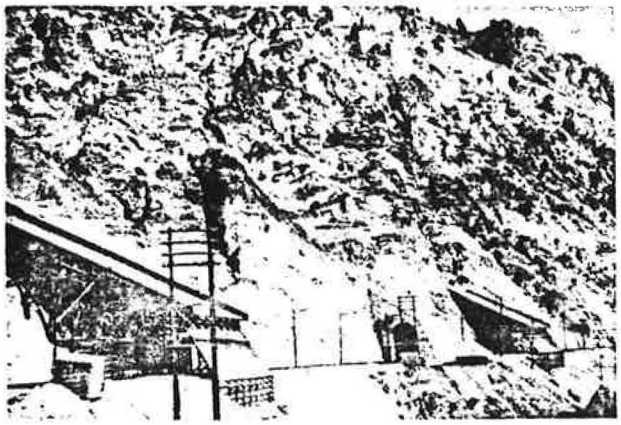

Figure 7. Wire mesh over raveling rock slope to prevent rockfall into grade.

New Construction

New construction and reconstruction sometimes require rock excavation. In the past, the general practice was to specify that new slopes in rock be cut to 0.25:1 and that shallow V-type ditches be used. These slopes were not designed according to the strength or quality of the rock. Current knowledge of rock mechanics, however, makes it possible to determine the stable slope angle with reasonable certainty and at a reasonable cost.

Figure 8. Catchment ditch.

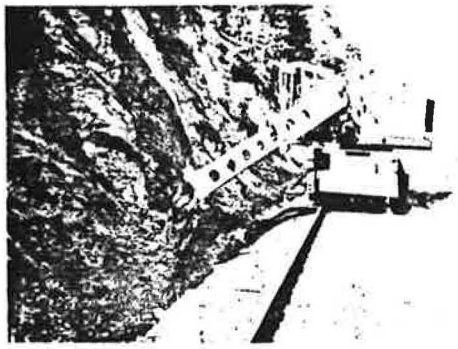

Figure 9. Catchment design using gabion walls.

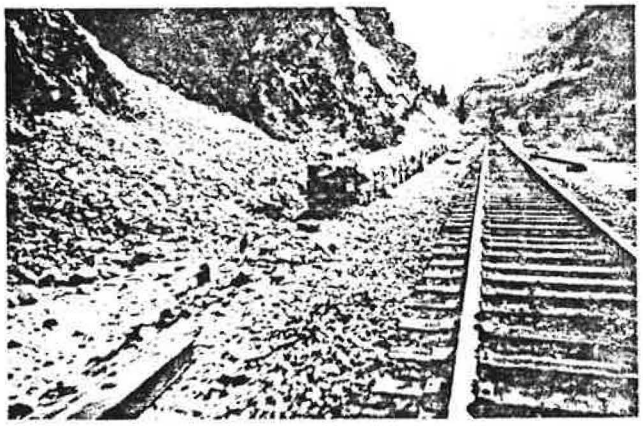

Where the rock strength or the geologic structure are favorable, rock slopes can and should be cut vertically. This will reduce quantities, allow the use of wider ditches, and result in rockfalls that drop vertically into the inner ditch rather than bouncing or rolling onto the track (see Figure 10). However, where geologic structural weaknesses dip out of the slope at an angle steeper than the effective angle of friction, the slope should be cut to this angle only.

Controlled blasting by using preshear or cushion tech-

niques should be used for the excavation of all rock slopes to minimize the damage to the rock in the slope from seismic acceleration forces (which can break rock and open joints for many meters back from the slope) (see Figure 11).

Typical Rock-Stability Assessment Program

To illustrate a working approach to the development of a rock-stability program, the program developed for the Canadian Pacific Railway on more than 2400 km (1500 miles) of track is described.

In stage 1, a variety of air photographs, topographic maps, climatic data, and railway plans were reviewed. This was followed by an inspection of the cut slopes by a division engineer, a roadmaster, or an assistant roadmaster. The stability of the slopes was then rated into five categories according to an estimate of the probability of failure based on the geology and rock conditions, slope geometry, ditch dimensions, hydrology and slope seepage, and past experience with slides or falls at the site:

1. Moderate probability of a failure of sufficient volume to cause derailment if undetected,
2. Some probability of a failure of sufficient volume to cause derailment if undetected,
3. Moderate probability of a small-volume failure that might reach the track,
4. Moderate probability of a localized rockfall during extreme climatic conditions such as very heavy rainfall or runoff or an extreme freeze-thaw cycle, and
5. Slight possibility of a localized failure under extreme climatic conditions (generally shallow cuts).

A program was instituted to record all slides and rockfalls large enough to be dangerous to train traffic. This included data on time, location, size, sight visibility, weather conditions preceding movement, type and size of movement, estimated cause of movement, problem created, and action taken. Areas of more frequent occurrences were investigated in detail on a priority basis to assess the need for and method of improving stability. Finally, a lecture and site-inspection workshop was prepared and attended by engineering staff, roadmasters, and foremen, and numerous case examples were reviewed.

In the stage 2 program, priority areas for stabilization were established, a detailed inspection was made of each, stabilization requirements were defined, and specifications were prepared. Construction has begun on these priority areas and will continue until the annual budget allocation is expended. At that time, further priority areas will be defined to establish the next year's program.

Figure 10. Design for rock slope.

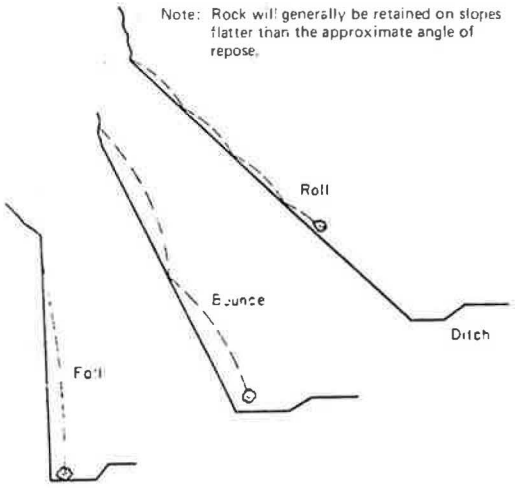

Figure 11. Comparison of rock slopes cut by using controlled versus uncontrolled blasting techniques.

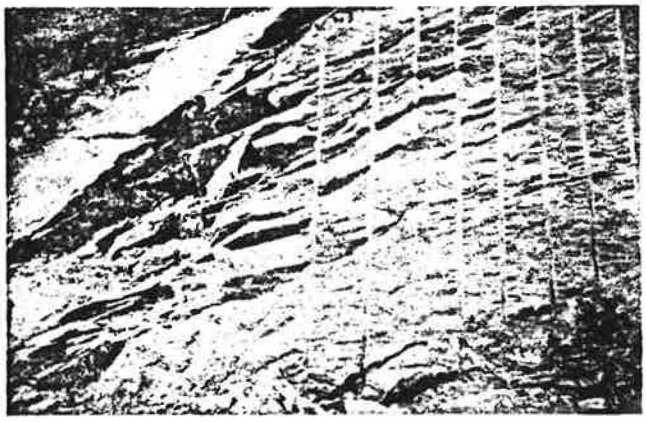

Figure 12. Effect of a major rockfall from zone of fractures and weathered rock.

EXAMPLES OF INSTABILITY AND STABILIZATION

Figure 12 shows the effect of a major rockfall from a zone of fractures and weathered granite. This fall was precipitated by very heavy rainfall that increased the water pressure in the rock discontinuities. The rock fell across a highway, broke a concrete wall, and then fell onto the rail track below. The lead engine of a train hit the rockfall and derailed. Stabilization of this area involved removal of the remaining weathered rock and rebuilding the wall. The addition of horizontal drain holes to relieve the water pressure would have been desirable.

Figure 13 shows the results when a unit train hit a rockfall having a volume of about 11 m^3 (15 yd^3) on a curve. The train was derailed, and the engines and several cars went over the bank. The cause of this rockfall is shown in Figure 14—sliding on a soil-infilled joint (a) that dipped about 45° out of the slope of a block bounded by two through-going joints that were steeply inclined (b and c) and partially filled with calcite. Factors that contributed to the failure were the presence of the adversely dipping joints, a soil infill that became saturated by heavy rain, and train vibration. In this case, the slope was stabilized by selective scaling, installation of

Figure 13. Train derailment caused by train hitting rockfall.

Figure 14. Cause of rockfall that caused train derailment shown in Figure 13.

Figure 15. Potential failure site found during annual track inspection.

tensioned and grouted rock bolts, and construction of drain holes.

The potential failure site shown in Figure 15 illustrates the importance of periodic inspections of rock slopes by specialist rock mechanics engineers. This site was found during an annual inspection of rock slopes by track car. The near-vertical crack observed ex-

Figure 16. Stabilization: construction of wider catchment ditch.

Figure 17. Location at which rockfall punctured gasoline tank.

Figure 18. Track threatened by weak rock on adjacent rock face.

tended from the base of the slope to the top [about 30 m (100 ft)] above the track, where it was about 0.3 m (12 in) wide. The crack, which was of recent origin, had been caused by vibration due to blasting to develop holes for poles on which to construct a warning fence. Action to stabilize the crack was taken immediately and involved removal within a week of about 1500 m^3 (2000 yd^3) of material. During the blasting to remove this material, the track was covered with sand and gravel for protection.

Figure 19. Track threatened by snow and ice sliding from adjacent rock face.

Figure 20. (a) Location where shifting rock block resulted in movement within rock masonry abutment and (b) close-up of anchor cable installed for stabilization.

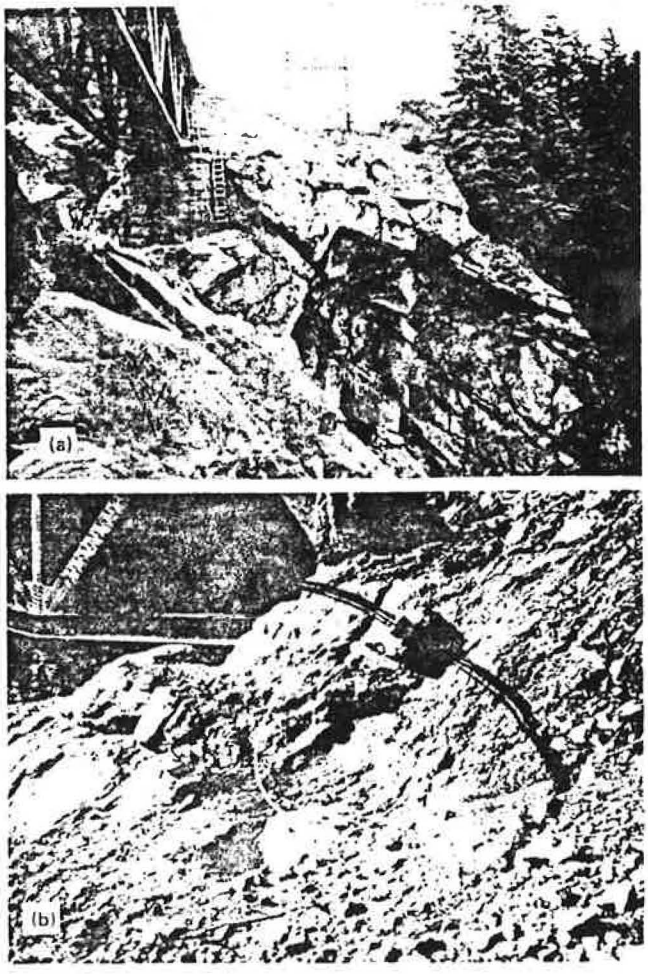

Figure 21. (a) Bridge where crack developed between abutment wall and approach retaining wall, (b) location below wall where rock block had fallen, and (c) stabilization of area.

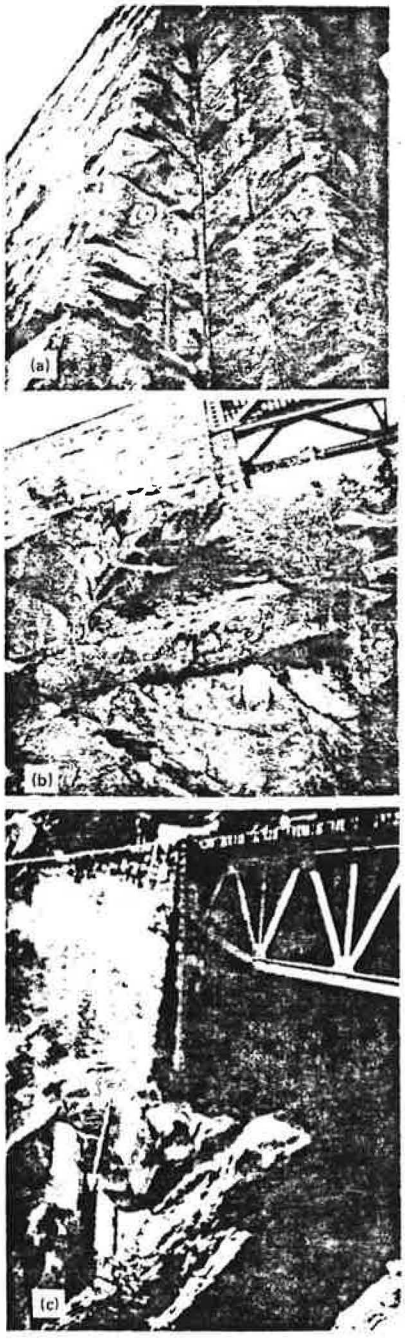

Figure 22. Stabilized concrete retaining wall.

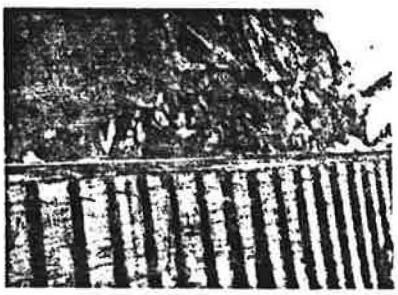

At the site shown in Figure 16, there was only a very narrow shallow ditch, and rock from slopes extending up to 122 m (400 ft) above periodically fell on the track. The rock is bedded shales, slates, and limestones, and the strike of the bedding was approximately perpendicular to the rock face. The jointing dipping out of the face was negligible. A wider catchment ditch was constructed by removing the toe of the rock bottom by controlled preshear blasting in which the drill holes were spaced 0.3-0.5 m (12-18 in) apart. Due to the favorable joint orientation, the rock face was cut vertically.

Figure 23. Construction of rock pillar support to control rockfall.

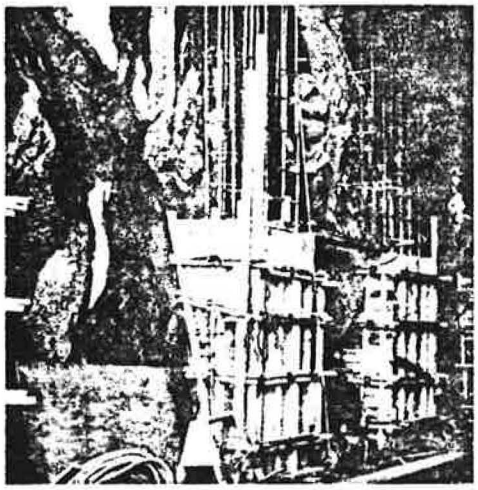

Figure 24. (a) Excavation at toe of rock slope and (b) rockfall precipitated by excavation.

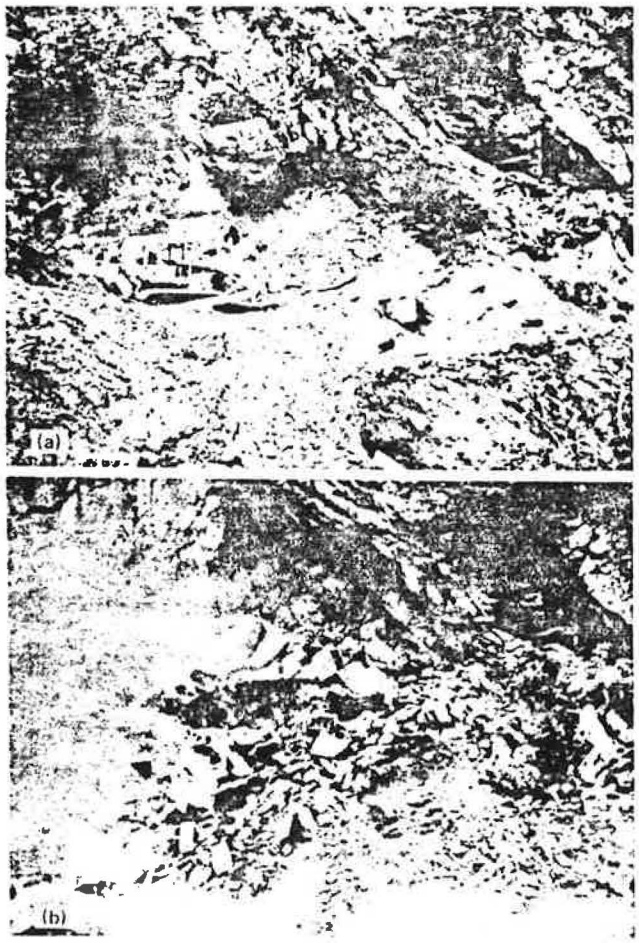

Figure 17 shows a location where a rockfall from high up a slope bounced across the tracks and punctured a large tank filled with gasoline. The gasoline spilled out onto the track, road, and adjacent inlet and created a serious fire and explosion hazard. The left-hand tank should never have been constructed at that location, which was close to both the rockfall path a (denuded of vegetation above the tank) and the second, larger path b. It was recommended that the tank be removed or protected by thick timbers on the slope side.

The track shown in Figure 18 is threatened by the adjacent rock face, in which weak rock exists below hard competent rock and is weathering and undercutting the support of the hard rock. It has been recommended that the weak rock be covered with wire-mesh-reinforced shotcrete to halt deterioration.

At the site shown in Figure 19, snow and ice develop on the smooth surface of the steeply dipping granite rock face and, during periods of melting, have sometimes slid off and derailed cars and locomotives. It has been recommended that dowels of old rail be grouted into the surface of the rock to increase the resistance to sliding and to hold the snow in place until it melts.

Figure 20a shows a location where shifting of a major rock block along a steeply dipping rock joint (a) resulted in movement within the rock masonry abutment. High-capacity anchor cables were installed, tensioned, and grouted to increase the shear strength along the joint and to halt the movement. Figure 20b shows a close-up of an anchor cable installation; each cable is 25 m (80 ft) long and full-length grouted to ensure that there is no loss of tension and to reduce the risk of corrosion.

Figure 21a shows a bridge where a crack up to 2.5 cm (1 in) wide developed between the abutment wall and the approach retaining wall (a). The geometry of the crack indicated that the wall was rotating outward, and inspection of the rock slope below the wall showed that a large block of rock (b) had fallen from the face, which had removed support for the rock forming a portion of the foundation of the wall (see Figure 21b). The rockfall area was cleaned of foreign material and loose rock, and the area was stabilized by grouting steel dowels into the rock and then filling the cavity with concrete (see Figure 21c).

At a location where the track was supported by concrete retaining walls constructed more than 70 years ago, cracks had begun to develop in the walls and several had tilted, some as much as 15 cm (6 in). A support system of no. 16 steel bars anchored and grouted into the rock and steel channels was installed at 3- to 3.5-m (10- to 12-ft) centers. One of the stabilized walls is shown in Figure 22.

Figure 23 shows a stabilization project in which rock pillars were constructed to control rockfalls near a major fault zone at the spring line of a tunnel. No. 8 dowels were grouted into the rock to tie the pillars to the rock.

Figure 24a shows an excavation being carried out at the toe of a rock slope to key in a road cut, and Figure 24b shows the major rockfall this excavation precipitated.

REFERENCES

1. C. O. Brawner. Slope Stability in Open Pit Mines. Western Miner, Oct. 1966.
2. C. O. Brawner. Rock Slope Stability in Highway Construction. 48th Conference, Canadian Good Roads Association, 1967.

3. C. O. Brawner and V. Milligan, eds. Stability in Open Pit Mining. American Institute of Mining Engineers, New York, 1971.
4. E. Hoek and J. W. Bray. Rock Slope Engineering. Institution of Mining and Metallurgy, London, 1974.
5. A. M. Ritchie. Evaluation of Rockfall and Its Control. HRB, Highway Research Record 17, 1963, pp. 13-28.

Publication of this paper sponsored by Committee on Soil and Rock Properties and Committee on Tunnels and Underground Structures.

Labor-Intensive Technology: Promises and Barriers

Mathew J. Betz and Ronald Despain

The numerous criteria for technology evaluation in developing countries are discussed with emphasis on labor-intensive appropriate technologies. Historical technologies, current technologies of reduced scale, the adaptation and improvement of indigenous technologies, and the need for research and development in labor-intensive techniques are presented. The technical factors in road construction are investigated as they relate to labor intensity. Special emphasis is given to evaluation of design standards, location criteria, and scheduling. It is possible to combine labor-intensive techniques where appropriate with more-conventional capital-intensive methods. The susceptibility of the various construction components to labor-intensive applications is briefly reviewed. Finally, the barriers to the adoption of labor-intensive techniques in road construction are presented. These include technical barriers; psychological barriers; bureaucratic barriers; educational barriers; managerial barriers; and the general lack of research, development, financing, marketing, and distribution systems to support labor-intensive alternatives. Labor-intensive alternatives are but one in a continuum of technologies. Developing countries will probably retain capital-intensive techniques for primary road projects. Labor-intensive techniques are probably best suited to the construction of feeder and rural-development roads.

APPROPRIATE TECHNOLOGY

During the past half decade, the terms "appropriate technology" and "labor-intensive technology" have become widely used, and the number of publications addressing their numerous aspects has grown.

The term "appropriate technology" can vary broadly in its application. It is currently being applied, not only to the developing countries, but also to Western Europe and the United States. Philosophically, appropriate technology implies that the decision makers should have the sophistication to devise, plan, evaluate, and select from a range of technical solutions to a given problem. Furthermore, it suggests that their selection should be based on a broader range of criteria than has been true in the past. Appropriate technology advocates the use of a greater number of economic indicators than is addressed in the traditional economic-feasibility study and emphasizes the need to include social as well as economic factors.

Stated in another way, appropriate technology could be expressed as the provision of technical solutions that are appropriate to the economic structure of those influenced, appropriate to their ability to finance the activity, appropriate to their ability to operate and maintain the facility, appropriate to the environmental conditions, and appropriate to the management capabilities of the population. There are numerous criteria, and appropriate technology challenges all of them. Not only the engineer, technologist, and economist but also the sociologist, anthropologist, historian, and others need to become involved in the evaluation and selection procedures of technological decision making.

In an extensive review, Eckaus has developed the following criteria for appropriate technology (1):

1. To maximize product output,
2. To maximize the availability of consumer goods,
3. To maximize the rate of economic growth,
4. To reduce unemployment,
5. To encourage regional development,
6. To reduce balance-of-payment deficits,
7. To provide greater equity in income distribution,
8. To promote political development, and
9. To improve the quality of life.

And, although conceding that the list is still far from comprehensive, we add the following:

10. To reduce the population flow to urban centers,
11. To provide an adequate food base for the local or national population,
12. To be as consistent as possible with the indigenous social structure, and
13. To preserve the indigenous cultural continuity and heritage.

It is obvious that these criteria are themselves in conflict. This is the real-world situation where no solution, technical or otherwise, will improve all factors impacted by a project. The strength of this approach is that it can identify both negative aspects and those that can be improved. This should lead to more-rational decision making because the positive and negative aspects can be compared as trade-offs. It presumes, however, that the criteria and the relative importance of each can be agreed on. Paradoxically, this advantage may also be a weakness. It may fail at times because it cannot be all things to all people. Considerable delay, which may in the end be disadvantageous to all, may be encountered in the extensive analysis and evaluation required. The decision making becomes very complex because of the number of criteria involved and of disagreement as to which have priority. Because of its broad definitional base, one can honestly say that, given appropriate conditions, any technology from tool-less hand labor to earth satellites can be appropriate.

LABOR-INTENSIVE APPROPRIATE TECHNOLOGY

One category of appropriate technology is that of labor-intensive appropriate technology. For example, the remaining sections of this paper will address such technologies as related to road construction and maintenance. In the economic sense, these are technologies that look for greater input of labor, often, but not necessarily, unskilled and a corresponding decrease in the requirements for capital investment. The obvious advantages of such technologies are the decrease of the number of underemployed and the reduction in foreign exchange. The underemployment problem in the world need not be documented. Labor-intensive technologies have implications in terms of slowing the migration from rural to urban areas and, perhaps most important of all, in making developing countries as self-sufficient as possible in basic commodities through rural development. We are not so naive as to feel that labor-intensive technology can completely stem the current migrations from rural areas; no such technologies are likely to be that effective or pervasive throughout any developing country. The emphasis should be to consider labor-intensive appropriate technologies as part of the range of alternatives available and possibly to give greater weight to some of the criteria that would tend to encourage and justify experimentation with and implementation of such technologies.

The idea of labor-intensive technologies, especially as applied to rural areas, goes back to the colonial era. Village industries were encouraged in India before the 1930s (2). Gandhi's writings and philosophies were intimately tied to labor-intensive technologies. More recently, the writings of Schumacher have emphasized some of the limitations of capital-intensive development and some of the advantages of labor intensity. It was Schumacher, whose thoughts have had significant impact on the young American reader (3), who coined the term "intermediate technologies" to identify those of moderate capital investment per employee. This led to the development of various intermediate technology groups in Great Britain and elsewhere. It is unfortunate that, at least in the United States, the term intermediate technology has been superseded by the term appropriate technology.

DEVELOPMENT OF LABOR-INTENSIVE TECHNOLOGY

The literature on labor-intensive technologies is a rapidly expanding one. These technologies can be developed from any of four primary sources. First, there is the revival of older technologies. These technologies were used to build the original manufacturing plants and basic infrastructure of the developed countries and were much more labor intensive than is the technology of today. The construction of railroads in the American West is a classic example. There are those who feel that a reintroduction of such technologies to Third World countries is appropriate. Much of the literature of labor-intensive technology, both that directed toward economic development and that directed toward a different life-style, is fundamentally based on this source, which might be called the Whole Earth Catalog approach. It has the advantage of being easily and quickly identifiable and having demonstrated success in the past. Thus, it can produce many good ideas at a very low research cost. It is often the approach of the instant expert, a breed not unknown in this field. It has the disadvantage of lack of depth once the initial inventory has been conducted. It has a very strong psychological disadvantage for the receiving country, which is being advised to use techniques perhaps a century old. It has the technical disadvantages that the tools are no longer manufactured and that maintenance and repair parts that may have been readily available when they were broadly used are not available today. One would have to establish a century-old production and technology base to broadly implement such technology. Where this can be done on a local level with minimal manufacturing and easily maintained tools, it can be effective. If the technology identified has much sophistication, these technical limitations are difficult to overcome. This type of solution should be among the first investigated in any comprehensive research effort, but it should not be overemphasized or become the primary intellectual base.

The second source of labor-intensive technologies is to adapt current technologies to a smaller scale for implementation in a receiving country. This is done daily as new plants and techniques are introduced. Even substantial manufacturing plants are often not to the scale that would be built in the developed world. The adoption of smaller lightweight tractors as opposed to heavier commercial ones is an example.

A third source is the adaptation and improvement of indigenous technologies. The fact that the populations concerned have existed within their geographical location and physical environment for centuries, if not millennia, is often overlooked. The methods and technologies developed have certainly been successful in those conditions. Thus, the folklore methods of doing things may form a fundamental base of knowledge from which to develop improvements and modifications. Furthermore, any new technique or tool must be introduced into the social and cultural environment that exists. This is the same environment that has successfully adopted or adapted the traditional techniques. Why they work and how they work is fundamental to either improving existing techniques or to the insertion of new techniques into the cultural and social milieu. It would seem obvious that the less disruptive a new technique is to its environment (social and cultural), the more likely it is to be readily adopted. This is particularly true in labor-intensive technologies for road construction and maintenance, which apply to large numbers of people in open environments, rather than to limited numbers in the closed environment of a factory.

The fourth source of labor-intensive technologies, probably least used currently, is simply the invention of new technologies that are labor, rather than capital, intensive. The difficulties are substantial. We have established educational and research facilities aimed at the invention and development of tools and techniques that tend to be more capital intensive rather than less so. The difficulties to be addressed in looking at the opposite side of this coin cannot be overemphasized. The concept of small research for small technology is naive. However, it is more than a question of financial resource. It is a question of the entire matrix of the education system from preschool through the Ph.D. In both the developed and the developing countries, training tends to establish biases, capabilities, and value structures that make it very difficult to conceptualize and invent low-capital-investment alternatives. This is not to imply that it cannot or should not be done. If labor-intensive techniques are to be broadly or even moderately effective, such research emphasis must be developed. Most of these techniques require extensive development and implementation projects that are best done in Third World locations.

TECHNICAL FACTORS IN TECHNOLOGY SELECTION

In road construction, labor-intensive projects require the integration of multiple activities, on a relatively large scale and employing many people. Road construction is illustrative of the diverse difficulties encountered when using labor-intensive techniques in large rural development projects. A linkage, normally a road of some type, is a necessity for rural development. Without the physical interconnection of a transportation link, importation of needed commodities and services and export of surplus production is impossible. [This need has been discussed elsewhere (4), as has the construction of low-volume roads (5).]

Most road projects have emphasized the use of capital-intensive heavy equipment, imported from a limited number of developed countries. However, adequate roads were built long before the invention of such equipment. Also, not all roads in developing countries need or should be of a high-quality or a paved type. The Sudan, which instituted a road-building program a few years ago, is about to complete the first paved road from Khartoum to the sea. Is is clear that the Sudan with its large area cannot afford either the cost or the time necessary to develop high-quality roads throughout. Roads can be built in as broad a spectrum of design and quality as any other works of humans.

One of the basic technical factors affecting the attractiveness of labor-intensive technologies in road construction is the original design of the facility. The higher the design standards, the more likely that capital-intensive technology will appear desirable. The overdesign of rural roads in developing countries is probably widespread. The design of penetration and agricultural-access roads to lower standards, including accepting a greater risk of temporary closure, should be carefully evaluated. The selection of a paved design versus an improved gravel facility is often critical. Many of the functions involved in even a simple bituminous-surface-treatment design are not realistically feasible when labor-intensive techniques are used. Such designs usually call for higher-quality base materials and more-uniform compaction standards than does an unpaved facility. As material specifications increase, the likelihood of use of adjacent soil is decreased. This, in turn, increases the need for capital equipment, as efficient methods of transporting material greater than 1 km by labor-intensive techniques are not generally available (5).

The performance of the system, which is exposed to the physical environment and to the abuses of an uncontrolled user group (overloaded lorries being a prime example), is an additional engineering concern. Most engineers feel responsible and consider inadequate performance of roads as a failure. The tendency, therefore, is to overdesign. If the engineers (rather than the real causes) are to be held responsible for the lack of performance, then overdesign will continue to be a problem. There is a myth that, the higher quality the road and the more sophisticated the design, the greater the quality control (i.e., the more mechanized equipment) and the easier and cheaper the maintenance. Over the last 15 years, an expanding amount of research has indicated that, although there is some truth to this in the narrow range, it is misleading in the broad range of design alternatives. In other words, a paved road is not necessarily cheaper or easier to maintain than a gravel road, nor is a gravel road necessarily cheaper or easier to maintain than a dirt road. The local manufacture of road construction equipment is of importance. Such activity has been developed in Kenya through a rural-access road program (6).

The initial location of a proposed facility can bias the technology choice. A direct route between two points generally requires more earth work, involving both excavation and embankments, than would a longer route that takes advantage of the natural terrain. Although the longer route might cost more because of its extra length, the shorter route, because of its technical requirements, may mandate capital-intensive techniques. In other cases, the route might be lengthened to take advantage of locally available materials. This route lengthening could actually decrease the length of haul from material site to building site and thus increase the attractiveness of labor-intensive techniques.

The construction schedule is another variable that can encourage or discourage labor intensity. Labor-intensive techniques require that unemployed or underemployed local labor be available. In the rural situation, there may be relatively little underutilized labor during planting and harvesting seasons. Thus, construction schedules that call for intensive activity spanning either or both of these seasons may require capital intensity. However, time is not critical in most rural road projects, and it should be possible to devise a schedule that supports the use of excess labor.

Road construction represents a collection of different and semi-independent functions, including (but not limited to) site clearance, excavation, hauling, embankment building, compaction, placement of selected material, and grading. There is no reason why a mixture of capital-intensive and labor-intensive technologies cannot be used on a given project. In studying construction of gravel roads in Kenya, one analysis of a variety of construction techniques that ranged from wholly labor-intensive to wholly capital-intensive technology concluded that a combination of labor- and capital-intensive techniques required the minimal amount of capital per person day of work and employed a substantial labor force at a minimal increased total cost (7). Muller (8) has discussed his personal experiences using labor-intensive construction. The project was the construction of 480 km of all-weather gravel road, including drainage and bridges, by capital-intensive methods using mostly imported equipment. The production rate was 1 km of road graveling each 2.3 days at a direct operations cost of approximately $500. Actual experience indicated production rates of 30-70 percent of the anticipated. Increased numbers of laborers were employed when excavators had mechanical problems. Occasionally, these laborers were retained even when the machinery was working, which resulted in increased productivity. Based on this experience, other methods of increasing the labor intensity were devised; Muller found that all operations except hauling (because of the long haul distance from quarry to site) and watering could be performed economically by labor-intensive methods. Maximizing the labor intensity and maintaining the same operational speed (2.3 days/km) resulted in a cost of approximately $550 or about 10 percent higher than the capital-intensive methods. Both Muller's conclusions and those of the International Labor Organization indicate that the direct transfer of capital-intensive technologies into the African social-economic environment is probably not justified. A balance between capital- and labor-intensive techniques would seem to meet current broader criteria.

LABOR-INTENSIVE TECHNIQUES FOR ROAD CONSTRUCTION

Labor-intensive methods of construction are not neces-

sarily limited to the use of the simplest techniques and tools available, e.g., carrying excavation materials in baskets or using hand shovels. The techniques should include the design and construction of new tools and equipment.

In excavation and loading, the traditional techniques of picks, hoes, and shovels can be implemented. Hand-held stretchers or head baskets are effective over short distances and where changes in elevation are small. Somewhat more-sophisticated and more-productive tools can be devised by using teams of labor, draft animals, or machines that develop mechanical advantage (such as those based on the principle of the bicycle). Depending on the soil type and the difficulty of excavation, labor-intensive techniques can be used in immediate conjunction with mechanical excavators. As haul distances increase, more-sophisticated equipment should be devised, but this can still fall far short of modern capital-intensive hauling vehicles. Locally built carts with rubber tires can be drawn by teams of men or draft animals and carry embankment materials significant distances. Small tipping trucks on steel rails may be animal or human powered and are an effective hauling device, although the tracks must be moved as construction progresses. For intermediate distances, the adaptation of the small scraper (possibly made from a half of an oil drum) is feasible. The design for and productive capacity of similar equipment (including carts, wagons, plows, drags, scrapers, fresnos, and wheel scrapers) can be found in older American highway engineering publications (9). The spreading and leveling of road materials is generally not effectively accomplished by hand. Some type of scraper, broom, or drag is necessary but, again, labor, draft animals, or light mechanization can provide the power.

Most engineers feel that soil compaction is the function for which labor-intensive methods have the greatest difficulty in competing with methods involving heavy equipment. Heavy equipment gives rapid compaction that is often significantly higher than can be produced manually. In addition, there is probably greater uniformity of compaction. This does not require, however, that all compaction be done with heavy equipment. Hand compaction can be effective (even in developed countries, it is often used in areas where heavy equipment cannot operate, such as back filling behind retaining walls). Compaction can be achieved by small hand-controlled mechanical compactors, but it can also be accomplished solely by hand. Many feel, however, that hand compaction has serious economic as well as technical disadvantages. A real alternative that should be investigated is the reduction of compaction standards traded off against greater depths of compacted material. It should also be noted that traffic itself can supply considerable compactive capability. For example, a discussion (9) of the construction of sand clay roads in the United States early in the century stated that

> The ordinary method that has been utilized to obtain this result (compaction) has been the mixing and packing due to hooves of animals and wheels of vehicles going over the road. This gives surprisingly good results, but it usually takes several months before the road is thoroughly consolidated and packed. It is necessary, while this packing is going on, that after each rain, the surface be immediately reshaped and crowned.

For a high-quality gravel surface, some type of roller having a significant weight (probably 8 Mg or more) was generally advised.

The haulage of water for construction is usually somewhat more complicated than the haulage of construction materials. Nonetheless, the use of animal-drawn water tanks of local manufacture (e.g., drums on rubber-tired carts) can be effective.

These are just a few specifics that illustrate the feasibility of using more labor-intensive technologies. In addition, as noted by Marsden (10), "New technology should stimulate output in indigenous industries and be capable of being reproduced locally."

BARRIERS TO USE OF LABOR-INTENSIVE TECHNOLOGIES

What are the barriers to the use of labor-intensive techniques? For one, the experts do not agree. Eckaus tends to classify the advantages of Schumacher's proposals under his (Eckaus') criteria of improvement of quality of life and specifically limits them to rural village development. He further states that the advantages of such intermediate technologies are limited and indicates that they fly in the face of major trends throughout the world by resting almost entirely on a village-oriented life-style (1).

Most of the technology available to the Third World is the technology of the developed world. This technology has survived and prospered under a narrow range of solely economic indicators that emphasize minimal cost of production, capital investment, and quality control and are generally based on an economy that has almost full employment and high wage rates. It is not surprising that such an environment encourages high-capital-investment projects.

Project feasibility studies conducted by American or European consultants tend to have a capital-investment bias, intentionally or unintentionally. The bias may be unintentional in that these consultants are trained and experienced in and technically more comfortable with high-capital alternatives. Or, the bias may be intentional because of the realization that the sources of the high-capital construction items are, for the most part, the developed countries. In addition, labor-intensive-technology alternatives may involve fewer expatriates in their implementation and operation (7).

As most development projects are either conducted or channeled through the national government, the selection of projects is greatly influenced by the local bureaucracy. It is clear that, for a given amount of capital to invest, the larger the capital component of each project, the fewer the total number of projects. Thus, from the bureaucratic standpoint, it may be advantageous to have a limited number of projects (which can be realistically followed and controlled) rather than a large number of low-capital-investment projects (which tend to be impossible to control by a central agency).

A country's tariff and tax structures may be another bias toward high-capital projects. These may result in subsidized capital. Such policies tend to undervalue capital investment in terms of other alternatives. Capital may be provided through the central government at low rates or by reduced import duties for foreign machinery, thus subsidizing those who wish to place their resources in a capital investment as opposed to investment in labor components.

Labor-intensive techniques require large numbers of people. The training of these people, their organization and management, becomes a substantial problem. People who have such training and management skills are in short supply in most Third World countries (11). In addition, the developed countries have not provided the organizational structures nor the training tools to support such projects. More imagination is needed in these areas. We suggest consideration of highly sophisticated tools to do this very unsophisticated job. The use of modern, highly portable, audiovisual training techniques may be very effective where the trainees are illiterate. Their audiovisual capabilities may be more acute than

those of a more literate, book-based society.

Because a large number of people are involved, they probably represent a substantial portion of the total indigenous population in a given location. Therefore, the ability to institute and carry through such projects benefits from maximizing the use of the existing social and organizational systems. This calls for a substantial input from sociologists, cultural anthropologists, and other social scientists.

The desire of the private entrepreneur to capitalize is seldom addressed in the literature, other than in terms of lowering unit production cost to maximize profits. Increased capital investment may also increase capacity and improve quality control, which may broaden the potential market. If this is supported by governmental capital subsidization, so much the better from the entrepreneur's standpoint. In addition, one of the factors that is almost never mentioned and may be a consideration, even at a very low level of capitalization, is the fundamental truth that the capital investment belongs to the capitalist. If an individual has given resources, he or she generally can select a technology that will place some of these into capital investment in plant and equipment, some in operational costs, and some in labor costs. There may be a feeling that operational and labor costs are dispersed, whereas investment in plant and equipment is under the control and ownership of the investor. In other words, expenditure in capital tends to be a long-term asset whereas expenditures in operations and labor are not. The importance of this as a psychological bias is probably underrated. The impact of this becomes even greater when the economies have high inflation rates.

The barriers discussed above are basically economic and structural limitations to the implementation of labor-intensive technology. There are others.

A system for innovation in labor-intensive techniques is lacking. There is only a weak technological invention base and little or no incentive for private investment in the invention of low-capital-investment tools. Most Third World countries lack a well-defined research and development laboratory, either in the private or in the public sectors.

There is the absence of the innovation and implementation system represented by the individual firm in the private economy. There tends to be a lack of marketing and distribution systems for those labor-intensive technologies that are used. The weak financial infrastructure to support innovative systems for labor-intensive technologies reflects an absence of private incentives and public interest.

Because of the limitations described above, there would seem to be little incentive for increased emphasis on labor-intensive technologies. The primary justification is the possibility of dispersing economic development by placing some of the emphasis on the number of individuals benefited rather than all of it on the national economic factors.

CONCLUSIONS

The purpose of this paper has been to identify the potentials and problems of labor-intensive technology as applied to low-volume road construction and maintenance. Clearly, because of the multidisciplinary nature of the problems, there is a need for an integrated approach. This is especially true if labor-intensive techniques are to be applied broadly. Although substantial work and much imagination are necessary inputs to the development of new tools, the successful implementation of labor-intensive techniques is fundamentally a people problem; therefore, training, management, social structure, and cultural systems become the four corner posts on which success of the technical activities must rest. The failure of any one will cause failure, or at least substantial impediments to the success, of the others.

Finally, the emphasis on labor-intensive techniques reflects the fundamental belief that the most-valuable resource of any country is its people. The development of this resource cannot be instantaneous. It requires time and patience. More important, it requires opportunity and resources. The use of capital-intensive technologies has led to the development of dualistic economies in many nations. Some would say that this is wrong. These persons feel that development should be entirely focused on the rural development element to improve the quality of life for all of the population simultaneously. A more moderate view would seem appropriate. Modern developing countries wish to become just that—modern. There is a place for the most-advanced 21st-century technologies. There is a place for modern capital-intensive production. As we have emphasized, there is also a place for labor-intensive activities. In this paper, we have identified some of the real barriers, internal and external, technical and social, to greater and more-accelerated application of labor-intensive techniques. Greater efforts by all concerned must be made to encourage and implement these techniques.

REFERENCES

1. R. S. Eckaus. Appropriate Technologies for Developing Countries. National Academy of Sciences, Washington, DC, 1977, pp. 37-52.
2. N. Jaquier, ed. Appropriate Technology: Problems and Promises. Organization for Economic Cooperation and Development, Paris, 1976, p. 175.
3. E. F. Schumacher. Small Is Beautiful: Economics As If People Mattered. Blond and Briggs, Ltd., London, 1973.
4. Transportation Technology Support Project. TRB, Transportation Research News, No. 78, Sept.-Oct. 1978, pp. 10-11.
5. M. Allal, G. A. Edmonds, and A. S. Bahalla. Manual on the Planning of Labor-Intensive Road Construction. International Labor Office, Geneva, 1977.
6. J. Baranson. Road Construction Equipment for Local Manufacturer: Kenya. Ekistics, June 1977, pp. 369-372.
7. United Nations Development Program. Employment Incomes and Equality: A Strategy for Increasing Productive Employment in Kenya. International Labor Office, Geneva, 1972, pp. 383-390.
8. J. Muller. Labor-Intensive Methods in Low-Cost Road Construction: A Case Study. International Labour Review, Vol. 101, No. 4, April 1970, p. 372.
9. A. H. Blanchard, ed. American Highway Engineers Handbook. Wiley, New York, 1919, pp. 430-440.
10. K. Marsden. Progressive Technologies for Developing Countries. In Third World Employment (R. Jolly and others, eds.), Cox and Wyman, Ltd., London, 1973, p. 328.
11. C. P. Timmer, J. W. Thomas, L. T. Welk, and D. Morawetz. The Choice of Technology in Developing Countries. Center for International Affairs, Harvard Univ., Cambridge, MA, 1975, pp. 3-15.

Publication of this paper sponsored by Committee on Low-Volume Roads.

Abridgment

Stability Charts for Effective Stress Analysis of Nonhomogeneous Embankments

Yang H. Huang

New stability charts have been developed for the effective stress analysis of nonhomogeneous embankments subjected to seepage and seismic conditions. These charts are applicable to soils that have a small effective cohesion, which is the case encountered most frequently in engineering practice. The procedure is based on the normal method and is unique in that, although a large number of factors are considered, only a limited number of charts are needed. The theory by which these charts have been developed, the suggested procedures for their use, and their application to practical cases are presented. The factors of safety determined by using the charts are compared with those obtained by using the available computer programs, based on both the simplified Bishop and the normal methods. When the most-critical failure surface is a shallow circle, the factor of safety determined by using the charts agrees closely with the computer solutions. However, if the most-critical failure surface is a deep circle, the factor of safety determined by using the charts will be somewhat smaller than that obtained by using the computer solution based on the simplified Bishop method but slightly greater than that based on the normal method. Compared with the simplified Bishop method, the use of the stability charts is therefore conservative.

In a previous paper (1), I presented two new charts for the stability analysis of earth embankments. The chart for short-term stability is based on a total stress analysis, uses $\phi = 0$, and can be applied to a nonhomogeneous slope composed of various layers. The chart for long-term stability is based on an effective stress analysis, uses given values of $\bar{c}$ and $\bar{\phi}$, and is applicable only to a homogeneous slope that has a ledge at a considerable distance from the surface. It was indicated that the assumption of a homogeneous slope for effective stress analysis was not a serious limitation because the long-term shear strength parameters (i.e., $\bar{c}$ and $\bar{\phi}$) for most soils might not change significantly and average values could easily be estimated. However, if the strength parameters for different materials in different parts of the slope are significantly different, it will be difficult to obtain average values. Another difficulty in the use of the chart for effective stress analysis is the estimation of pore pressures. Unless the phreatic surface and the location of failure circle are known a priori, pore pressures cannot be estimated with certainty.

The purpose of this paper is to present an additional chart that can be used for the effective stress analysis of both homogeneous and nonhomogeneous slopes subjected to steady-state seepage and seismic conditions. The method requires an iterative determination of the factors of safety for a number of potential failure circles, so that a minimum factor of safety can be obtained. [Due to space limitations, only one chart and a simple example will be presented here; additional charts and detailed procedures for their use are given elsewhere (2).]

The chart presented here can be used only where the effective cohesion of the materials is small. These materials include granular soils and normally consolidated clays. The potential failure surfaces through these materials generally consist of shallow circles, so only a few charts involving shallow circles are needed. It is believed that the assumption of a small cohesion is realistic and can be used in many practical cases.

DESCRIPTION OF METHOD

Figure 1 shows a slope that has a height H and an outslope S:1 (horizontal: vertical). It is assumed that the effective cohesion of the soil in the slope is small, so that the most-critical failure surface is a shallow circle, the two endpoints of which lie at a distance of 0.1 SH from the top edge and the toe. This assumption of 0.1 SH, i.e., one-tenth the horizontal distance between the edge and the toe, is arbitrary. In fact, I have developed other charts that have endpoints passing through or at varying distances from the edge and the toe, so the factor of safety for any given circle can be determined. However, it has been found that the factor of safety for most slopes can be estimated by using this assumption.

When a failure circle is assumed, the average shear stress developed along it can be determined by equating the moment at the center of the circle due to both the weight of the sliding mass and the corresponding seismic force with that due to the average shear stress distributed uniformly over the failure arc. This developed shear stress is proportional to the unit weight of the soil and the height of the slope and can be expressed as

$$\tau = (\gamma H/N_s) + (C_s \gamma H/N_e) \quad (1)$$

where

- τ = developed shear stress,
- γ = total unit weight of soil,
- N_s = stability number,
- C_s = seismic coefficient (the ratio between seismic force and weight), and
- N_e = earthquake number.

Both N_s and N_e depend on the geometry of the slope and the location of the circle. The average shear strength along the failure surface varies with γ and H and, according to the Mohr-Coulomb theory, can be expressed as

$$s = \bar{c} + [(1 - r_u)\gamma H \tan \bar{\phi}]/N_f \quad (2)$$

where

- s = shear strength,
- $\bar{c}$ = effective cohesion,
- r_u = pore pressure ratio (ratio between the pore water pressure and the overburden pressure),
- $\bar{\phi}$ = effective angle of internal friction, and
- N_f = friction number (which also varies with the geometry of the slope and the location of the circle).

The factor of safety (F) is the ratio between the shear strength and the shear stress. By dividing Equation 2 by Equation 1, F can be expressed as

$$F = [(\bar{c}/\gamma H) + (1 - r_u)\tan \bar{\phi}/N_f]/[(1/N_s) + (C_s/N_e)] \quad (3)$$

Figure 1. Potential failure circles in a typical slope.

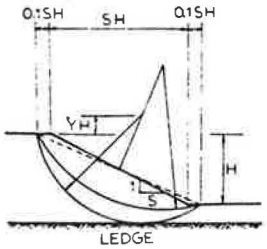

Figure 2. Stability chart.

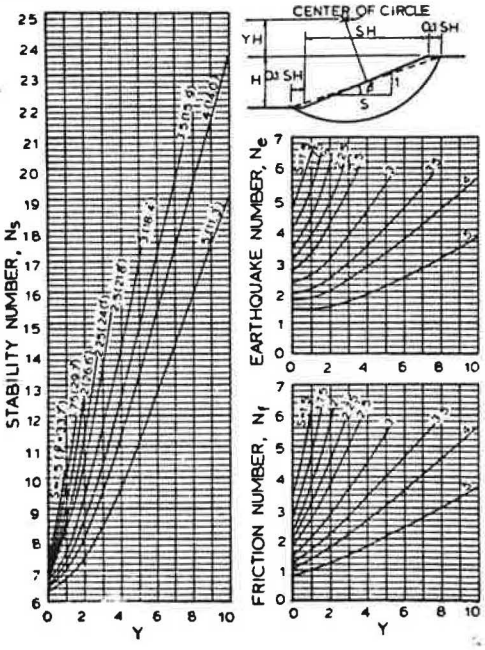

Figure 3. Analysis of nonhomogeneous slope.

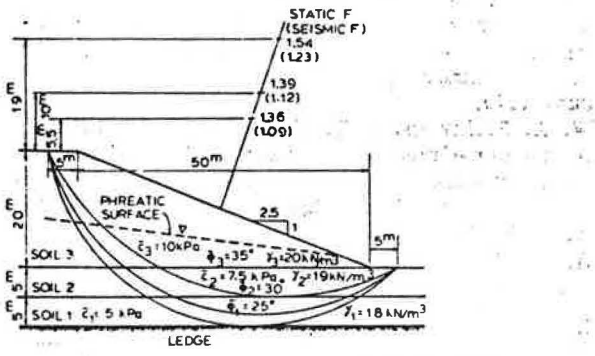

Note: 1 m = 3.28 ft; 1 kPa = 20.9 lbf/ft^2; 1 kN/m^3 = 6.37 lbf/ft^3.

Equation 3 shows that F depends on four geometric parameters (H, N_s, N_f, and N_e) and four soil parameters (r_u, γ, $\bar{c}$, and $\bar{\phi}$). N_s, N_f, and N_e can be obtained from the stability chart, and r_u can be determined from the location of the phreatic surface with respect to the failure circle. If the slope is homogeneous, γ, $\bar{c}$, and $\bar{\phi}$ are given directly. If the slope is nonhomogeneous, average values of γ, $\bar{c}$, and $\bar{\phi}$ must be determined. [To facilitate the computation of average soil parameters, a special table and form were developed but are not presented here (2).] The method for computing γ, $\bar{c}$, $\bar{\phi}$, and r_u for a nonhomogeneous slope is illustrated below.

The value of F obtained by using Equation 3 is similar to that obtained by the normal method, which is one of the two methods used in the ICES-LEASE computer program (3) [the other is the simplified Bishop method (4)]. When the pore pressure ratio = 0 or there is no seepage, the normal method and the well-known Fellenius method (5) are identical. When the pore pressure ratio $\neq$ 0, the normal method differs from the Fellenius method because the former is based on the concept of submerged weight, which acts vertically, while the latter is based on the pore pressure normal to the failure surface. The simplified Bishop method was not used because the assumption that the shear stress varies with F makes it impossible to express F in the simple form shown by Equation 3.

Figure 2 shows N_s, N_f, and N_e in terms of the dimensionless parameters Y and S, where Y = ratio between the distance from the center to the top of the slope and the height of the slope. Because the slope angle (β) is related to S by S = cotβ, the slope angles corresponding to each value of S are also shown.

In using the stability chart, it is necessary to plot a cross section of the slope. A bisector perpendicular to the dashed line is drawn, as shown in Figure 1, and the values of F for several circles that have centers on the bisector are determined and compared. If the ledge or stiff stratum is close to the surface, the circle tangent to the ledge is usually the most critical.

EXAMPLE

Figure 3 shows a 2.5:1 slope, 20 m (66 ft) high, composed of three different soils. Soil 1 has an effective cohesion of 5 kPa (104 lbf/ft^2), an effective friction angle of 25°, and a total unit weight of 18 kN/m^3 (115 lbf/ft^3); soil 2 has an effective cohesion of 7.5 kPa (157 lbf/ft^2), an effective friction angle of 30°, and a total unit weight of 19 kN/m^3 (121 lbf/ft^3); and soil 3 has an effective cohesion of 10 kPa (209 lbf/ft^2), an effective friction angle of 35°, and a total unit weight of 20 kN/m^3 (127 lbf/ft^3). The location of the phreatic surface is as shown. Assuming a seismic coefficient of 0.1, determine both the static and the seismic values of F.

Because the weakest material (soil 1) lies immediately above the ledge, the most-critical circle is probably tangent to the ledge. Thus, a circle that cuts through all three soils is drawn tangent to the ledge and passing through the two endpoints 5 m (16 ft) from the edge and the toe. The center of the circle is 5.5 m (18 ft) above the top of the slope, or Y = 5.5/20 = 0.275. For S = 25 and Y = 0.275, Figure 2 gives N_s = 7.0, N_f = 2.0, and N_e = 2.8.

To determine the average soil parameters, the sliding mass is divided into a number of subareas, as shown in Figure 4. The area of each subarea is measured; the sums for soils 1, 2, and 3 are 131, 221, and 534 m^2, respectively.

The average unit weight for the entire sliding mass (γ) = [(131 × 18) + (221 × 19) + (534 × 20)]/(131 + 221 + 534) = 19.5 kN/m^3 (124 lbf/ft^3).

The length of the failure arc through soils 1, 2, and 3 is measured; these values are 40, 17.6, and 24 m (131, 57, and 79 ft), respectively.

$\bar{c}$ = [(40 × 5) + (17.6 × 7.5) + (24 × 10)]/(40 + 17.6 + 24) = 7.0 kPa (146 lbf/ft^2).

Because only the component of weight normal to the failure surface is effective in producing friction, tan$\bar{\phi}$ is determined by multiplying the weight above the failure surface by cos θ, where θ = angle of inclination of the chord, as shown by θ_1, θ_2, and θ_3 in Figure 4.

The weight normal to the failure arc in soil 1 = [(131 × 18) + (187 × 19) + (293 × 20)] × 0.95 = 11 182 kN/m

Figure 4. Area, arc length, and chord inclination of critical circle.

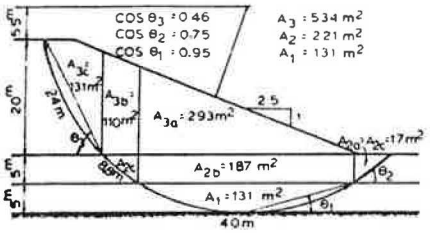

Note: 1 m = 3.28 ft; 1 m² = 10.7 ft².

(771 172 lbf/ft), that in soil 2 = [(2 × 17 × 19) + (110 × 20)] × 0.75 = 2135 kN/m (147 241 lbf/ft), and that in soil 3 = 131 × 20 × 0.46 = 1205 kN/m (83 103 lbf/ft).

Therefore, $\tan\bar{\phi}$ = (11 182 tan 25° + 2135 tan 30° + 1205 tan 35°)/(11 559 + 2135 + 1205) = 0.502.

The average pore pressure can be estimated by using

r_u = area of sliding mass under water × unit weight of water ÷ total area of sliding mass × average unit weight of soil (4)

The area of sliding mass under water is measured and found to be 527 m² (5571 ft²).

r_u = (527 × 9.8)/(886 × 19.5) = 0.299.

From Equation 3, the static factor of safety = [[7.0/(19.5 × 20)] + [(1 - 0.299) × 0.502]/2.0]/(1/7.0 + 0) = (0.0179 + 0.1760)/0.1429 = 1.36.

The seismic factor of safety = (0.0179 + 0.1760)/(0.1429 + 0.1/2.8) = 0.1939/0.1786 + 1.09.

Two more circles, as shown in Figure 3, were also evaluated; their factors of safety were greater than the above values, thus confirming that the circle tangent to the ledge is the most critical.

The factors of safety obtained by using the REAME computer program (6) are summarized below:

	Method	
Factor of Safety	Simplified Bishop	Normal
Static	1.508	1.206
Seismic	1.129	1.002

Thus, the normal method yields a factor of safety somewhat smaller than does the simplified Bishop method. It was also found that the discrepancy decreased as the most-critical circle became shallower. The factor of safety determined by using the stability chart always lies between that found by using the normal method and that found by using the simplified Bishop method, as is expected. Compared with the simplified Bishop method, the use of stability charts is conservative.

SUMMARY AND CONCLUSIONS

A new stability chart for the effective stress analysis of slopes is presented. This chart is a valuable supplement to the stability chart presented in a previous paper (1). The advantages of the new chart over the earlier one are that (a) it can be used for both homogeneous and nonhomogeneous slopes that have a ledge or a stiff stratum either close to or far from the surface, (b) it can be used to determine both the static and the seismic factors of safety, and (c) it makes possible a more accurate evaluation of the pore pressure ratio. However, the application of the chart to a nonhomogeneous slope requires the determination of average soil parameters by measuring the arc length and the cross-sectional area of different soils in various regions.

The application of the stability chart is based on the normal method, which is a modified version of the Fellenius method. If the foundation is good or the ledge is near to the ground surface, the most-critical circle will be a shallow circle, and the factor of safety obtained by using the normal method will be only slightly smaller than that obtained by using the simplified Bishop method. If the foundation is poor or the ledge is far from the surface, the most-critical circle will be a deep circle, and the factor of safety obtained by using the normal method will be much smaller than that obtained by using the simplified Bishop method. Because the circle used in conjunction with the stability chart may not be the most-critical circle, the factor of safety determined by using the chart generally lies between the minimum factor of safety obtained by using the normal method and that obtained by using the simplified Bishop method. If the acceptance of a design is based on the simplified Bishop method, the use of the stability chart is conservative.

ACKNOWLEDGMENT

The work reported in this paper was part of an overall study of the stability of slopes that was supported by the Institute for Mining and Minerals Research, Kentucky. The support given by the Computing Center, University of Kentucky, Lexington, for the use of the IBM 370 computer is appreciated.

REFERENCES

1. Y. H. Huang. Stability Charts for Earth Embankments. TRB, Transportation Research Record 548, 1975, pp. 1-12.
2. Y. H. Huang. Stability Charts for Refuse Dams. Proc., 5th Kentucky Coal Refuse Disposal and Utilization Seminar, Univ. of Kentucky, Lexington, June 1979.
3. W. A. Bailey and J. T. Christian. ICES-LEASE-I: A Problem-Oriented Language for Slope Stability Analysis—User's Manual. Massachusetts Institute of Technology, Cambridge, Soil Mechanics Publication 235, April 1969.
4. A. W. Bishop. The Use of the Slip Circle in the Stability Analysis of Slopes. Geotechnique, Vol. 5, No. 1, 1955, pp. 7-17.
5. W. Fellenius. Calculation of the Stability of Earth Dams. Trans., 2nd Congress on Large Dams, Washington, DC, Vol. 4, 1936, pp. 445-462.
6. Y. H. Huang. User's Manual for REAME: A Computer Program for the Stability Analysis of Slopes. Office of Engineering Continuation Education, Univ. of Kentucky, Lexington, 1980.

Publication of this paper sponsored by Committee on Embankments and Earth Slopes.

The Transportation Research Board is an agency of the National Research Council, which serves the National Academy of Sciences and the National Academy of Engineering. The Board's purpose is to stimulate research concerning the nature and performance of transportation systems, to disseminate information that the research produced, and to encourage the application of appropriate research findings. The Board's program is carried out by more than 250 committees, task forces, and panels composed of more than 3100 administrators, engineers, social scientists, attorneys, educators, and others concerned with transportation; they serve without compensation. The program is supported by state transportation and highway departments, the modal administrations of the U.S. Department of Transportation, the Association of American Railroads, and other organizations and individuals interested in the development of transportation.

The Transportation Research Board operates within the Commission on Sociotechnical Systems of the National Research Council. The National Research Council was established by the National Academy of Sciences in 1916 to associate the broad community of science and technology with the Academy's purposes of furthering knowledge and of advising the federal government. The Council operates in accordance with general policies determined by the Academy under the authority of its Congressional charter, which establishes the Academy as a private, nonprofit, self-governing membership corporation. The Council has been the principal operating agency of both the National Academy of Sciences and the National Academy of Engineering in the conduct of their services to the government, the public, and the scientific and engineering communities. It is administered jointly by both Academies and the Institute of Medicine.

The National Academy of Sciences was established in 1863 by Act of Congress as a private, nonprofit, self-governing membership corporation for the furtherance of science and technology, required to advise the federal government upon request within its fields of competence. Under its corporate charter, the Academy established the National Research Council in 1916, the National Academy of Engineering in 1964, and the Institute of Medicine in 1970.